



**EFFECT OF MIXTURE PRESSURE AND EQUIVALENCE RATIO ON
DETONATION CELL SIZE FOR HYDROGEN-AIR MIXTURES**

THESIS
JUNE 2015

Curtis A. Babbie, Captain, USAF

AFIT-ENY-MS-15-J-045

**DEPARTMENT OF THE AIR FORCE
AIR UNIVERSITY**

AIR FORCE INSTITUTE OF TECHNOLOGY

Wright-Patterson Air Force Base, Ohio

DISTRIBUTION STATEMENT A.
APPROVED FOR PUBLIC RELEASE; DISTRIBUTION UNLIMITED.

The views expressed in this thesis are those of the author and do not reflect the official policy or position of the United States Air Force, Department of Defense, or the United States Government. This material is declared a work of the U.S. Government and is not subject to copyright protection in the United States.

AFIT-ENY-MS-15-J-045

EFFECT OF MIXTURE PRESSURE AND EQUIVALENCE RATIO ON
DETONATION CELL SIZE FOR HYDROGEN-AIR MIXTURES

THESIS

Presented to the Faculty

Department of Aeronautics and Astronautics

Graduate School of Engineering and Management

Air Force Institute of Technology

Air University

Air Education and Training Command

In Partial Fulfillment of the Requirements for the
Degree of Master of Science in Aeronautical Engineering

Curtis A. Babbie, BS

Captain, USAF

June 2015

DISTRIBUTION STATEMENT A.
APPROVED FOR PUBLIC RELEASE; DISTRIBUTION UNLIMITED.

AFIT-ENY-MS-15-J-045

EFFECT OF MIXTURE PRESSURE AND EQUIVALENCE RATIO ON
DETONATION CELL SIZE FOR HYDROGEN-AIR MIXTURES

Curtis A. Babbie, BS

Captain, USAF

Committee Membership:

Dr. Paul I. King
Chair

Dr. Marc Polanka
Member

Dr. Fred Schauer
Member

Abstract

Cell sizes of fuel and oxidizer combinations are the fundamental length scale of detonations. The detonation cell size is correlated to dynamic detonation properties. One of the properties, detonability is the motivation for this research. In order to design combustion chambers for detonating engines, specifically PDEs and RDEs, the cell size is needed. Higher than atmospheric mixture pressure detonation cell sizes are important for scaling the combustion chambers, and before this research no data existed for hydrogen and air detonation cell sizes at mixture pressures up to 10.0 atm. This research successfully validated a new detonation cell size measurement technique and measured 15 cases for varying mixture pressures up to 10 atm and equivalence ratios. The results were concurrent with previous trends, as increase in mixture pressure decreased detonation cell size and a decrease in equivalence ratio from stoichiometric increased detonation cell size. The experimental results were used to establish a correlation that estimates hydrogen and air detonation cell size given initial mixture pressure and equivalence ratio. The 15 new data points will be added to the detonation database for future experiments involving detonations.

Acknowledgments

I would like to express my sincere appreciation to my faculty advisor, Dr. Paul I. King, for his guidance and support throughout the course of this thesis effort. The insight and experience was certainly appreciated. I would, also, like to thank my sponsor, Dr. Fred Schauer, from the Air Force Research Laboratory for both the support and latitude provided to me in this endeavor. Last and most importantly, I would like to thank my wife. Without her love and support over the last year and a half I would not have been able to accomplish what I have.

Curtis A. Babbie

Table of Contents

	Page
Abstract	iv
Table of Contents	vi
List of Figures	viii
Nomenclature	xii
List of Abbreviations	xiii
I. Introduction	1
General Issue	1
Research Objectives	2
Methodology.....	3
Assumptions/Limitations.....	4
II. Literature Review	5
Chapter Overview.....	5
Background.....	5
Previous Research	12
Summary.....	32
III. Methodology	33
Chapter Overview.....	33
Experimental Methods.....	33
Analysis Method.....	43
IV. Analysis and Results.....	51
Chapter Overview.....	51
Results	51
Investigative Questions Answered	58

Summary.....	59
V. Conclusions and Recommendations	60
Chapter Overview.....	60
Conclusions of Research	60
Significance of Research.....	62
Recommendations for Future Research.....	63
Summary.....	63
Appendix A - Previous Research Data	64
Appendix B - Raw Schlieren Images.....	71
Appendix C - Results by Equivalence Ratio and Pressure	102
Bibliography	112

List of Figures

	Page
Figure 1. Detonation triple point (Ciccarelli et al., 1994).....	6
Figure 2. Single detonation cell (Ciccarelli et al., 1994)	7
Figure 3. Multiple cells with detonation front (Ciccarelli et al., 1997)	8
Figure 4. RDE dimensions	11
Figure 5. Open air detonation tube (Guirao et al., 1982).....	14
Figure 6. Soot foil trace (Moen et al., 1982).....	15
Figure 7. Soot trace end cap (Stevens et al., 2014).....	19
Figure 8. Dominant mode method (Moen et al., 1982)	20
Figure 9. Cell size vs. equivalence ratio (temperature range 277K to 650K) (Ciccarelli et al., 1994, Ciccarelli et al., 1997, Guirao et al., 1982, Stamps et al., 1991, and Tieszen et al., 1987).....	24
Figure 10. Cell size vs. equivalence ratio (temperature range 277K to 373K) (Ciccarelli et al., 1994, Ciccarelli et al., 1997, Guirao et al., 1982, Stamps et al., 1991, and Tieszen et al., 1987).....	25
Figure 11. Cell size vs. mixture pressure (Ciccarelli et al., 1994, Ciccarelli et al., 1997, Guirao et al., 1982, Stamps et al., 1991, and Tieszen et al., 1987)	27
Figure 12. Cell size vs. mixture pressure with varying curve fits (Ciccarelli et al., 1994, Ciccarelli et al., 1997, Guirao et al., 1982, Stamps et al., 1991, and Tieszen et al., 1987)	29
Figure 13. Cell size vs. mixture pressure predictions with experimental data (Stamps et al., 1991)	32

Figure 14. High pressure detonation tube	34
Figure 15. Detonation tube viewing section	34
Figure 16. Detonation tube viewing section cross section.....	35
Figure 17. High pressure detonation tube exterior schematic.....	36
Figure 18. High pressure detonation tube cut-away schematic	37
Figure 19. Detonation tube and optics configuration.....	38
Figure 20. Hydrogen and oxygen detonation critical initial pressure versus critical tube diameter (Matsui and Lee, 1979)	40
Figure 21. Test matrix.....	42
Figure 22. Raw schlieren images of detonation at 1.0 atm and 1.0 equivalence ratio.....	43
Figure 23. Detonation triple point movement.....	45
Figure 24. Schlieren image of hydrogen and air detonation ($P = 4.0$ atm, $\Phi = 1.0$).....	46
Figure 25. Schlieren image of hydrogen and air detonation transverse shocks annotated (P $= 4.0$ atm, $\Phi = 1.0$).....	47
Figure 26. Figure 27. Schlieren image of hydrogen and air detonation with transverse shocks annotated ($P = 4.0$ atm, $\Phi = 1.0$)	48
Figure 28. Hydrogen-air detonation raw image and processed image comparison ($P = 4.0$ atm, $\Phi = 1.00$)	48
Figure 30. Hydrogen/air detonation cell size vs mixture pressure by equivalence ratio ..	54
Figure 31. Hydrogen/air detonation cell size vs equivalence ratio by mixture pressure ..	55
Figure 31. Hydrogen-air detonation cell size vs equivalence ratio, experimental data with model overlay.....	58

Figure C - 1. Hydrogen/air detonation cell size vs mixture pressure (P=1.0-4.0 atm, $\Phi=1.00$)	103
Figure C - 2. Hydrogen/air detonation cell size vs mixture pressure (P=2.0-10.0 atm, $\Phi=0.80$)	104
Figure C - 3. Hydrogen/air detonation cell size vs mixture pressure (P=4.0-10.0 atm, $\Phi=0.70$)	105
Figure C - 4. Hydrogen/air detonation cell size vs mixture pressure (P=6.0-10.0 atm, $\Phi=0.65$)	106
Figure C - 5. Hydrogen/air detonation cell size vs equivalence ratio (P=2.0 atm, $\Phi=0.80$ - 1.00)	107
Figure C - 6. Hydrogen/air detonation cell size vs equivalence ratio (P=4.0 atm, $\Phi=0.70$ - 1.00)	108
Figure C - 7. Hydrogen/air detonation cell size vs equivalence ratio (P=6.0 atm, $\Phi=0.65$ - 0.80)	109
Figure C - 8. Hydrogen/air detonation cell size vs equivalence ratio (P=8.0 atm, $\Phi=0.65$ - 0.80)	110
Figure C - 9. Hydrogen/air detonation cell size vs equivalence ratio (P=10.0 atm, $\Phi=0.65$ - 0.80)	111

List of Tables

	Page
Table 1. Pressure and equivalence ratios	42
Table 2. Summary of results	52
Table 3. Error results.....	56
Table A - 1. Detonation data, Ciccarelli et al., 1994	64
Table A - 2. Detonation data, Ciccarelli et al., 1997	66
Table A - 3. Detonation data, Guirao et al., 1982.....	67
Table A - 4. Detonation data, Stamps et al., 1991	68
Table A - 5. Detonation data, Tieszen et al., 1987.....	69

Nomenclature

atm	atmospheres
cm	centimeters
dpi	dots per inch
fps	frames per second
ID	inside diameter
λ	cell size (mm, cm)
m	meters
mJ	millijoule
mm	millimeters
n	sample size
N/A	not available
Φ	equivalence ratio
P	pressure (torr, atm)
P_i	initial pressure (torr, atm)
psia	absolute pounds per square inch
R^2	R-squared, goodness of fit
s	sample standard deviation
s^2	sample variance
\bar{x}	sample mean

List of Abbreviations

AFIT	Air Force Institute of Technology
DDT	Deflagration to Detonation
MAPE	Mean Absolute Percent Error
PDE	Pulsed Detonation Engine
RDE	Rotating Detonation Engine
ZND	Zel'dovich von Neumann Döring

EFFECT OF MIXTURE PRESSURE AND EQUIVALENCE RATIO ON DETONATION CELL SIZE FOR HYDROGEN-AIR MIXTURES

I. Introduction

General Issue

Pressure gain combustors have the potential to replace traditional combustions systems in gas turbine engines (Tellefsen et al., 2012). There is ongoing research into pressure gain combustion systems, specifically RDEs, as standalone systems. At this point, pressure gain combustion has not been fully incorporated into turbine engines. In order to fully integrate RDEs into turbine engines, RDEs must be able to function using pressures from high pressure compressors. At a turbine jet engine design point altitude of approximately 30k ft, the inlet pressure is approximately 0.31 atm. Current jet engines in aircraft have compressor pressure ratios of 30 and above (Millhouse et al., 2000). In an RDE were to replace a traditional combustor, the RDE at 30k ft would have an input pressure of approximately ten atm or higher. However, current RDE testing has not been accomplished with input pressures at or above 10 atm (DeBarmore et al., 2013).

RDEs are sized based on the cell size of a detonation of the fuel and oxidizer mixture. RDEs have three major design dimensions, the internal channel width, length, and height, where the channel length is the circumference of the RDE and channel height is measured perpendicular to the circumference. Two of the RDE dimensions are of interest to cell size, channel length and channel height. Detonations can propagate into two dimensional areas where the third dimension is less than the size of one detonation cell; however, the other two dimensions must be larger than a cell width (Lee, 2008).

The internal channel width of an RDE can be less than the size of the detonation cell, and the detonation will continue without transitioning into a deflagration. However, the channel length and channel height must be greater than the cell size to sustain a detonation.

In order to size RDEs correctly, the cell size of the detonation must be known. In order to replace traditional combustors with RDEs, testing and design of RDEs are necessary at pressures equal to post-compressor pressures greater than 2.5 atm. Currently, there is no data available for cell sizes of non-diluted fuel and air mixtures at mixture pressures greater than 2.5 atm.

There are measurements of detonation cell sizes for a variety of fuels, oxidizers, and equivalency ratios at atmospheric pressures. As the mixture pressure is raised, the amount of data decreases (Kaneshige, and Shepherd, 1997). There are data points for mixtures at elevated mixture pressures where oxygen is used as an oxidizer (Kaneshige, and Shepherd, 1997). However, turbine engines will inevitably use air as an oxidizer. The difference in oxidizer will increase the cell size. There is also data for detonation cell sizes at elevated pressures with air as an oxidizer, but with diluents added (Shepherd, 1985). The diluents were added to increase the cell size for ease of measurements. There are known empirical formulas that show how much the diluent affects the cell size, but correlations are not substitutes for actual data.

Research Objectives

This research started with the measurement of hydrogen and air at atmospheric pressure to establish validity of the measurement technique used in this research. The

measurements were compared to historic data to establish a baseline. The mixture pressure was increased to 2.0, 4.0, 6.0, 8.0, and 10.0 atm. The equivalence ratio was decreased from 1.00 to 0.65 incrementally. The main goal of this research was to measure hydrogen and air detonation cell size at 10 atm.

After 10 atm was reached, other variations of mixture pressure and equivalence ratio were tested. The range of mixture pressures and equivalence ratios were used to make an algorithm to predict hydrogen and air detonation cell sizes in the range of mixture pressures and equivalence ratios tested.

This research developed a baseline method to measurement hydrogen and air mixtures at up to 10 atm. The same method is being used to measure propane and air detonation cell sizes. Eventually, methane and air and JP-8/10 and air mixtures will be detonated and measured using the techniques found in the current research to fulfill the need for data in the 10 atm mixture pressure regime.

Methodology

The experimental methods in this research included a detonation tube and an optics configuration. A detonation was started inside the detonation tube through a deflagration to detonation transition device. The detonation travelled through the tube with an inside diameter of 66.64 mm, through a viewing section with fused silica glass on two sides. The optics configuration then took images of the front of the detonation at the center of the cross section. The optics configuration consisted of: an extended light source, two parabolic mirrors, two flat mirrors, a knife-edge cut-off, and a high speed camera.

The images were used to measure the cell width of the hydrogen and air detonations at varying equivalence ratios and mixture pressures. The cell boundaries were determined by finding triple points at the detonation front, or, where the triple points were not visible, the transverse shock waves were used at the cell boundaries. There are two transverse shock waves for each detonation cell. In order to find the average cell size, the height of each image was divided by half the number of transverse shocks plus one. One more was added because the transverse shocks did not follow the exact edge of the window allowing for one more cell to be present.

Assumptions/Limitations

Experimental research in the detonation field is not exact due to the inherent irregular nature of detonations. This research captures attributes of detonations in such a way as to minimize the noise and irregularity in detonations. Though there are controls to help the consistency of the detonations, the data shows that detonation measurements are noisy and vary even within the same test.

II. Literature Review

Chapter Overview

The purpose of this chapter is to discuss what detonation cell size is and its importance. In order to develop an appreciation for detonation cell size, a brief definition of detonations is given followed by an in depth discussion of what a detonation cell is and how it can be measured. Photographs and diagrams of detonations and detonation cells are shown to support a complete understanding of the foundation of this research.

Further, this chapter will discuss previous research methods and the results obtained. The previous results are analyzed to show trends in the data that were used in the research for this paper. The previous research trends and data will be used to compare to the current research in Chapter V. The relevance and motivation of cell size to the current research is discussed.

Background

Definition of a detonation

A self-sustaining detonation is a wave consisting of a shock coupled with a deflagrating reaction zone (Ciccarelli et al., 1997). The shock wave adiabatically compresses the mixture, which quickly increases the temperature and pressure, allowing the reaction to occur more quickly than a deflagration alone. A detonation consists of an incident shock, transverse waves, and Mach stems (Ciccarelli et al, 1994). Transverse waves continually collide creating Mach stems and propel the incident shock forward and continuing the process until the reactants are no longer available or the mixture has reached the detonability limits due to the geometry of the vessel (Tieszen et al., 1987).

The Zel'dovich von Neumann Döring (ZND) model was once used to characterize detonations, but a detonation is not a simple planar wave with a reaction behind it. They are complex irregular transverse shocks that create Mach stems and triple points in varying patterns.

Definition of cell size

Detonation cell size is a fundamental physical characteristic of detonation waves. The cell size can refer to the length or width of a detonation cell. This research only measured the cell width, which will later be shown to be a more useful characteristic. A detonation cell is defined by its boundaries. The boundaries of a detonation cell fall at the triple point paths (Lee, 2008). A triple point is a point on the detonation front where the incident shock, Mach stem, and transverse shock wave intersect. Figure 1 shows a close up of the three components of a triple point. The trajectory shown in Figure 1 demonstrates the path the triple point takes while the detonation is moving.

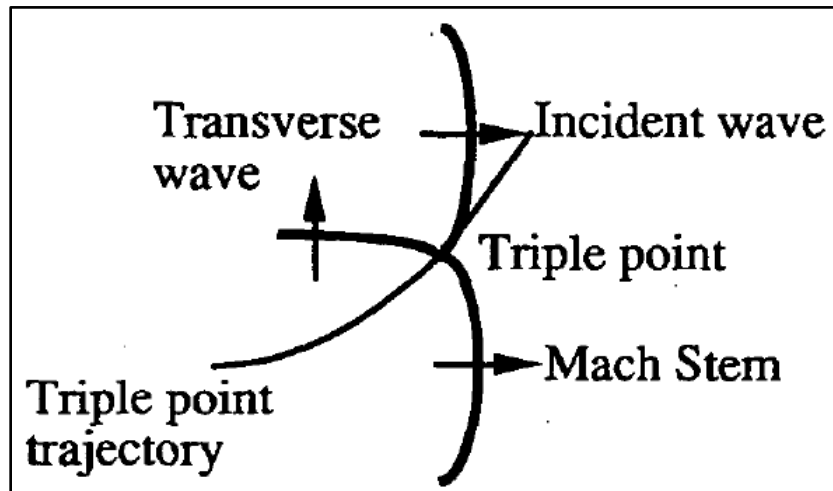


Figure 1. Detonation triple point (Ciccarelli et al., 1994)

When two triple point paths cross, the four outside boundaries of a detonation cell are formed. The triple point paths give the detonation cell a diamond shape or commonly referenced as a fish scale. Denisov was the first to discover the cell pattern and it has been called the fish scale pattern since (Denisov, 1960). Figure 2 shows a singular detonation cell.

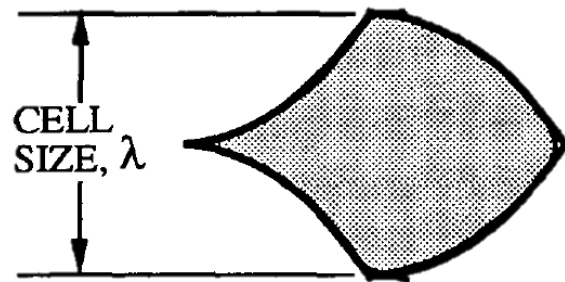


Figure 2. Single detonation cell (Ciccarelli et al., 1994)

In a detonation there is more than one cell. The number of cells depends upon the fuel and oxidizer combusting, whether diluents are added, mixture temperature, mixture stoichiometry, geometry of the facility, and mixture pressure in the facility (Lee, 1984). Adding diluents or changing the equivalence ratio from 1.0 increases detonation cell size (Ciccarelli et al, 1994). Increasing mixture pressure or temperature decreases detonation cell size (Tieszen et al., 1987). Figure 3 shows multiple cells within an arbitrary detonation. The cells are generally not of equal size and are referenced by the average cell size.

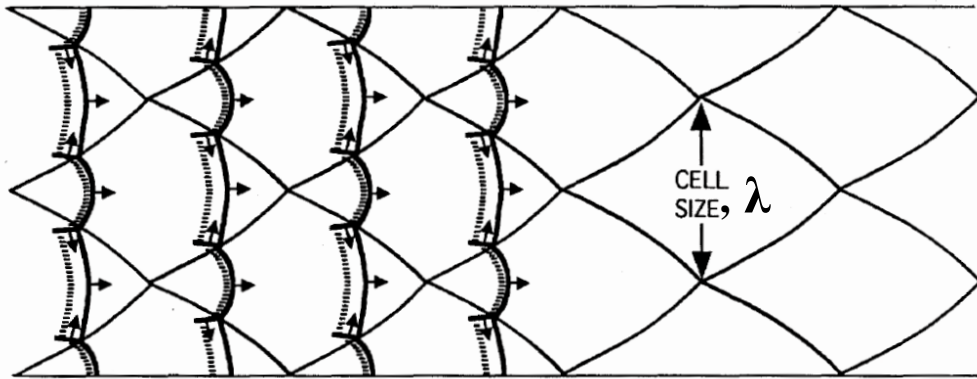


Figure 3. Multiple cells with detonation front (Ciccarelli et al., 1997)

Importance of cell size

Detonation cell size is the fundamental length scale of detonations (Tieszen et al., 1986). The cell size is correlated with other dynamic properties of detonations (Lee, 1984). These dynamic properties are detonation initiation energy, transmission, and propagation (Lee, 1977). The dynamic detonation properties are all based on cell size and detonation sensitivity, which is why the cell size has also been referred to as the sensitivity of a detonation. Detonation sensitivity has been shown to be inversely proportional to the cell size (Ciccarelli et al., 1997).

Detonation initiation energy is the minimum energy required to start a detonation in a gas mixture (Ciccarelli et al., 1994). The initiation energy has been shown through empirical correlations to be proportional to the cube of the detonation cell size (Lee, 1977). If the cell size were known, the minimum energy to start a detonation could be used, which would allow for a safer design. Often times in testing, a high-explosive was used to initiate a detonation inside a facility. They did not want to use more high-explosive than was required.

Detonation transmission refers to a detonation's ability to continue from one geometry to another. The most used geometry is the critical tube diameter referring to the minimum diameter a tube can be and allow a detonation to continue detonating into an unconfined environment (Tieszen et al., 1987). A correlation was found by Mitrofanov and Soloukhin that the critical tube diameter is approximately 13 times the detonation cell size (Mitrofanov and Soloukhin, 1965). This relation was further tested and verified by Moen et al., 1980.

Detonation cell size is most important for this research due to its correlation with detonability or detonability limits. A vessel must contain the correct geometry in order to allow a certain number of cells to form within (Dupre et al., 1985). The exact number of cells required is different for each geometry and fuel-oxidizer combination, the absolute minimum being one cell in height. If the internal height of a vessel is not at least as large as one detonation cell, at most a deflagration will occur but will not transition to a detonation. It was once thought that the detonability of a mixture was based only on the equivalence ratio. This was found to be only partially true, and in fact, the detonability was found to be based on the geometry of the vessel (Tieszen et al., 1987). The detonation cell size allows designers to build vessels that are no larger in cross-sectional height than needed to allow a detonation to propagate.

The detonation dynamic properties have made the detonation cell size the fundamental length scale for detonations. The cell size is also important in the reaction zone length behind the detonation. The reaction zone length is directly proportional to the speed of the detonation (Shepherd, 1986). The reaction zone length is important because it drives the detonation speed and sensitivity (Shepherd, 1986). The cell size is

equal to an empirically derived constant times the reaction zone length (Schelkin and Troshin, 1965). This relationship can help calculate the speed of the detonation wave. Detonation waves are not constant velocity waves because of the changing reaction zone. The detonation velocity can range from 0.6 to 1.6 times the Chapman Jouguet (CJ) velocity, where the CJ velocity is the velocity where the reaction zone reaches sonic velocity compared to the leading shock velocity (Shepherd, 1986). As the detonation starts to decay, the reaction zone lengthens and pushes the transverse waves which further accelerate the detonation wave (Shepherd, 1986). Therefore, the wave speed is closely tied to the reaction zone length and transverse wave motion, and the transverse wave motion is what creates the detonation cell boundaries.

The main motivation of this research was to find cell size for the use of detonability limits inside of RDEs. An RDE geometry design will be based on the cell size of the detonation it contains. Two of the three RDE channel dimensions are critical for detonations, the channel height and circumference. The circumference can be indefinite in size, but the minimum circumference is necessary for detonation propagation. The minimum circumference is related to the detonation cell length, however, the current research only measures cell width. Therefore, the current research is only concerned with RDE height. Figure 4 shows the three dimensions of the channel in an RDE. There is ongoing research to find the minimum channel height of an RDE, but channel height cannot be less than one cell in order for a detonation to propagate (Lee, 1984).

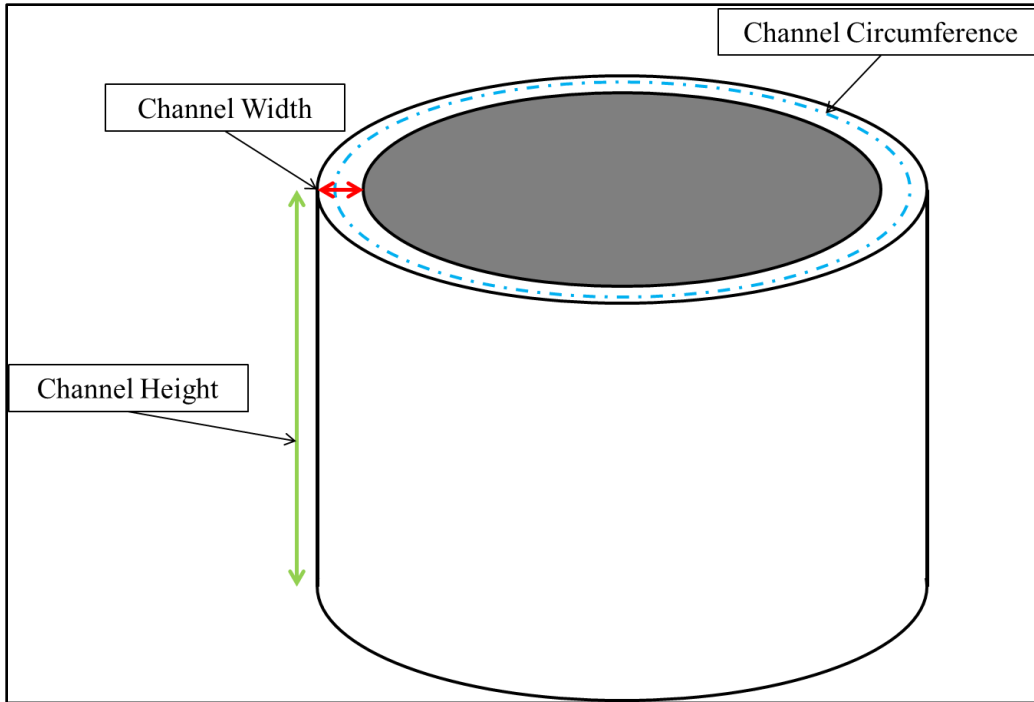


Figure 4. RDE dimensions

The RDE channel width is not a factor because detonations can propagate where the cell thickness is less than one cell. According to Lee, a detonation can propagate in a narrow channel where it is approximated by a two-dimensional model (Lee, 2008). However, the circumference must be larger than one cell length and height of the channel must be larger than one cell width. The actual dimensions will be different for each mixture used.

One goal for RDEs is to replace traditional deflagrating combustors in jet engines with an RDE. The combustor sits behind a compressor that can compress incoming air to 30 times the inlet pressure. At a design point altitude of about 30k feet, an inlet pressure would be approximately 0.3 atm. This would yield a combustor intake air pressure near ten atmospheres. For this reason, it would be advantageous to design an RDE combustor

for intake pressures in the ten atmosphere range. In order to design the RDE the cell size must be known at that pressure, but no cell size data for hydrogen and air detonations has been tested. Data for hydrogen and air detonations at less than one atmosphere is numerous (Ciccarelli et al., 1994, Ciccarelli et al., 1997, Guirao et al., 1982, Stamps et al., 1991, and Tieszen et al., 1987). There is also data for hydrogen and air detonations above one atmosphere, but the greatest mixture pressure used was approximately three atmospheres (Stamps et al., 1991, and Tieszen et al., 1987). The current research is an effort to fill the data gap for hydrogen and air detonation cell size for mixture pressures from one to ten atmospheres.

Previous Research

Previous research overview.

There have been other organizations and people measuring hydrogen and air detonation cell size since the 1960s. One of the forerunners of hydrogen and air detonation cell size was Sandia National Laboratories (SNL) and the associated universities who worked with SNL. The most common purpose to measure cell size in previous research was for nuclear reactors (Ciccarelli et al, 1994, Ciccarelli et al, 1997, Stamps et al., 1991, Tieszen et al., 1986, Tieszen et al., 1987, and Guirao et al., 1982). The reactors were dissipating hydrogen into the air in an enclosed facility which allowed conditions for a detonation to occur (Tieszen et al., 1987). One of the most well-known examples is the 3-mile Island incident. Though it was not proven whether a detonation actually took place, it is known that the hydrogen in the air at least deflagrated and created catastrophic failure. The reason for the SNL research in measuring hydrogen and

air detonation cell size was to find out how to prevent the mixture from detonating inside the nuclear reactor facilities (Cicarelli et al., 1994). If the cell size is large enough for a given geometry, a detonation cannot occur. The SNL research found that by adding steam to the mixture, the cell size was increased to render it safe from detonations (Cicarelli et al., 1994).

Previous experimental methods.

In the past, hydrogen and air detonation cell sizes have been measured through different techniques and tools. Most of the techniques included diluting the mixture with argon, helium, or steam which increase the cell size, but the current research is focused on measuring detonation cell size in a non-diluted mixture to keep in line with an operational purpose. To keep an aircraft as light as possible detonations would occur without the extra weight of onboard diluents in pressured vessels. Previous research was more concerned with avoiding ground detonations inside of nuclear reactors where extra weight is not an issue.

The simplest experimental technique incorporated a detonation tube that was open to the outside atmosphere. A soot foil was placed in the tube to record the detonation cells. The soot foil was a piece of thin metal, often aluminum, with soot coating one surface. The soot foil was placed inside the tube as a cylindrical shape. The first use of a soot foil to record detonation cells was conducted by Denisov and Troshin, 1959. The triple point paths leave an etching into the soot foil as they pass by. The exact reason that the triple point paths leave a trace on the soot foil is not known, but it is believed to be related to the vortices in the shear layer that extends from the triple points (Cicarelli et al., 1997).

In the simpler experiments the mixture pressure only had the option of being one atmosphere, as it was not sealed. Figure 5 shows a picture of the experimental setup from McGill University (Guirao et al., 1982). In the figure the end is not closed allowing the detonation to continue to an unconfined space.

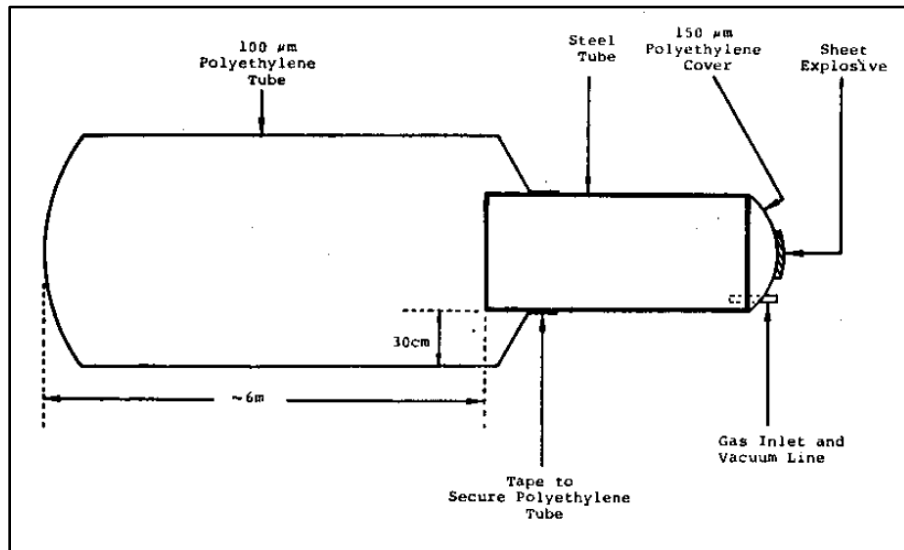


Figure 5. Open air detonation tube (Guirao et al., 1982)

The hydrogen and air gases were introduced through one end of the tube and ignited. The gases passed over a DDT device and became a detonation before approaching the exit of the tube. As the detonation passed through the tube, the higher density triple points removed soot from the foil. Figure 6 shows a picture of one of these soot foils. The traces along the soot foils effectively showed the outlines of detonation cells. These soot foils were then used to measure the cell sizes in the analysis.

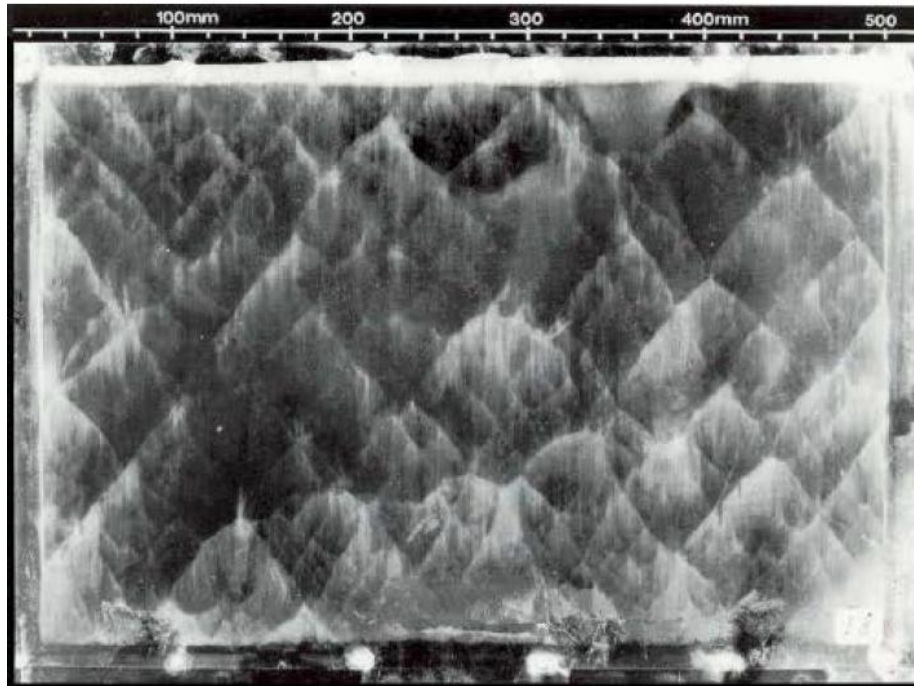


Figure 6. Soot foil trace (Moen et al., 1982)

The other dominant experimental setup mimicked a shock tube, with the exception that it contained a detonation. Brookhaven National Labs (BNL) built and tested several detonation tubes with hydrogen and air detonations. BNL's main detonation tubes were called the High-Temperature Combustion Facility (HTCF) and the Small-Scale Development Apparatus (SSDA) (Cicarelli et al., 1994 and (Cicarelli et al., 1997). SNL built and tested their Heated Detonation Tube (HDT) (Stamps et al., 1991). These differed from McGill University's in that they were sealed (Guirao et al., 1982).

Sandia's HDT was 0.43 m inside diameter and 13.1 m long (Stamps et al., 1991). It was enclosed on both ends to contain the detonation. They were able to heat the tube, change the equivalence ratio, and change the mixture pressure. Detonations were

initiated in their tube via direct initiation. This was composed of 110 g of DuPont Detasheet high-explosive. Direct initiation is the easiest to set off a detonation, but it has its drawbacks. A detonation requires a lot of energy to start and high-explosives contain the required energy in a simple to install package. However, high-explosives are unsafe and difficult to handle. A direct initiated detonation also will overdrive the detonation to a velocity faster than it would travel on its own. For this reason the tube had to be longer to allow the detonation to slow down to approximately its CJ velocity. At the end of the tube a 3.66 m soot foil was placed to record the detonation cells. Sandia's goal was to measure and predict hydrogen and air detonation cell size based on equivalence ratio, mixture temperature, and mixture pressure and to find the detonability limits with respect to equivalence ratio.

BNL's detonation tubes were similar to each other in setup, except the sizes were different (Cicarelli et al., 1994). The SSDA was an enclosed tube with an inside diameter of 0.10 m and a length of 6.1 m (Cicarelli et al., 1994). The HTCF was larger with an inside diameter of 0.27 m and a length of 21.3 m (Cicarelli et al., 1997). Both the SSDA and the HTCF had the ability to change the mixture temperature from 300 K to 650 K and the ability to change to mixture pressure from one atmosphere to just less than three atmospheres.

Before BNL designed their detonation tubes, it was common for detonation tubes to employ a gas driver initiation system (Cicarelli et al., 1994). The gas driver system worked by inserting a diaphragm between two gas mixtures and detonating a driver gas with less initial energy and letting the driver gas detonate the test gas. The driver gas was usually a mix of acetylene and oxygen or any other easily detonable mixture, and the test

gas could be any mixture for that test. The driver gas was easily detonated through a small exploding wire and detonated through the diaphragm, tearing it, and detonating the test gas. The gas driver initiation system was safer than using direct initiation and it would not allow the test gas to be overdriven. The main drawback to the gas driver initiation system was that the diaphragm had to be replaced after each test.

In order to save time from replacing the diaphragms, BNL designed a diaphragmless gas driver initiation system (Cicarelli et al., 1994). In their system, the driver gas was premixed in a separate container and injected quickly into one end of the detonation tube. At the instant the correct amount of gas was injected, a small exploding wire was ignited and started a detonation in the driver gas. In the same way as the diaphragm system, the diaphragmless system allowed the detonation to transfer from the driver gas to the test gas. In the diaphragm system, the diaphragm took some energy from the detonation, which was avoided in BNL's system. The drawback to the diaphragmless initiation system was that there existed a potential for the driver gas to mix with the test gas, but the time was so short and the tube was so long that BNL neglected any mixing effects. Both the SSDA and the HTCF employed soot foils to trace the detonation waves (Cicarelli et al., 1994, Ciccarelli et al., 1997).

The previous methods established for measuring detonation cell sizes worked well for each purpose. Most of the previous methods only included measuring cell sizes for mixture pressures less than one atmosphere, where some included limited data points less than three atmospheres. The current research required data points up to ten atmospheres; therefore, even though the previous methods worked for their purpose, they did not work

for elevated mixture pressures. The results from previous methods are discussed in the Previous results section.

More recently, an elevated mixture pressure setup has been tried using some of the previous methods (Stevens et al., 2014). This method included using a smaller detonation tube. The largest difference with this method was that it was designed to start at higher than atmospheric pressure before the detonation occurred. The tube was filled with air and hydrogen and mixed with a fan. After which a detonation was started by a spark and a DDT device. The DDT device was a Shelkin spiral. This method of detonation initiation is the safest, but it can make initiation more difficult.

The high pressure detonation tube at first used a soot foil around the inside of the tube as the previous examples (Stevens et al., 2014). A major issue was that the detonations started at higher mixture pressures up to 4.0 atm and crushed the soot foils lining the side walls. The same detonation tube was again used with soot directly on the end cap instead of lining the side walls (Stevens et al., 2014). This method traced the plane perpendicular to travel of the detonation instead of the plane parallel to the detonation. This method worked for lower mixture pressures, but when the pressure was elevated, the soot was blown off of the end cap from the detonation. The end cap soot traces were also more difficult to see. A picture of one of the soot foils is shown in Figure 7. Figure 7 shows an example of the difficulty in seeing detonation cell boundaries on an end cap soot foil from previous research.



Figure 7. Soot trace end cap (Stevens et al., 2014)

Previous analysis methods.

Each of the previous methods incorporated different approaches to measure detonation cell size on soot foils or soot traces. The two primary methods to measure cell size used in most of the previous research were based on Moen et al., 1982. The first method is referred to as the single cell method. In this method many cells are measured all over the soot foil and then the average is taken of the cells. This method leaves much subjectivity in what counts as a cell. Moen et al. found that there seemed to be a substructure within the cells that made it difficult to distinguish what counted as a cell or what was a substructure.

The second method to measure detonation cells was referred to as the primary cell method or dominant cell method (Moen et al., 1982). This idea was based on the idea that detonations have multiple modes of length scales for cell sizes. There can be different size cells within cells called substructures. The dominant mode is the largest

length scale. The dominant mode is observed on soot foils generally by looking for the darkest lines of cell boundaries. Figure 8 shows the dark lines as the primary modes. The cells were counted between two parallel lines and divided by the length of the lines. In Figure 8, the highlighted cells would be counted. The dominant cell method was used by Tieszen et al, 1994, Ciccarelli et al., 1997, Stamps et al., 1991, and Guirao et al., 1982.

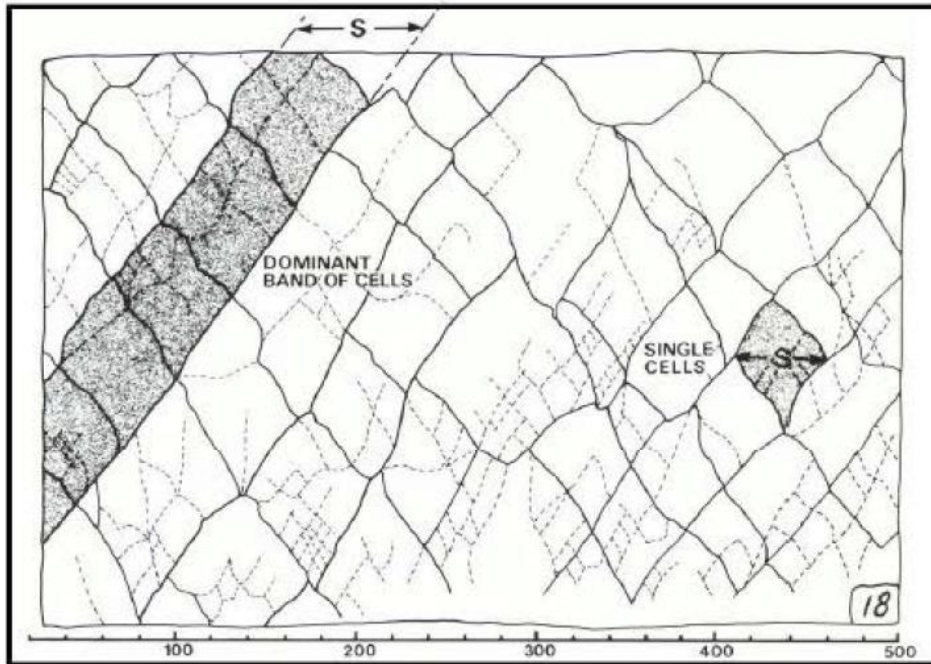


Figure 8. Dominant mode method (Moen et al., 1982)

There are some criticisms of the dominant mode measurement of cell size. Hydrogen and air detonations are generally irregular in cell structure which hampers the ability to distinguish the dominant cell structure from the substructure (Guirao et al., 1982). Moen et al., 1984 even later questioned whether there was a single dominant mode or if there was a range of widths for each mixture, which would render a cell size point estimate useless and bring about a need for a range of cell sizes where the maximum cell size may be more important. Stamps et al., 1991 admitted that there was

subjectivity in distinguishing the cell boundaries and the end number was heavily influenced by human error. Though the dominant mode method is subjective, it is still the most reliable method to measure cell size.

More recent research has measured cells perpendicular to the detonation direction (Stevens et al., 2014). The cells were viewed from an end cap of a detonation tube. The triple points removed soot from a soot foil that the detonation reflected. The measurement was done using the outside boundary of the end cap. The cells were measured from the circumference of the end cap using the traced portions from the edge. A cell was counted by dividing the circumference of the end cap by the number of cell boundaries. There were not measurements taken; the research's objective was to explore new ways of measuring detonation cell size (Stevens et al., 2014).

In any method there is some subjectivity that causes uncertainty. According to Tieszen et al., 1987, measuring detonation cell size is more of an art than a science. And because there is subjectivity in the measurement, there is also subjectivity in the error bounds. Tieszen et al., 1987 placed a subjective 25 percent error on cell size measurements when comparing with other measurements within the report, and a 100 percent error on cell size measurements when comparing to cell sizes from other research. They found error bounds by forcing the measured points into the known relationship of the "U" shape in the graph of cell size versus equivalence. Prior to finding the error, each author measured the cells using the dominant cell method and were each assigned a subjective weight to their measurement based on their confidence in their work. Then the weighted average was used as the cell size point estimate. The

weighted average was made to fit the “U” shaped graph and then the error bars were subjectively selected.

Stamps et al., 1991 used their own error bound methods. Each author measured the detonation cell size independently and the average was taken. On average one author’s measurements were 1.16 times the size of the second author’s measurements (Stamps et al., 1991). They assumed the standard deviation was 0.13 times the measured cell size. They suggested that the true average detonation cell size was within 0.372 to 1.628 times the measured cell size. Stamps et al used an error of approximately 63 percent that came from a subjective standard deviation and a difference in each authors’ measurement of the same soot foil.

In other research, error bounds are ignored and only a point estimate is given. It is clear from previous research that cell measurements and error bounds are subjective in nature and relied on the authors’ ability to locate the dominant cells instead of substructures..

Previous results.

Previous research came to many of the same conclusions about the effects of mixture pressure, temperature, and equivalence ratio on cell size, but contained different data points. Previous results are shown in Figures 9 to 13, as well as in Tables A-1 to A-5. Data was obtained from all sources from Cal-Tech’s Detonation Database and refined, corrected, and added to in order use only data from hydrogen and air detonations without any diluents added (Ciccarelli et al., 1994, Ciccarelli et al., 1997, Guirao et al., 1982, Stamps et al., 1991, and Tieszen et al., 1987). The data ranged in mixture pressure from approximately 0.40 atmospheres to 3.00 atmospheres. Though not as important in this

research, the data incorporated mixture temperature from 300 K to 650 K. The data was used to show relationships of detonation cell size versus equivalence ratio and cell size versus mixture pressure.

The data in Figure 9 was compiled from various research experiments from BNL, SNL, and McGill University (Cicarelli et al., 1994, Ciccarelli et al., 1997, Guirao et al., 1982, Stamps et al., 1991, and Tieszen et al., 1987). Figure 9 shows hydrogen and air detonation cell size versus the equivalence ratio. The only data that was used was from mixture pressures ranging from 0.97 to 1.05 atmospheres. The temperatures also ranged from 277 K to 650 K. From various research it was hypothesized that the cell would be a minimum at a stoichiometric equivalence ratio and the cell size would increase with a deviation from stoichiometric. The data is spread out a little more due to the temperature range, but it still shows the hypothesized correlation. The data is also broken down into pressure ranges of: under one atmosphere, one to two atmospheres, and two to three atmospheres. From the graph it appears that the higher pressures have a lower minimum cell size than the lower pressures. It also appears each pressure range creates its own “U” correlation.

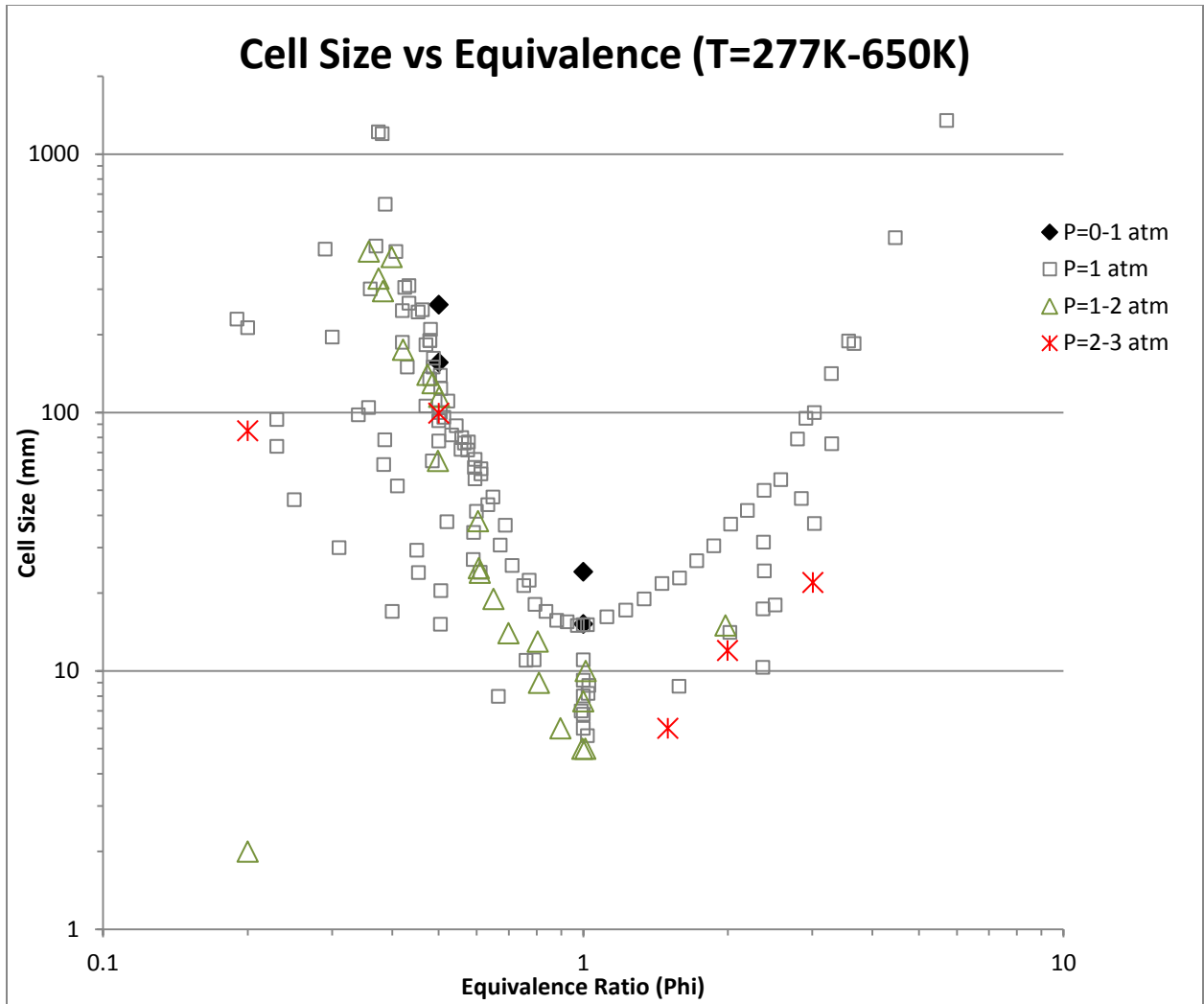
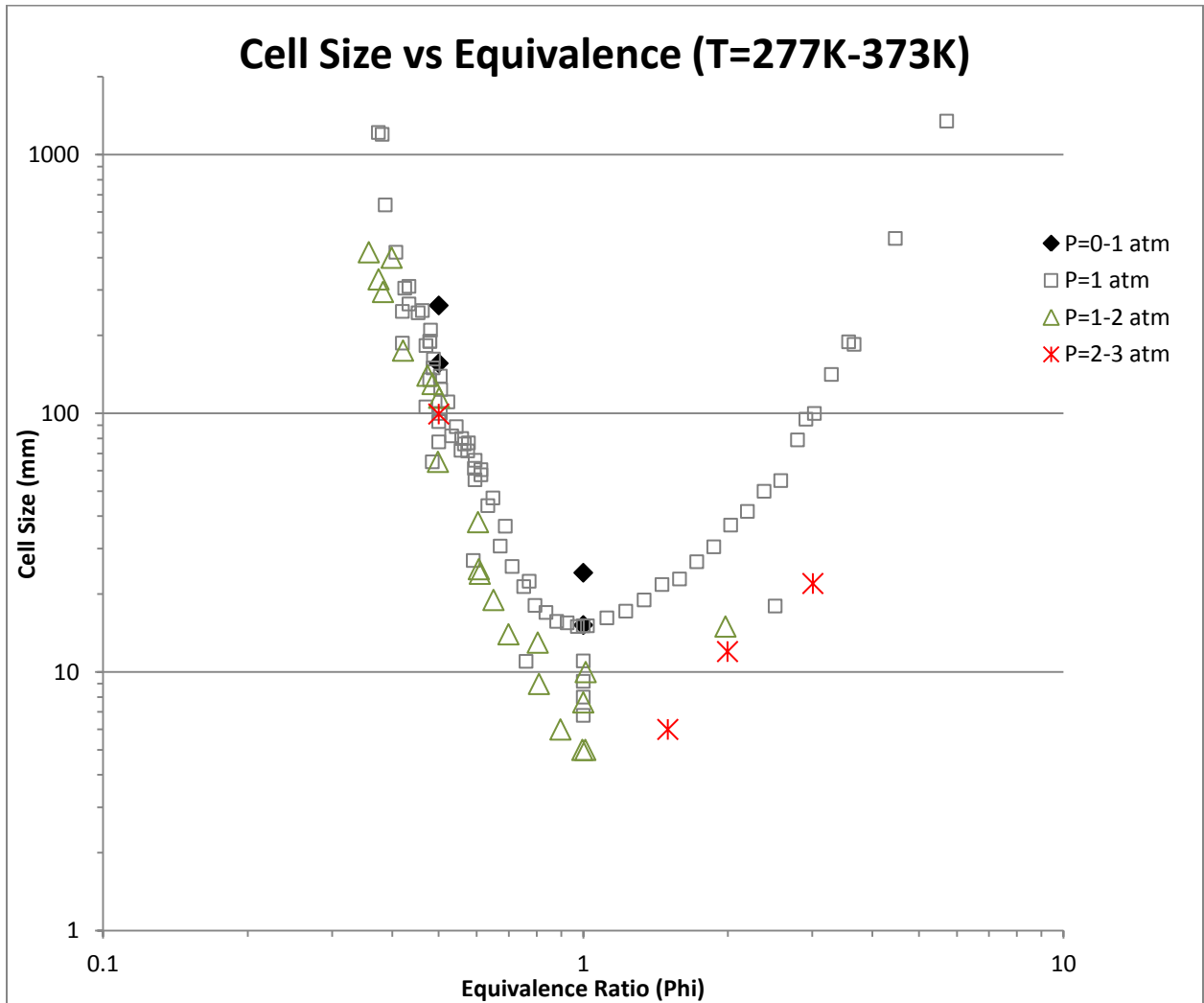


Figure 9. Cell size vs. equivalence ratio (temperature range 277K to 650K)
(Ciccarelli et al., 1994, Ciccarelli et al., 1997, Guirao et al., 1982, Stamps et al., 1991,
and Tieszen et al., 1987)

The same data from Figure 9 is shown in Figure 10 with the mixture temperature range restricted to 277 K to 373 K (Ciccarelli et al., 1994, Ciccarelli et al., 1997, Guirao et al., 1982, Stamps et al., 1991, and Tieszen et al., 1987). Without the temperatures above 373 K, the data is tighter and shows a more uniform shape, though there is less

data to show the curve fit. Equation 1 shows the curve fit for the left side of the data for equivalence ratios under 1.03 and mixture pressures less than 1.01 atm.

$$\lambda = 8.08x^{-4.07} \tag{1}$$



**Figure 10. Cell size vs. equivalence ratio (temperature range 277K to 373K)
(Ciccarelli et al., 1994, Ciccarelli et al., 1997, Guirao et al., 1982, Stamps et al., 1991,
and Tieszen et al., 1987)**

All data from Figure 9 and Figure 10 was also input into Figure 11 to show the effects of mixture pressure on hydrogen and air detonation cell size (Ciccarelli et al.,

1994, Ciccarelli et al., 1997, Guirao et al., 1982, Stamps et al., 1991, and Tieszen et al., 1987). Figure 11 shows hydrogen and air detonation cell size versus mixture pressure. The mixture pressures are divided into categories based on ranges of equivalence ratio with a trend line through them. The range of mixture temperatures is from 277 K to 373 K. Correlations were added to the data by equivalence ratio. The data is focused on 1.0 atm and is not consistent in the curve fits.

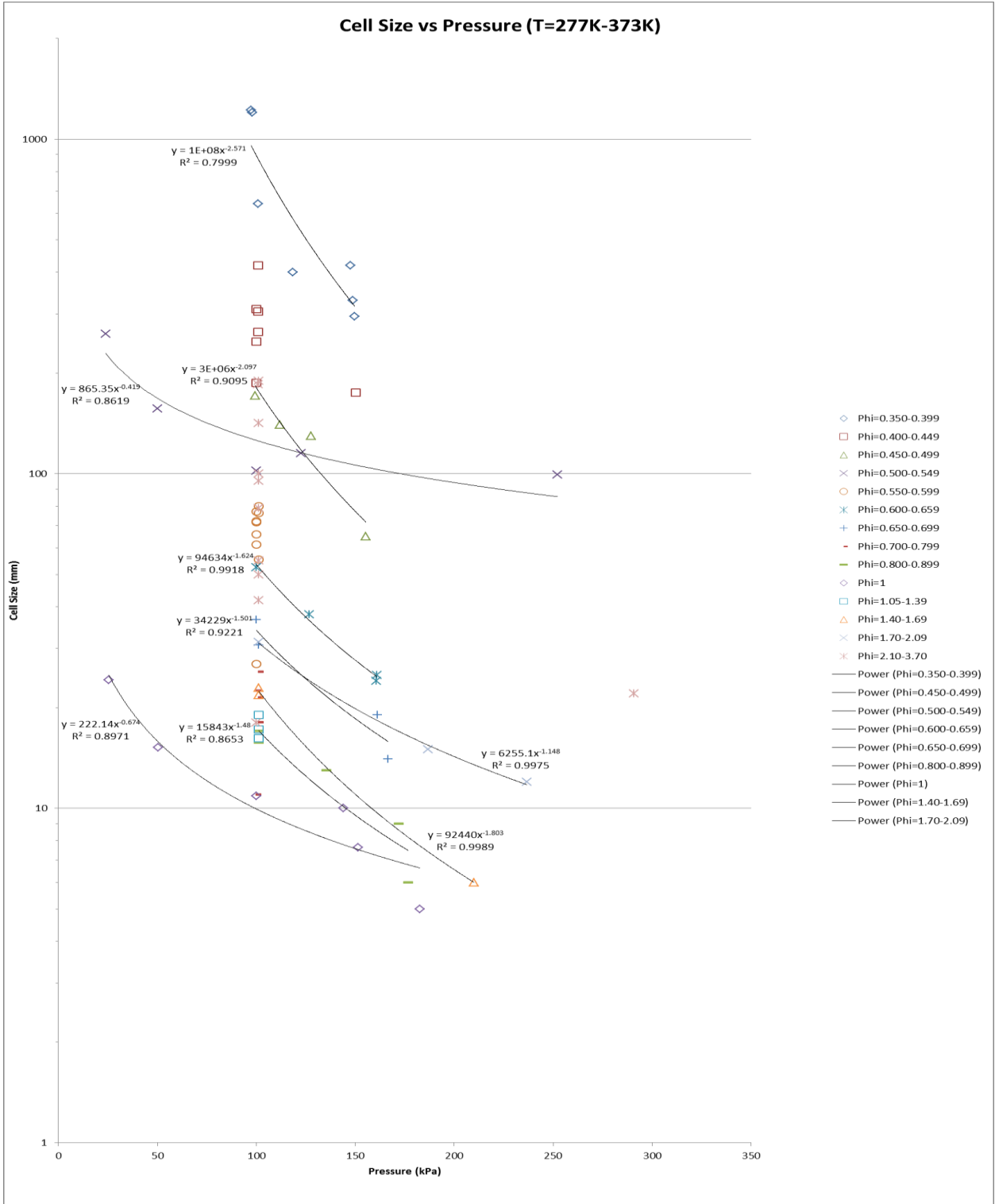


Figure 11. Cell size vs. mixture pressure (Ciccarelli et al., 1994, Ciccarelli et al., 1997, Guirao et al., 1982, Stamps et al., 1991, and Tieszen et al., 1987)

Figure 12 shows the same data as Figure 11 except pressure ranges with less than three data points has been removed for clarity (Ciccarelli et al., 1994, Ciccarelli et al., 1997, Guirao et al., 1982, Stamps et al., 1991, and Tieszen et al., 1987). The equivalence ratios where there are multiple data points have been averaged for trends and clarity. In both Figure 12 and Figure 11, it is evident that an increase in mixture pressure decreases the cell size. Each equivalence ratio range trend line has a different slope based on a power series curve fit added to the data. The exponent ranges from -0.5 to -2.4. The exponents do not appear to follow any trends when compared to changing equivalence ratios and mixture pressures. The range of exponents and the lack of a general trend shows that the previous results don't establish a clear baseline to make comparisons. The previous data trend fits do give a range to make generalized comparisons to the current research. There is not enough data to make any clear conclusions to a more exact empirical formula for all equivalence ratios for the previous data. The mixture pressures in Figure 11 and Figure 12 only reach just over 2.5 atmospheres. The slopes of the trend lines are unknown for mixture pressures greater than 2.5 atmospheres.

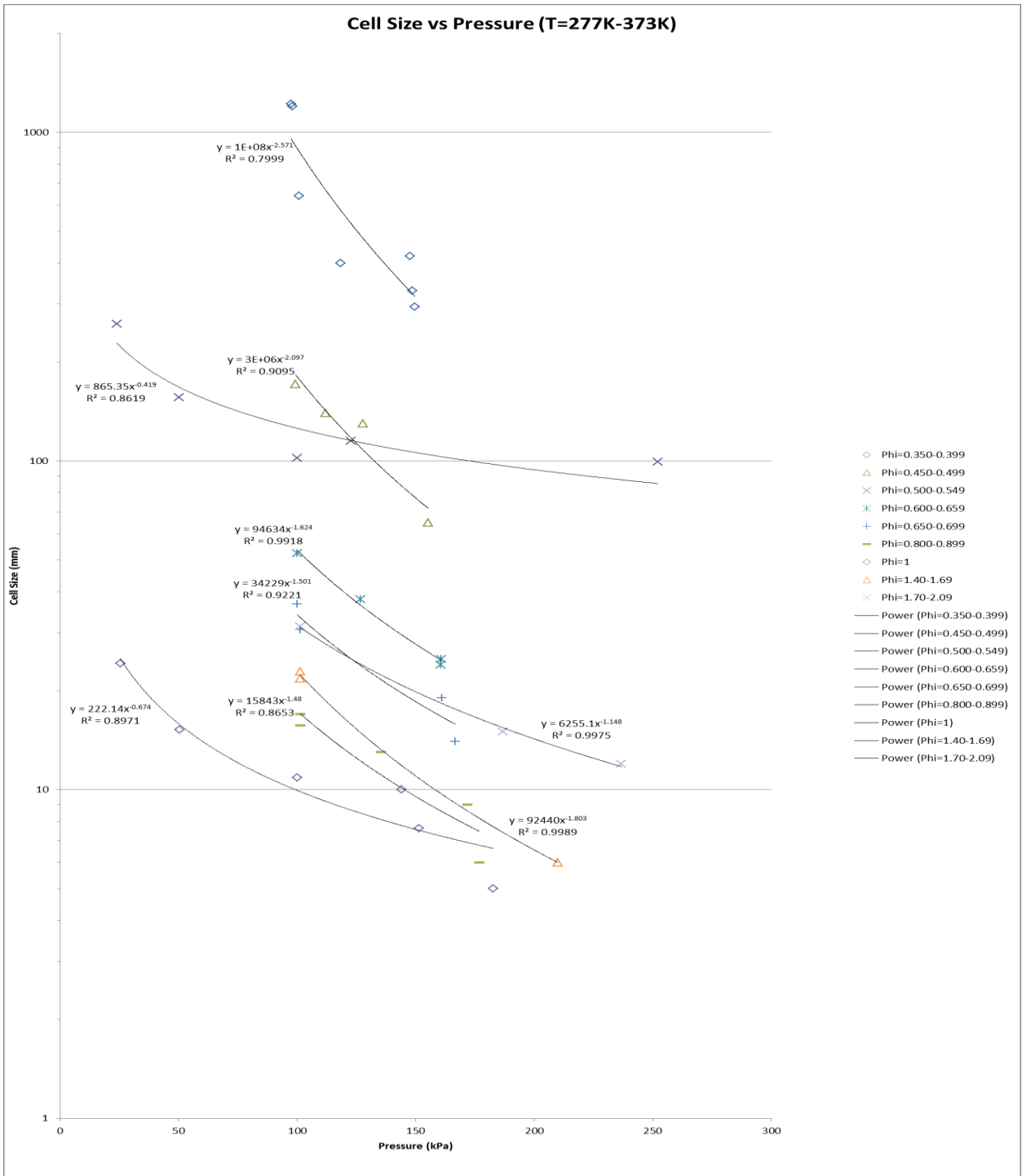


Figure 12. Cell size vs. mixture pressure with varying curve fits (Ciccarelli et al., 1994, Ciccarelli et al., 1997, Guirao et al., 1982, Stamps et al., 1991, and Tieszen et al., 1987)

All of the previous research as well as the analysis on the collective research agree on the overall trends of hydrogen and air detonation cell size compared to mixture conditions of pressure, temperature, and equivalence. It is agreed through experimentation that an increase in mixture temperature decreases the cell size (Ciccarelli et al., 1994, Ciccarelli et al., 1997, Guirao et al., 1982, Stamps et al., 1991, and Tieszen et al., 1987). The reasoning is that the increase in temperature increases the detonation sensitivity, and because detonation sensitivity and cell size are inversely correlated, the cell size decreases (Ciccarelli et al., 1994).

The previous research also agrees on the effect of changing the equivalence ratio on hydrogen and air detonation cell size. The cell size is minimized at stoichiometric conditions and increases with a change in equivalence in either direction (Ciccarelli et al., 1994, Ciccarelli et al., 1997, Guirao et al., 1982, Stamps et al., 1991, and Tieszen et al., 1987). The cell size gradient is greater when the equivalence ratio is less than one, than when the equivalence ratio is greater than one. The detonability limits of hydrogen and air due to stoichiometry were between equivalence ratios of 0.311 and 7.07 (Stamps, 1991).

The effect of a change in mixture pressure on hydrogen and air detonation cell size is the most important trend for the current research. In general it is agreed that an increase in mixture pressure is inversely related to cell size (Ciccarelli et al., 1994, Ciccarelli et al., 1997, Stamps et al., 1991, and Tieszen et al., 1987). However, the extent of the effect mixture pressure has on cell size is not. Ciccarelli et al. discussed the effect of a pressure change from 14.5 psi to 34.8 psi. They said the cell size was moderately affected by the change in mixture pressure, but the change in temperature had a much

larger effect on cell size (Ciccarelli et al., 1997). It is important to note that the pressure range they used is just over double the starting pressure. They did not gather enough data points to make clear quantifiable relationships to show how much mixture pressure and temperature independent of each other affected cell size (Ciccarelli et al., 1997).

Stamps et al. came to a similar conclusion that an increase in pressure did in general decrease the cell size, but with a local minimum (Stamps et al., 1991). They found that the cell size decreased by a factor of approximately two between the mixture pressures of 1.0 atmospheres and 3.0 atmospheres. Figure 13 shows a proprietary model Stamps et al. used to predict the cell size for a given pressure. They predicted that the cell size could have a local minimum depending on the equivalence ratio. Figure 13 shows four equivalence ratios predicted and two equivalence ratios tested. Stamps et al. predicted cell size for mixture pressures up to 3.0 atmospheres but only tested to about 2.5 atmospheres. There are only four and five data points for each equivalence ratio at a range of pressures from approximately 0.25 atm to 2.5 atm.

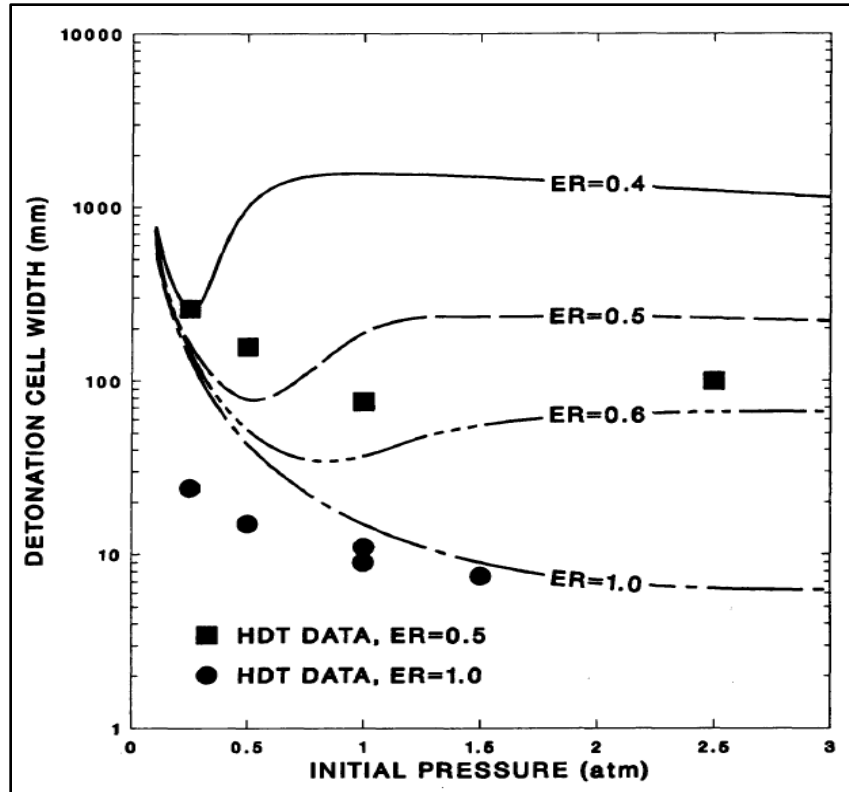


Figure 13. Cell size vs. mixture pressure predictions with experimental data (Stamps et al, 1991)

Summary

Detonation cell size is an important characteristic of detonations. It is the fundamental length scale that can be used to find other detonation properties. Detonation properties can be useful to designers for many reasons, but the most important reason for the current research is in helping design an RDE with the correct dimensions. Designers use cell size to determine the minimum circumference and length of an RDE that can sustain a detonation. There is much data available for hydrogen and air detonation cell size for mixture pressures less than three atmospheres, but until this research no data existed for mixture pressures between three and ten atmospheres.

III. Methodology

Chapter Overview

The purpose of this chapter is to explain the methods used to conduct the experiments and to analyze the data from the experiment. The experimental setup is similar to previous detonation tubes with differences in the optics section. The analysis methods use different techniques to measure detonation cells from the classic dominant mode of cell counting. With information on the setup and analysis, others should be able to replicate and improve upon the process in order to obtain more detonation cell size data for any gaseous mixture required.

Experimental Methods

Experimental Setup

The test and measurement system consisted of a high pressure detonation tube with a viewing section for the optical equipment. Figure 14 is a picture of the system. The high pressure tube is 4.42 m long and contains a viewing section 2.62 m from the right side of the highlighted detonation tube in Figure 14. The right end of the detonation tube contains an ignition system with a DDT device to transition the flame into a detonation before entering the viewing section. The tube has an internal diameter of 67 mm. The viewing section, shown in Figure 15, allows light to pass horizontally through 60 mm of Tosoh N grade quartz and then through the inside 47 mm passage width where the detonation passes. The window of the viewing section is 47.24 mm high and 101.6 mm long. This window allows for the observation of cells smaller than 47 mm.

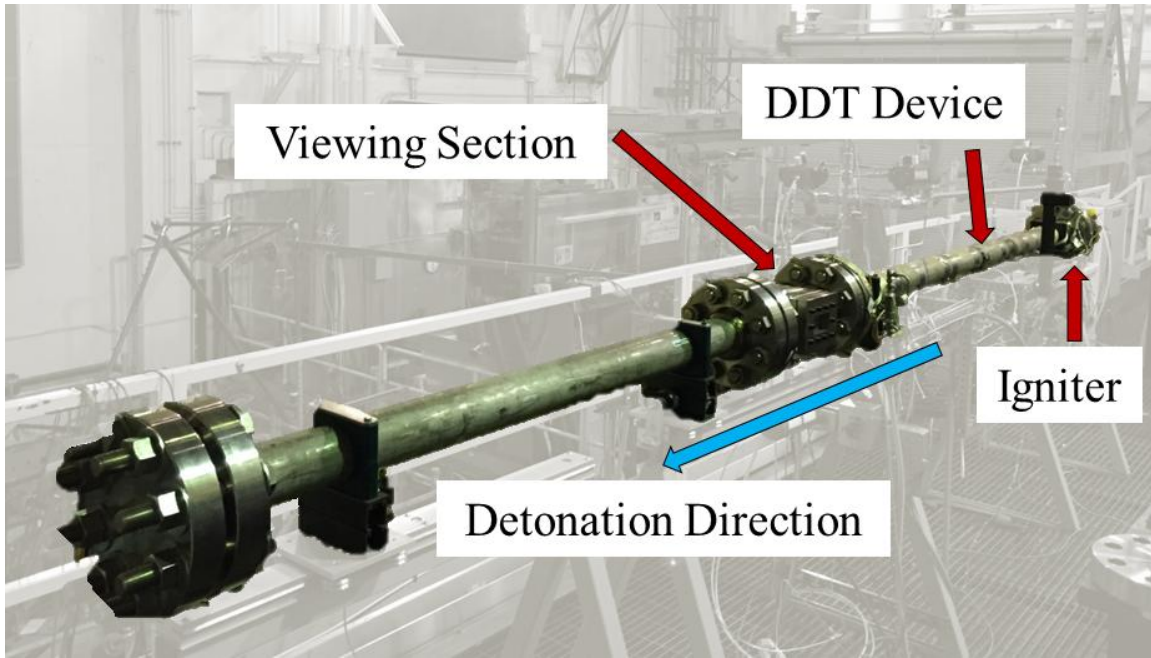


Figure 14. High pressure detonation tube

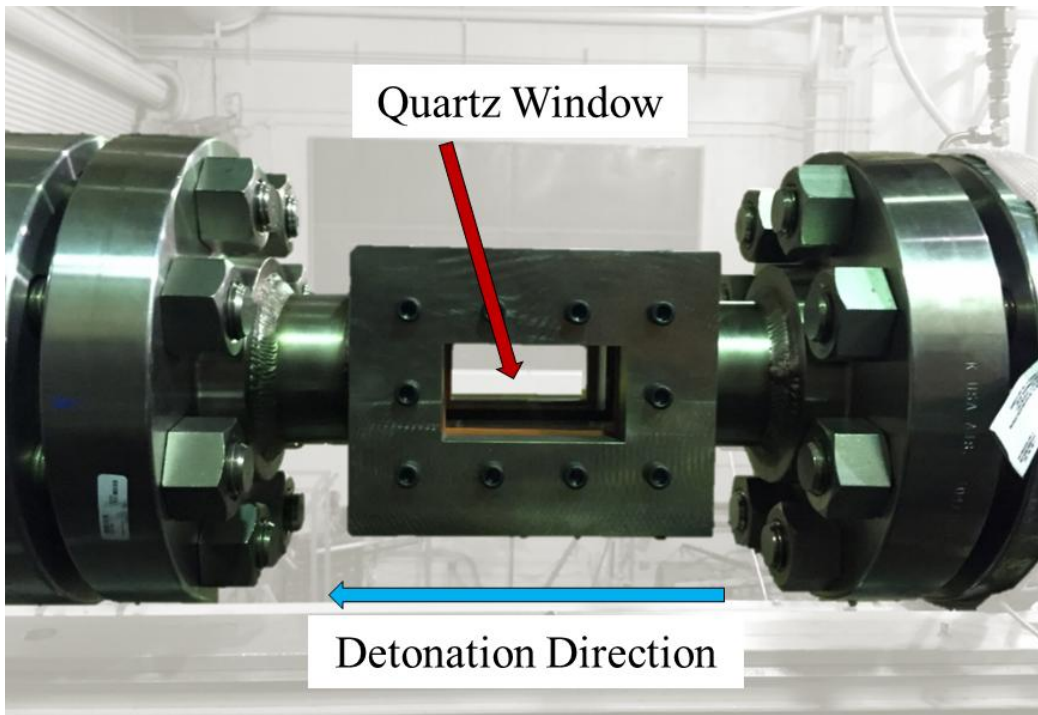


Figure 15. Detonation tube viewing section

The detonation tube has a circular cross section until it transitions at the flange in the viewing section. At the flange in Figure 15, the cross section changes to Figure 16. The transition is immediate and occurs approximately 18 cm before the viewing section window.

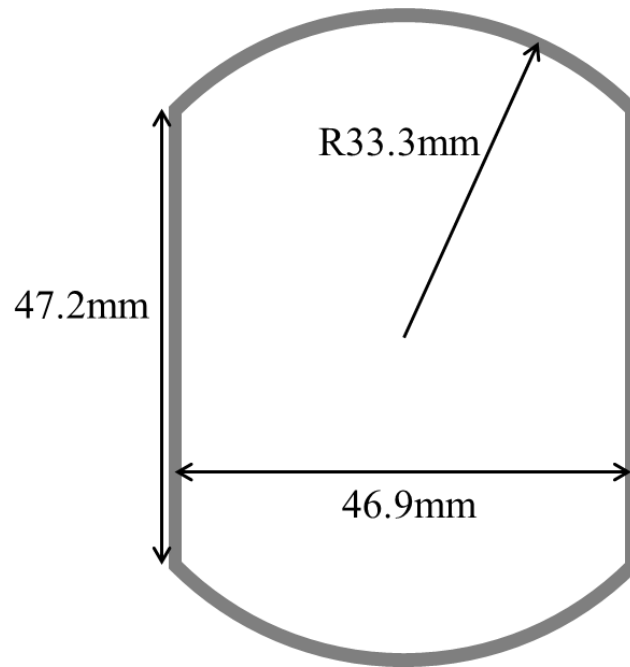


Figure 16. Detonation tube viewing section cross section

A schematic of the shock tube system is shown in Figure 17. To start each test, the system was evacuated to approximately 0.02 atm to remove impurities that could cause erroneous results. The tube was then filled with air to the correct partial pressure for that test's mixture total pressure and equivalence ratio. Then hydrogen was added to the tube to the total pressure for that test. Because of hydrogen's low density, it tends to move to the top of the tube; therefore, the mixture was circulated via a fan with a flow rate of 1.16 m³/min for 10 minutes.

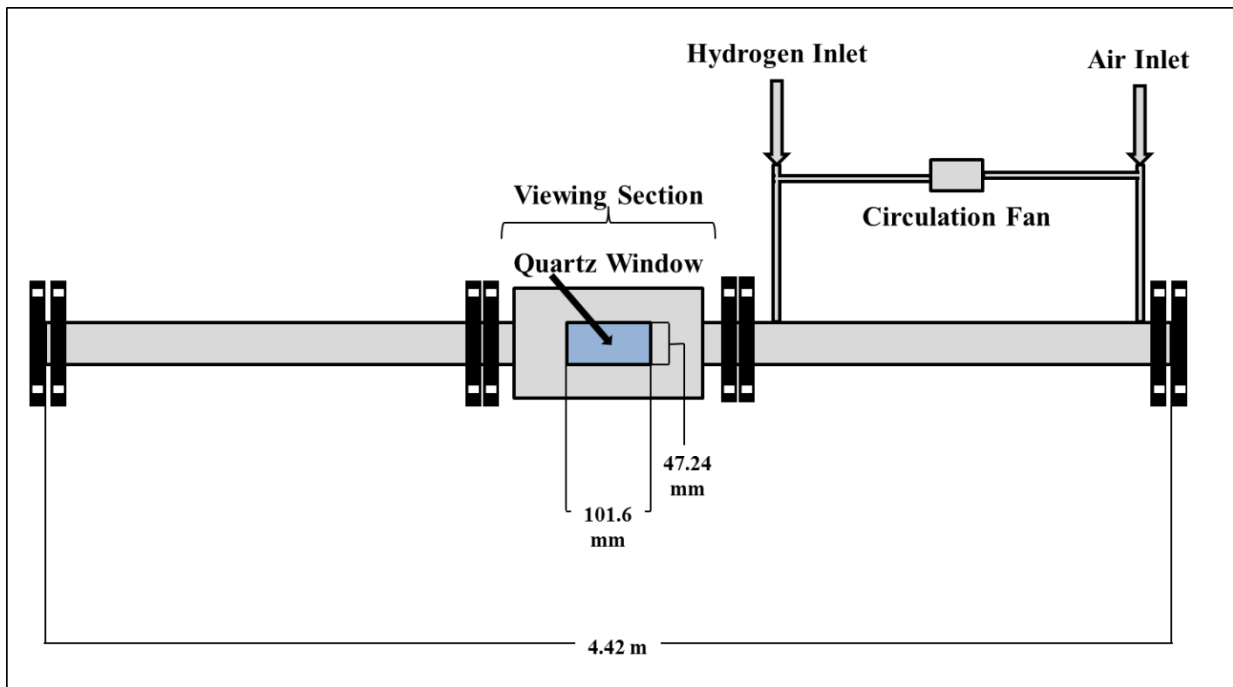


Figure 17. High pressure detonation tube exterior schematic

Figure 18 shows a cutaway schematic of the shock tube system. Less than 30 seconds after mixing, the hydrogen and air mixture was ignited via a 100 mJ spark plug. The deflagration traveled through a 1.200 m DDT device before passing through the viewing section. The detonation traveled from right to left in Figure 18. During the detonation's first pass through the viewing section, images were taken. After passing the viewing section, the detonation reflected off of the flange and back flowed through the viewing section several times. The reflected waves were normal shocks and were not used for measurements though they appeared on the schlieren images.

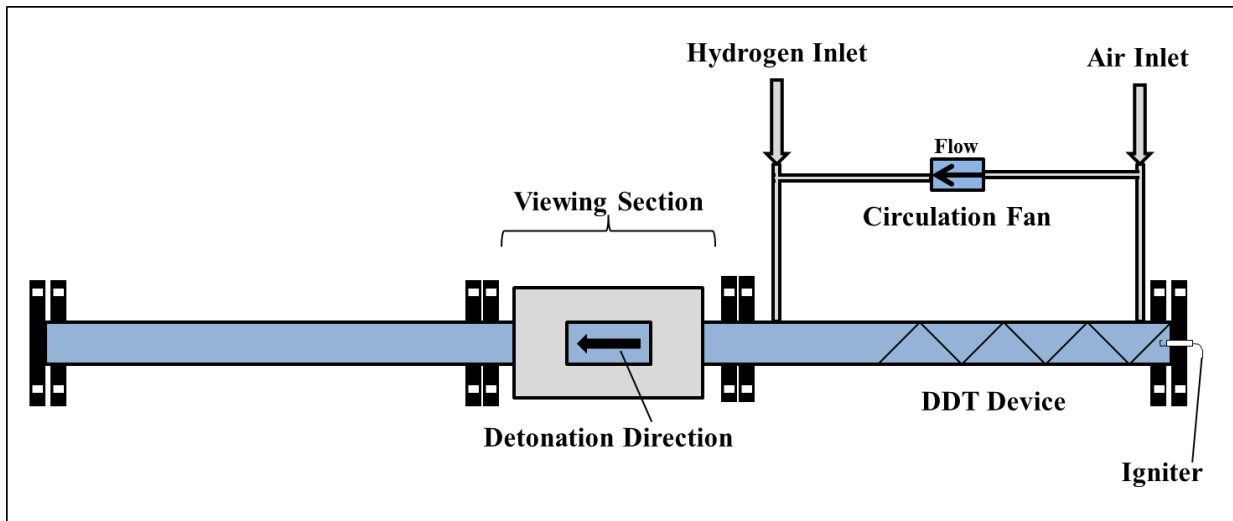


Figure 18. High pressure detonation tube cut-away schematic

The optics configuration was a schlieren setup that consisted of two flat mirrors, two parabolic mirrors, and a high speed camera. Schlieren imaging was used to take images of the density gradients in the detonation waves. The transverse, incident, and Mach shocks are higher density than the surrounding mixture. The higher densities show up as dark areas on the schlieren images. The darker transverse shocks are what are used to find the detonation cell boundaries.

Figure 19 shows the system configuration including the optics. The flat mirrors were used to extend the distance from the light source to the viewing section and from the high speed camera to the viewing section, due to physical size constraints of the lab floor area. If the area were larger, the flat mirrors would not be needed. An extended light source was used so that the focusing schlieren technique could be utilized. Simple schlieren systems use a point light source that has an infinite focal depth; therefore, the entire segment between the parallel mirrors is focused (Settles, 1985). In the focusing schlieren technique, the extended light source acts as multiple point light sources on the

object. Each light beam illuminates the object and the focal depth is shortened proportional to the source diameter. The extended light source configuration allows the schlieren image plane to be moved by moving the camera, mirrors, and light. By moving the image plane, the image can be focused on any plane in space. The system was focused on the center of the viewing section to measure the cells far from the walls to eliminate boundary effects.

A Phantom[®] 711 high speed camera recorded the density gradients at 49,000 fps and a pixel density of 20,000 dpi. The mirrors were set up so that the image the camera sees is at the center of the viewing window. An object was placed at the focal plane, and the camera was focused by adjusting the camera's focus until the object was in focus.

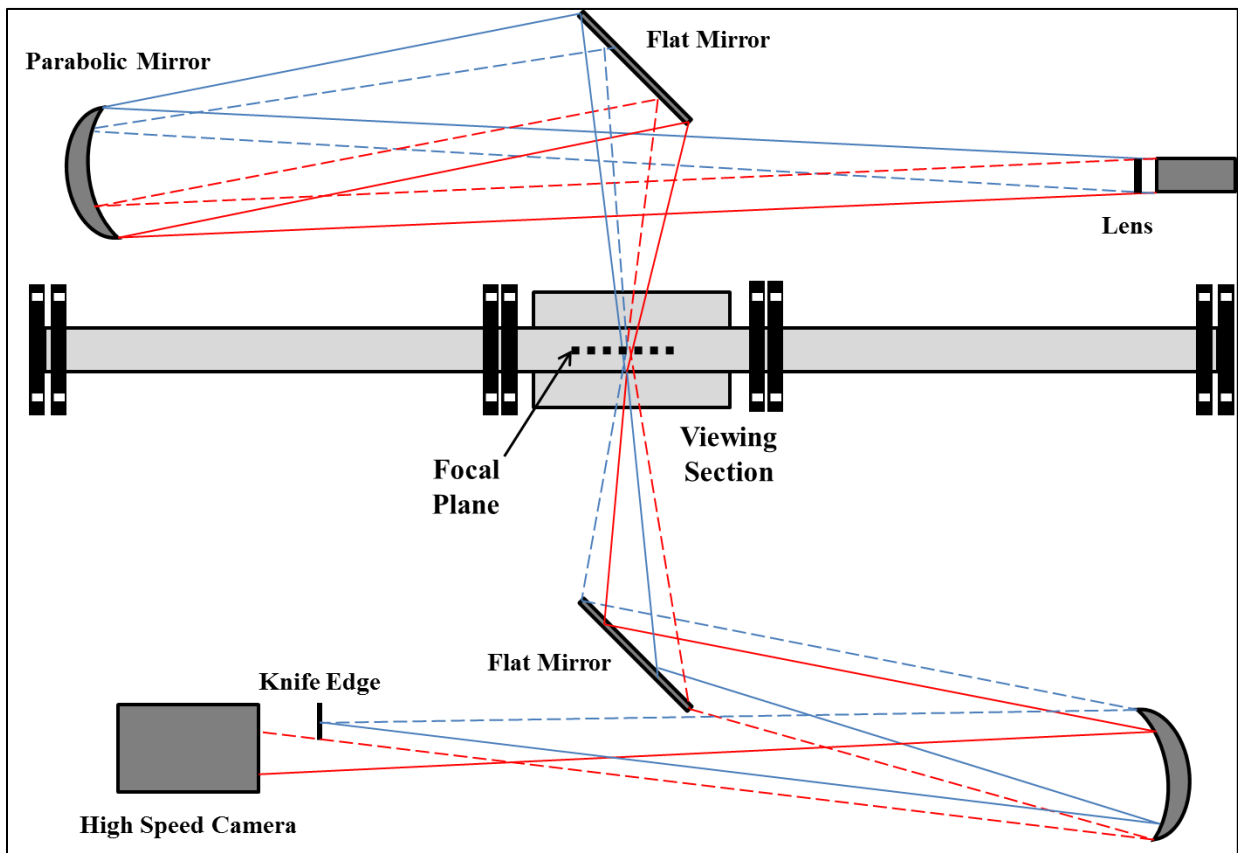


Figure 19. Detonation tube and optics configuration

Execution

The tests were completed at increasing pressures with decreasing equivalence ratios in order to increase cell size so that the cells would be large enough to measure using the techniques in this research. As the pressure is increased the cell size is decreased. This relationship can be modeled by Equation 2 at stoichiometric conditions, where P_i is the mixture pressure in torr and λ is in cm (Lee, 2008). For a hydrogen and oxygen mixture 'a' and 'b' are approximately 1,452 and 0.928, respectively. The current experiment used air as an oxidizer which will have an effect on cell size. Even though cell size is different for hydrogen and air, this equation was used to find the approximate cell size at each pressure to find out if the cells would be visible on the schlieren images.

$$\lambda \cong \frac{1}{13} \left(\frac{a}{P_i} \right)^{1/b} \quad (2)$$

Using Equation 2, the approximated cell size for a mixture pressure of 2.0 atm was 0.073 cm and the approximated cell size for an mixture pressure of 4.0 atm was 0.035 cm. Cell sizes less than two mm were too small to measure with the techniques used in this research due to camera constraints. The camera speed setting selected was 49,000 fps. At 49,000 fps the pixel dimensions available was 512 pixels long and 256 pixels high. The pixels were approximately 0.02 cm in height. In order to be able to see cell boundaries, it was assumed that at least ten pixels per detonation cell were needed; therefore, detonation cell sizes had to be at least 0.2 cm in order to measure them. A greater number of pixels decreased the uncertainty of the results. In order to keep the uncertainty less than 50 percent, which is the approximate maximum uncertainty discussed later, the number of required pixels was increased. In order to make the cells

visible with the given camera constraints and minimize uncertainty, the cell size had to be increased.

A known relationship was used to increase the cell. Figure 20 shows a relationship of how the mixture pressure affects critical tube diameter for hydrogen and oxygen detonations (Lee, 2008). The critical tube diameter is approximated as 13λ (Lee, 2008). Therefore, the relationship in Figure 20 can be used to approximate cell size.

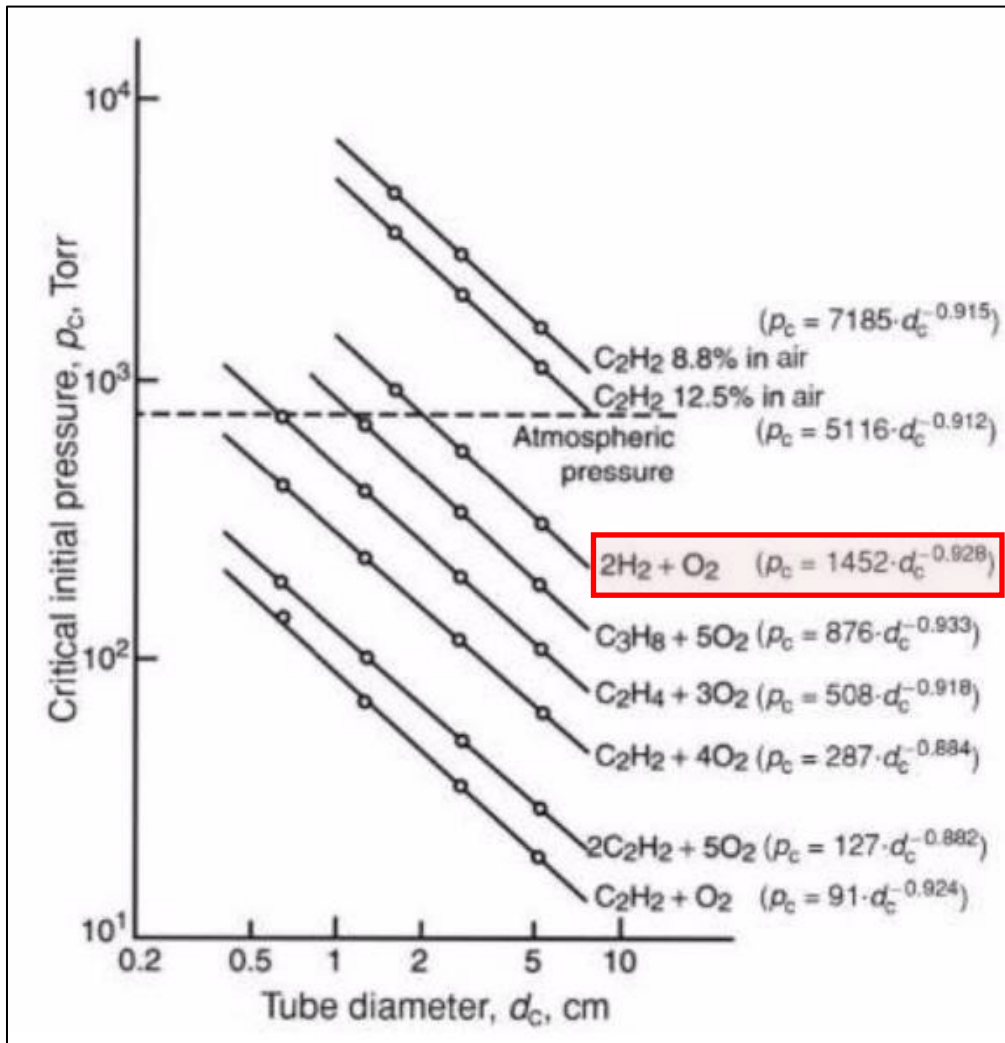


Figure 20. Hydrogen and oxygen detonation critical initial pressure versus critical tube diameter (Matsui and Lee, 1979)

In order to increase the size of the cells in a range that would be measurable within the camera constraints, the equivalence ratio was decreased. There are data for known relationships of cell size versus equivalence ratio discussed in Chapter II (Cicarelli et al., 1994, Ciccarelli et al., 1997, Guirao et al., 1982, Stamps et al., 1991, and Tieszen et al., 1987). The smallest cell size occurs at an equivalence ratio of approximately one. As the equivalence ratio decreases from unity with all other variables held constant, the cell size increases rapidly.

Hydrogen and oxygen detonation data on cell size versus equivalence ratio were used as approximations of hydrogen and air detonation cell size (Lee, 2008). The approximations were used to find equivalence ratios that would allow the detonation cells be measurable within the viewing section. The values chosen for each test case are in Table 1. The first four cases were first calculated then tested. The remaining 11 cases were each tested with the knowledge of the cell size from the previous case. The pressure was increased and the equivalence ratio was changed to keep the cells large enough to be viewable. Table 1 shows the order of testing. Due to time constraints each case was tested once.

Table 1. Pressure and equivalence ratios

Case	P	Φ
1	1.0 atm	1.00
2	2.0 atm	1.00
3	2.0 atm	0.80
4	4.0 atm	0.80
5	4.0 atm	0.70
6	6.0 atm	0.70
7	6.0 atm	0.65
8	8.0 atm	0.65
9	10.0 atm	0.65
10	10.0 atm	0.70
11	8.0 atm	0.70
12	10.0 atm	0.80
13	8.0 atm	0.80
14	6.0 atm	0.80
15	4.0 atm	1.0

The goal was to reach 10.0 atmospheres. Once that goal was reached, the next goal was to measure cell size for 10.0 atmospheres at a range of equivalence ratios. After multiple equivalence ratios were measured at 10.0 atmospheres, the rest of the cases were tested in order to fill in Figure 21. Figure 21 shows the test cases by mixture pressure and equivalence ratio.

Test Matrix

Pressure (atm)	10.0		X	X	X
	8.0		X	X	X
	6.0		X	X	X
	4.0	X	X	X	
	2.0	X	X		
	1.0	X			
		1.00	0.80	0.70	0.65

Equivalence Ratio (Φ)

Figure 21. Test matrix

Analysis Method

The cell size was measured for all of the 15 cases. The schlieren images from the high speed camera were used to visually count the cells in each detonation. For each case, there were two images that were analyzed. There were two images from each test due to the camera frame rate and detonation speed. Due to time constraints, there are two images available for each case. Figure 22 shows two of the raw images from a single detonation at a mixture pressure of 1.0 atm and an equivalence ratio of 1.0. The wave is moving from right to left. There is approximately 20.40 micro seconds between each image.

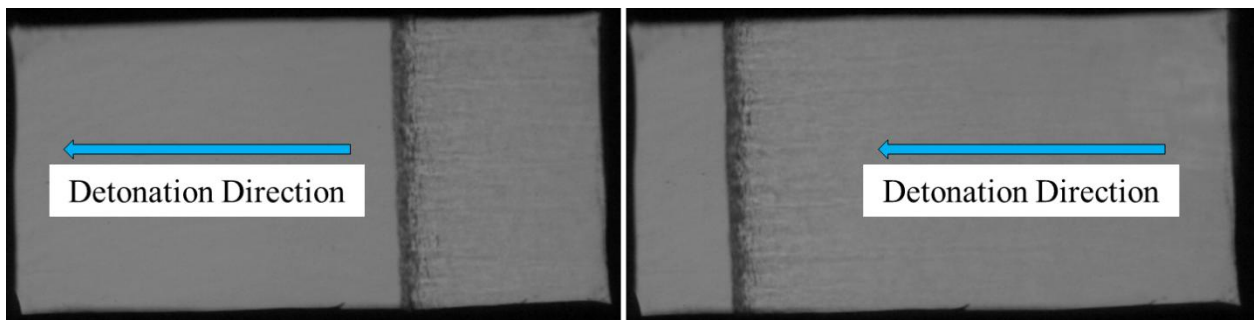


Figure 22. Raw schlieren images of detonation at 1.0 atm and 1.0 equivalence ratio

In order to calculate the cell size, the number of triple points was counted at each shock front. The number of triple points varies depending on where the image was taken of the detonation. Therefore, an average of the number of triple points was taken from the two images to calculate the number of cells in each case.

A detonation produces cells where the cell boundaries are defined by transverse shocks. Triple points are the points where the transverse shock, Mach stem, and incident shock intersect (Lee, 2008). The triple points are visible in the images taken by the high speed camera. The triple points visible by the naked eye are counted to find the number

of cell boundaries in a vertical cross section of the detonation. When the triple points are difficult to see due to chemiluminescence, transverse shockwaves are counted instead. Transverse shockwaves stem from the triple point; therefore, the number of transverse shock waves will be equal to the number of triple points.

In the current research triple points are viewed at the incident shock wave of the detonation. Figure 23 shows an example of one cell in green, where the green lines indicate the triple point paths that form cell boundaries (Lee, 2008, Lefebvre, 1993). The detonation shock fronts are shown in blue, located at different steps in time at points A, B, and C (Lefebvre, 1993). The incident shock front represents the density gradients visible in the schlieren images. If the cell triple point path intersections also intersected the detonation front, one triple point would be visible for two cells. Figure 23 at point A shows the detonation front intersecting a triple point path intersection. If the cell triple point path intersections were located exactly at the edge of the inside of the tube where they intersect the detonation shock front, the number of cells would be defined by the number of triple points plus one. Figure 23 at point B shows a detonation front with no triple points because the triple point path intersection is located at the edge of the tube. The likelihood of the capturing the image when the detonation wave front is at points A or B is practically zero. Because it is highly unlikely that the triple points would intersect the detonation front at the triple point path intersection (Figure 23, point A) or where the triple point path intersection meets the edge of the image (Figure 23, point B) there is approximately twice the number of triple points as there are cells as shown in Figure 23 at point C. This shows that there are two triple points in a detonation wave front for each detonation cell.

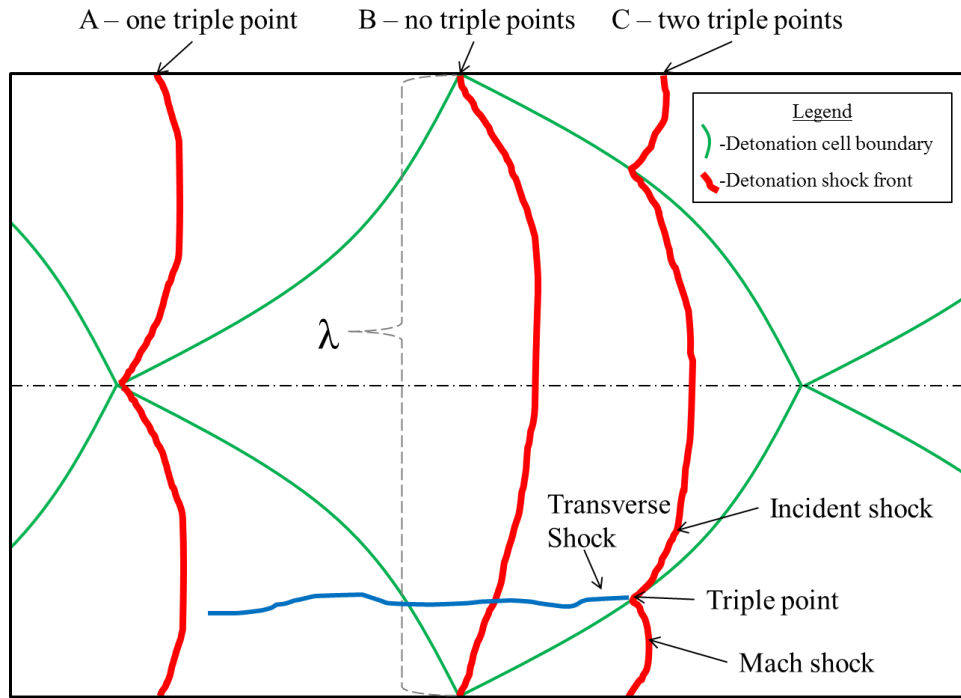


Figure 23. Detonation triple point movement

The number of cells within the vertical cross section of the tube is then equal to half the number of triple points plus one. The height of the image was divided by the number of cells plus one to find the cell size for each test. Figure 24 shows one of the raw images used to measure the cell size. It is a hydrogen and air detonation at equivalence ratio of 4.0 and a mixture pressure of 1.0 atm. The detonation is moving from right to left.

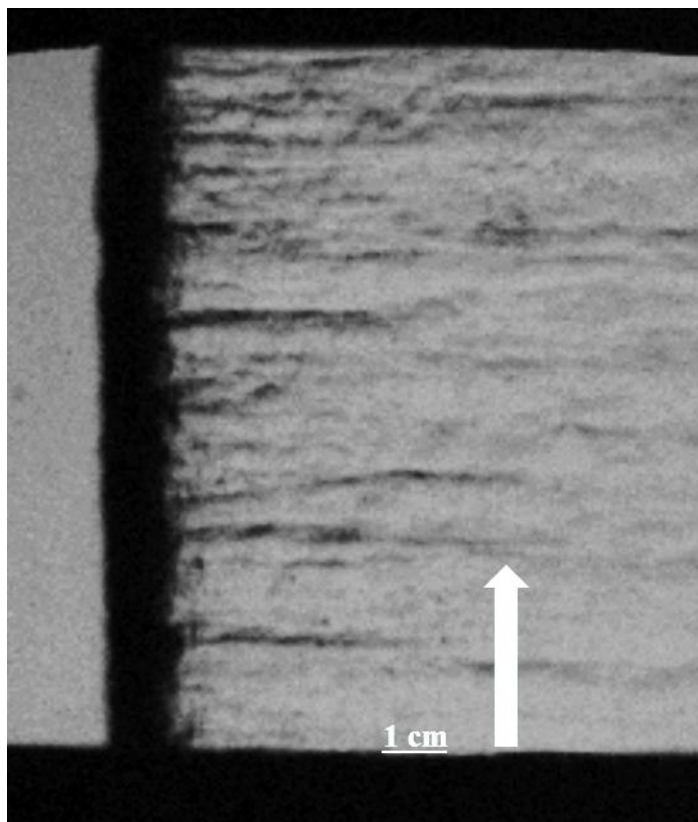


Figure 24. Schlieren image of hydrogen and air detonation ($P = 4.0 \text{ atm}$, $\Phi = 1.0$)

Figure 24 was used to count the number of triple points that were in the detonation wave front, using the transverse wave. Figure 25 is a copy of Figure 24 with the transverse shocks annotated. The images were analyzed in software to find edges and then invert the colors for more clear pictures. The drawn-in lines show the transverse shock waves that lead to the triple points. When the triple points were not clearly evident, which was in most cases, the transverse shocks were used to count the number of cell boundaries. The horizontal white lines in Figure 25 show the transverse shocks.

In order to count the horizontal line as a transverse shock, several criteria had to be met. The horizontal line had to start at the reaction zone. It had to have an aspect ratio of at least 10:1. The potential transverse shock had to be at least twice as long as the

reaction zone. If these criteria were met, the white horizontal line was counted as a transverse shock.

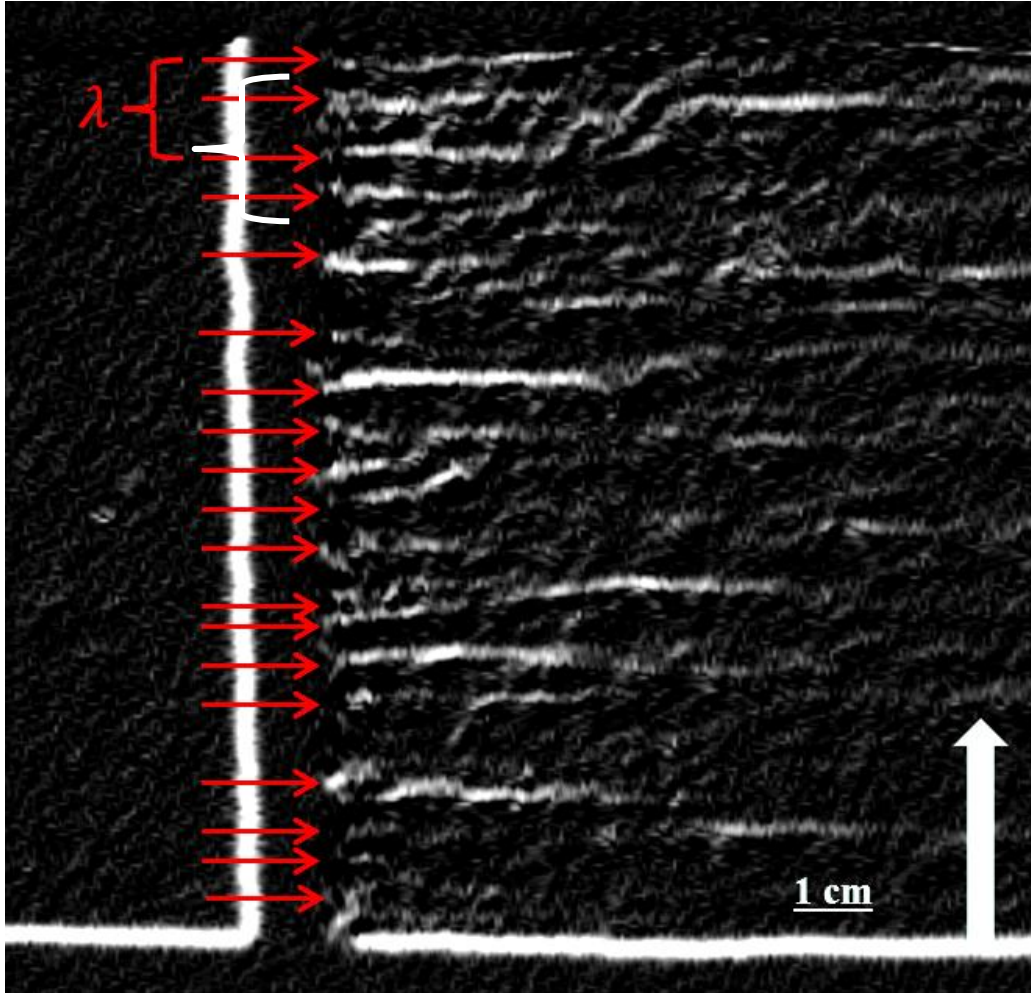


Figure 25. Schlieren image of hydrogen and air detonation transverse shocks annotated ($P = 4.0$ atm, $\Phi = 1.0$)

Often the image had to be increased in size to accurately find the cell boundaries. Figure 25 shows the same image from Figure 24 zoomed to see the cell boundaries.

Figure 25 shows two transverse shocks forming detonation cells. Each of the transverse shocks were counted to find the average cell size.

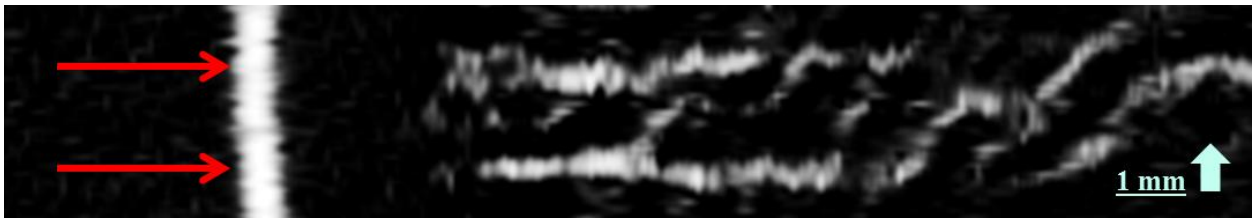


Figure 26. Schlieren image of hydrogen and air detonation with transverse shocks annotated ($P = 4.0 \text{ atm}$, $\Phi = 1.0$)

Error! Reference source not found. is the raw image beside the processed image of a detonation wave at a mixture pressure of 4.0 atm and an equivalence ratio of 1.00. The two images show how the transverse waves match up to the original image.

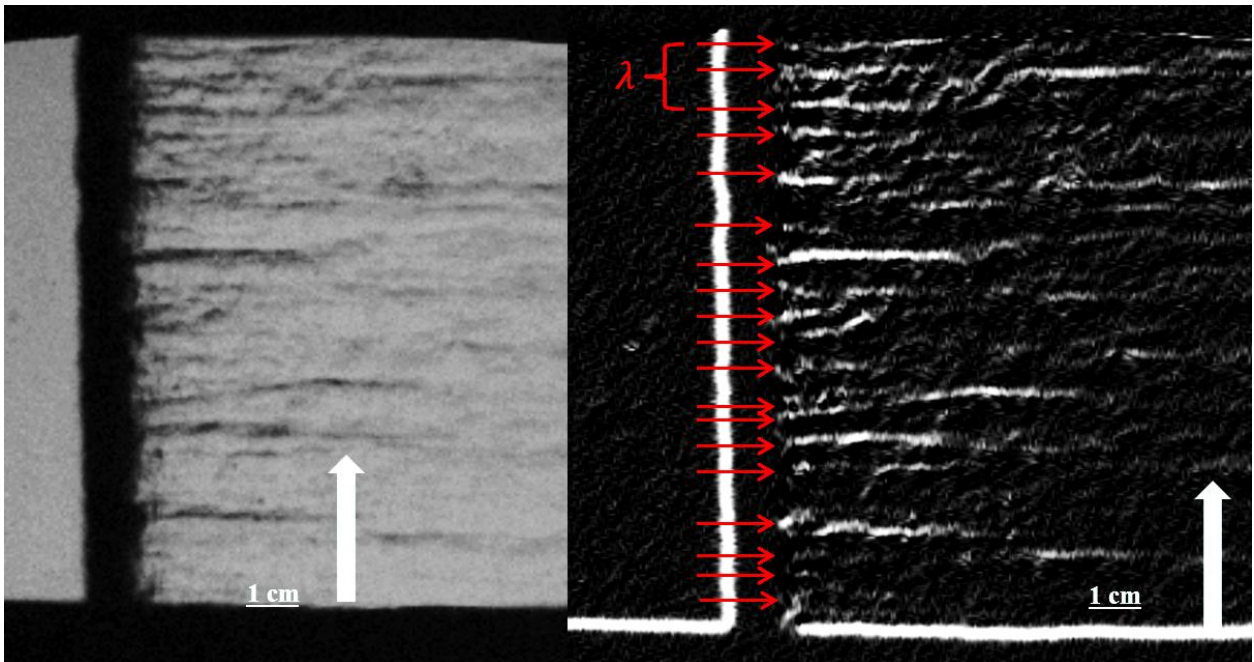


Figure 27. Hydrogen-air detonation raw image and processed image comparison ($P = 4.0 \text{ atm}$, $\Phi = 1.00$)

All of the raw Schlieren images are in Appendix B. The images were zoomed or softened in order to read them more clearly. All 15 cases are shown in Figure B - 1 to Figure B - 60. Each case has two unique images with a color image based on pixel density and a grey scale from the actual image, yielding four images for each case. It is important to note that in two of the cases, one of the images was too blurry to find cell boundaries. This was most likely due to the chemiluminescence from the reaction. Filters were added to the camera to reduce the chemiluminescence, but in two cases it was not enough to make the image visible.

With limited data points per test, the error tends to be high. There were two types of error in the analysis. There was random uncertainty or statistical error and systematic uncertainty or system induced error (Wheeler, 2004). Random uncertainty originates from the variation in cell sizes in each image. The random uncertainty was found by using a 95 percent confidence interval for each case. The student's t-distribution was used to find the confidence interval. The assumption was made that the measurements of the cell sizes would be normally distributed about the population mean in order to use the t-distribution. The t-distribution was used instead of the z-distribution because there were less than 30 samples for each case. The number of sample data points was based on the number of total counted detonation cells in two images. The total counted detonation cells ranged from 12 to 25 detonation cells. The variance and standard deviation were found by measuring each cell independently.

The second source of error was from systematic uncertainty. Systematic uncertainty was introduced from visual analysis. The main source of this error was in counting the number of visible cell boundaries through either triple points or transverse

shocks. To account for this error, the number of counted cell boundaries was assumed to have an uncertainty of 25 percent. This is a subjective uncertainty based on previous research using 25 to 100 percent uncertainty in measurements. In order to find the total uncertainty for each case, the root sum of the squares of random uncertainty and systematic uncertainty were calculated. The uncertainty values are discussed in Chapter IV.

IV. Analysis and Results

Chapter Overview

Schlieren images were analyzed in order to measure the hydrogen and air detonation cell size. The raw images are shown in the Appendix B. The raw images are presented to show the differing degrees of clarity for each combination of mixture pressure and equivalence ratio and for the reader to analyze the images. The current chapter displays the results through tables and charts to show trends, as well as empirically derived formulas for cell size predictions.

Results

The results from the experiments and analysis are divided into five sections: summary results, results by mixture pressure and equivalence ratio, error analysis, and empirical formulas. The summary results show all 15 cases in the same tables and charts. The summary results give the big picture view of the trends between the different mixture pressures and equivalence ratios. The results by mixture pressure and equivalence ratio divide the results into charts with a few cases of either a single equivalence ratio or single mixture pressure. The error analysis shows how the error was calculated for each measurement. The empirical formulas use the formula from the methodology section and update it with results from the current research.

Summary results

The results, as outlined in Table 2, include 15 cases with varying mixture pressures and equivalence ratios. The mixture pressure ranges from 1.0 atm to 10.0 atm and the equivalence ratios range from 0.65 to 1.00. The cases are not in order of being

tested and are rearranged in an order with ascending mixture pressures and descending equivalence ratios. Each case contains data from one to three schlieren images. The hydrogen and air mixture temperature for all cases was 296 ± 1 K. The error is included with each point estimate cell size.

The historic measured cell sizes are annotated in Table 2 where available. There is limited historic data available for hydrogen and air detonation cell sizes over 1.0 atm mixture pressure. The historic data available is presented in Appendix A (Cicarelli et al., 1994, Ciccarelli et al., 1997, Guirao et al., 1982, Stamps et al., 1991, and Tieszen et al., 1987). There is data for hydrogen and air cell size with diluents added, but the current research is only concerned with detonations without diluents. Where Table 2 says N/A, the data is not available for hydrogen and air detonation cell sizes without diluents.

Table 2. Summary of results

Case	Pressure (atm)	Equivalence Ratio	Measured Cell Size (mm)	Historic Cell Size Values (mm)
1	1.0	1.00	8.3 ± 3.1	10.4 ± 4.8
2	2.0	1.00	5.8 ± 2.2	5.5 ± 0.5
3	2.0	0.80	7.0 ± 2.8	N/A
4	4.0	1.00	4.9 ± 1.6	N/A
5	4.0	0.80	5.4 ± 1.8	N/A
6	4.0	0.70	8.6 ± 3.7	N/A
7	6.0	0.80	4.6 ± 2.2	N/A
8	6.0	0.70	5.9 ± 2.6	N/A
9	6.0	0.65	7.6 ± 3.6	N/A
10	8.0	0.80	4.3 ± 2.1	N/A
11	8.0	0.70	5.9 ± 5.2	N/A
12	8.0	0.65	7.9 ± 5.6	N/A
13	10.0	0.80	4.0 ± 2.4	N/A
14	10.0	0.70	5.1 ± 2.5	N/A
15	10.0	0.65	7.9 ± 3.8	N/A

The data from all 15 cases is presented in Figure 28 to show trends. Trends are based on lines of constant equivalence with different mixture pressures. The pressures are in atm and cell sizes are in cm. There are four trend lines for equivalence ratios of: 0.65, 0.70, 0.80, and 1.00. Each trend line has a different number of data points. Equivalence ratios of 0.65 and 1.00 have three data points. Equivalence ratio of 0.7 has four data points, and equivalence ratio of 0.80 has five data points.

Figure 28 shows that increasing the mixture pressure decreases the cell size. Based on Figure 28, the preliminary changes in pressure from 1.0 atm to about 4.0 atm represent a greater negative gradient in cell size. After approximately 4.0 atm, the change in mixture pressure has less of an effect on changing cell size. All five trend lines follow a power law decay with an exponent between -0.177 and -0.381.

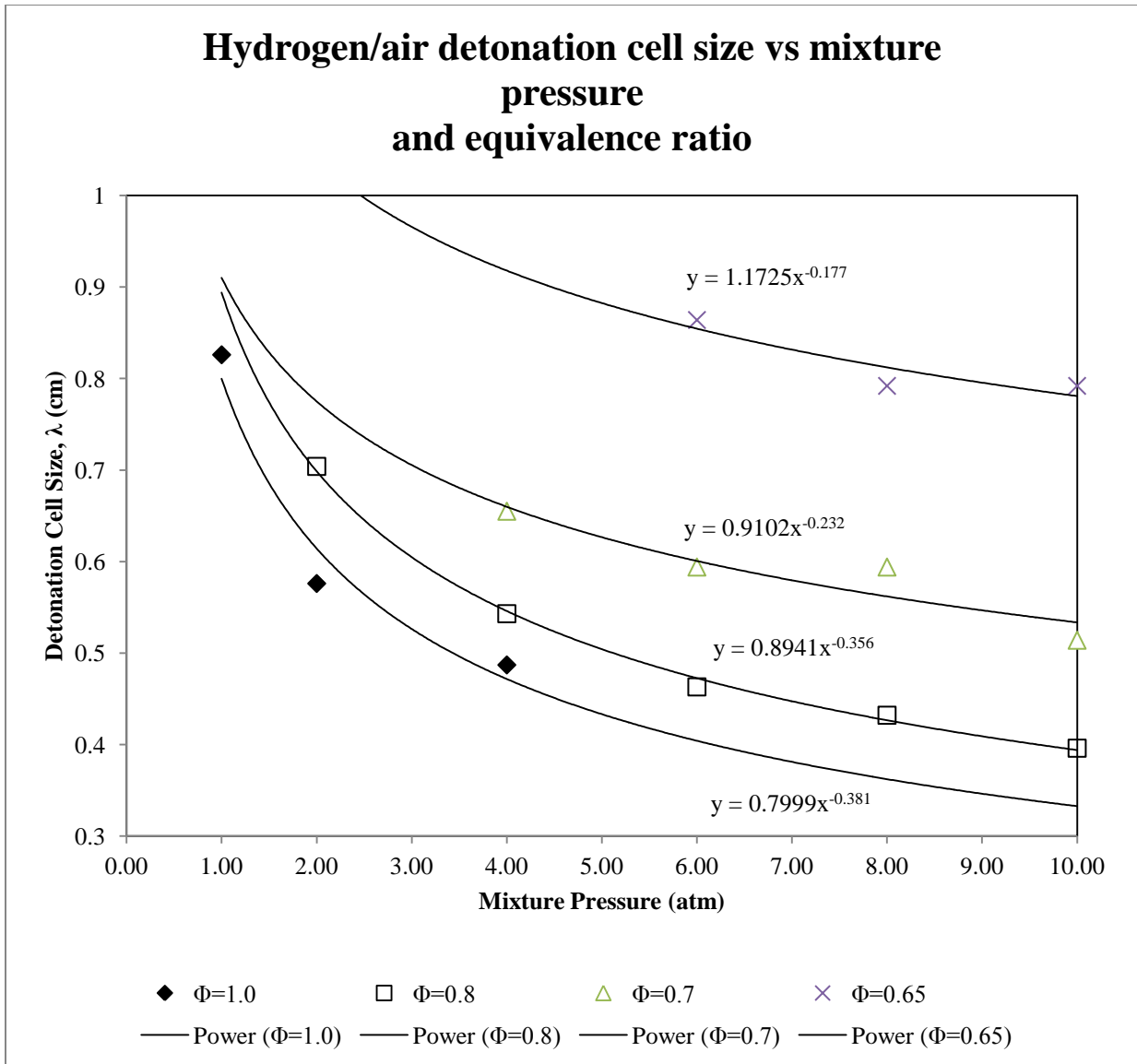


Figure 28. Hydrogen/air detonation cell size vs mixture pressure by equivalence ratio

Figure 29 shows the 15 cases from Figure 28 arranged by mixture pressure. There are five trend lines for mixture pressures of: 2.0 atm, 4.0 atm, 6.0 atm, 8.0 atm, and 10.0 atm. All trend lines except for the 2.0 atm line contain three data points; therefore the 2.0 atm trend line has lower accuracy than the other trend lines and is displayed for comparison purposes.

In Figure 29 the trend lines for 6.0 atm, 8.0 atm, and 10.0 atm follow a similar slope with an exponent of approximately -3.0. The 4.0 atm trend line has a more gradual slope. The difference between the slopes may be due the equivalence ratios not spanning the same range. The 2.0 atm trend line is only two points, so no conclusions can be drawn from it.

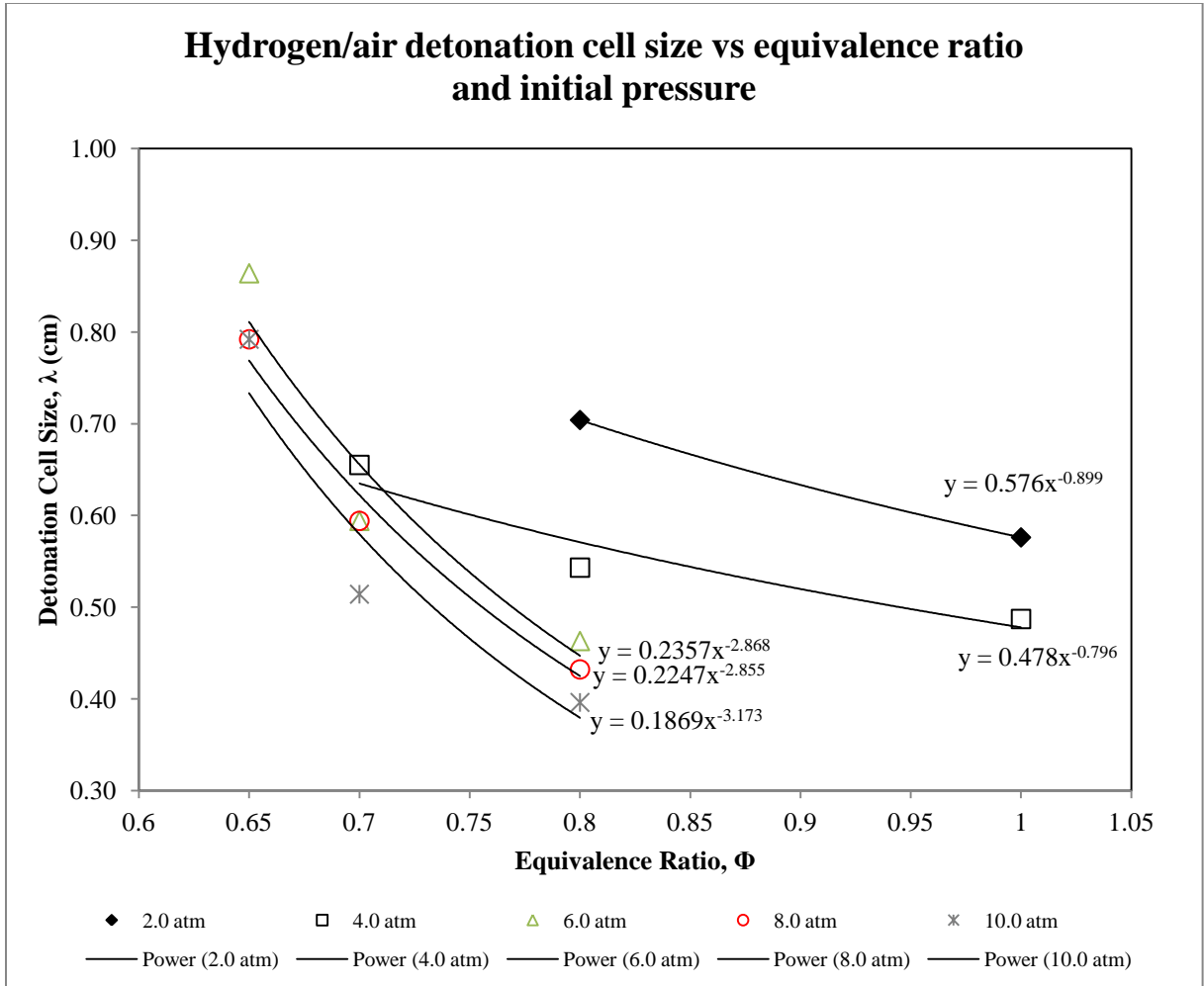


Figure 29. Hydrogen/air detonation cell size vs equivalence ratio by mixture pressure

Error analysis

The error analysis included systematic error and random error. The results from the error calculations for each of the 15 cases are shown in Table 3. The total error is the root sum squares of the random error and systematic error. The random error is a 95 percent confidence interval using the standard deviation and sample size, n, for each case. The systematic error is the error introduced in the measurements from visual error in counting the detonation cell boundaries. The systematic error is somewhat subjective due to the subjectivity of measuring detonation cell sizes. The systematic error includes a 25% assumed error for counting the transverse waves in the schlieren images.

Table 3. Error results

Case	P (atm)	Φ	n	\bar{x} (mm)	s^2 (mm)	s (mm)	Random Error (mm)	Systematic Error (mm)	Total Error (mm)
1	1.0	1.00	12	8.3	5.8	2.4	± 1.5	± 2.7	± 3.1
2	2.0	1.00	17	5.8	4.6	2.2	± 1.1	± 1.9	± 2.2
3	2.0	0.80	13	7.0	6.3	2.5	± 1.5	± 2.3	± 2.8
4	4.0	1.00	19	4.9	0.60	0.78	± 0.36	± 1.6	± 1.6
5	4.0	0.80	25	5.4	0.88	0.94	± 0.39	± 1.8	± 1.8
6	4.0	0.70	6	8.6	4.6	2.2	± 2.3	± 2.9	± 3.6
7	6.0	0.80	20	4.6	7.8	2.8	± 1.3	± 1.5	± 2.0
8	6.0	0.70	7	5.9	9.7	3.1	± 1.7	± 2.0	± 2.6
9	6.0	0.65	8	7.6	16	4.0	± 2.5	± 2.5	± 3.6
10	8.0	0.80	22	4.3	12	3.5	± 1.6	± 1.4	± 2.1
11	8.0	0.70	8	5.9	17	4.1	± 3.4	± 3.9	± 5.2
12	8.0	0.65	6	7.9	22	4.7	± 5.0	± 2.6	± 5.6
13	10.0	0.80	12	4.0	10	3.2	± 2.0	± 1.3	± 2.4
14	10.0	0.70	18	5.1	14	3.7	± 1.8	± 1.7	± 2.5
15	10.0	0.65	6	7.9	19	4.3	± 2.7	± 2.6	± 3.8

Empirical formula

After finding measurements for hydrogen and air detonation cell sizes, Equation 3 was found using linear regression techniques in statistic software. Equation 3 optimized the amount of error produced between the experimental data and predicted data using the equation. All 15 data points were used to find Equation 3. The R^2 value is 0.90 and the adjusted R^2 is 0.88. The equation met the assumptions that the residuals were normally distributed, independent, and displayed constant variance. The Mean Absolute Percent Error (MAPE) is the average absolute error between the predicted points and the experimental points. The MAPE for Equation 3 was 5.3%, meaning that the average point was 5.3% different in the model than the experimentally measured points.

$$\lambda = -1.12 + 9.04P^{-0.400} + 0.376\Phi^{-6.00} \quad (3)$$

Figure 29 has one point that does not follow the same trends as the rest; the point is a mixture pressure of 4.0 atm and an equivalence ratio of 0.70. That point was removed and a new model was made. The second model is shown in Equation 4. The R^2 value increased to 0.96 and the adjusted R^2 increased to 0.95. The MAPE for Equation 4 was reduced to 3.8%, showing an overall improvement of the correlation for finding cell size.

$$\lambda = -0.435 + 8.33P^{-0.4} + 0.219\Phi^{-7.00} \quad (4)$$

Equation 4 was used to predict all 15 data points found experimentally. The model data points are overlaid with the experimental results in Figure 30. The red lines are the model predictions and the black symbols are the experimental results. The point from the 4.0 atm and 0.70 equivalence ratio experiment is much lower than the model prediction. The model

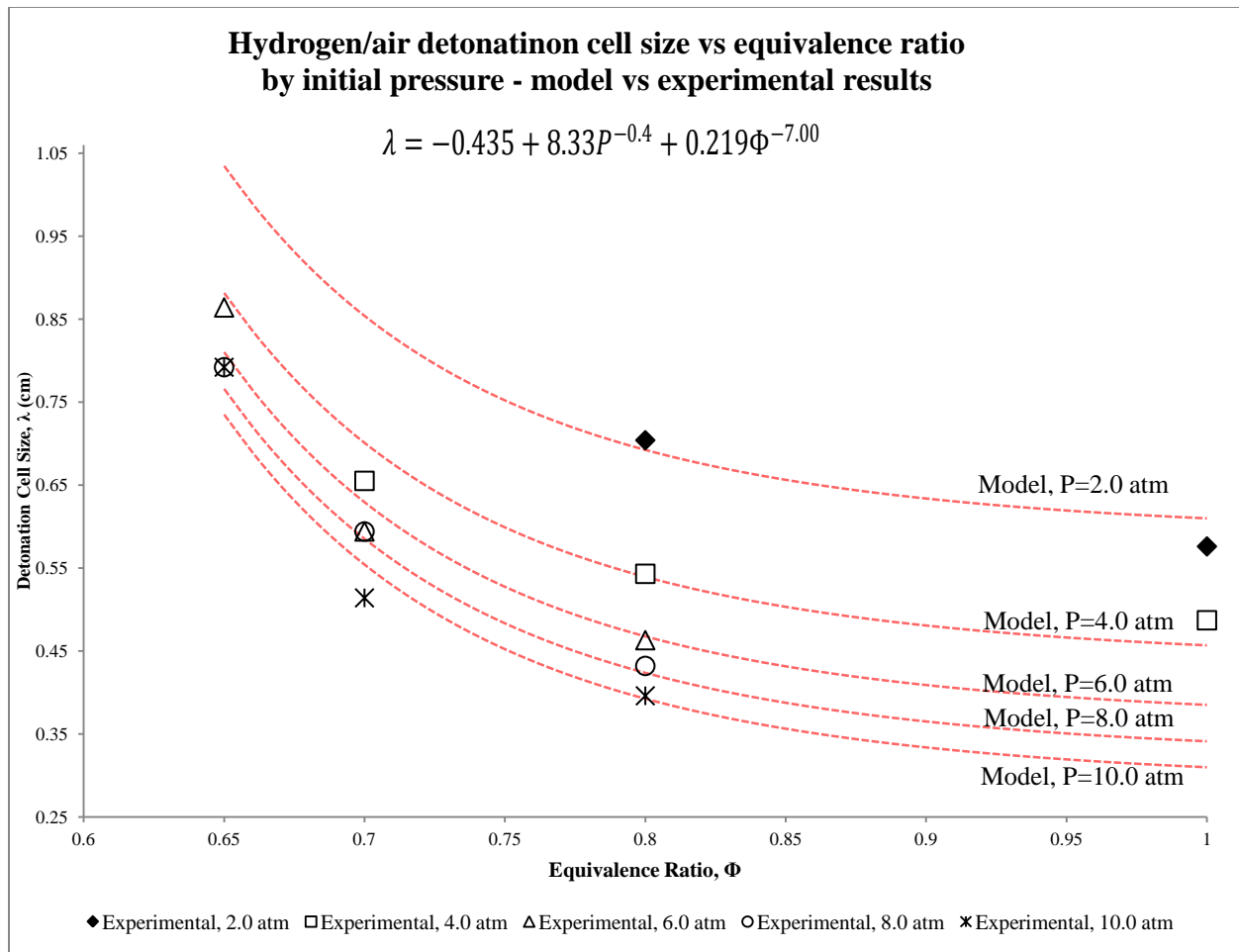


**Figure 30. Hydrogen-air detonation cell size vs equivalence ratio, experimental data
with model overlay**

Investigative Questions Answered

The goal of this research was to measure the cell size of hydrogen and air detonations at mixture pressures of up to 10.0 atm. The measurements were successful and trends were established that allow empirical formulas to help predict cell sizes for a larger variety of mixture pressure and stoichiometry combinations. At 10.0 atm and an equivalence ratio of 0.80, hydrogen and air detonations have a cell size of 4.0 mm.

Summary

The 15 test cases provided more insight into hydrogen and air detonation cell sizes with mixture pressures from 1.0 atm to 10.0 atm. The trend lines give the ability to predict true cell size for mixture conditions that fall within the tested limits. The trend lines appear to show that the closer the detonation mixture was to stoichiometric conditions, the higher the R^2 value was which yielded more accurate prediction models.

V. Conclusions and Recommendations

Chapter Overview

The results from this research give more insight into hydrogen and air detonation cell sizes. The cell size information can be used to derive the dynamic detonation properties of hydrogen and air detonations. Specifically, the detonability of hydrogen and air can be found for specific geometries of RDEs for future design.

Conclusions of Research

The measured cell sizes for hydrogen and air detonations are within expectations. A baseline case was used to assess the accuracy of the measurement system. Historic point estimate values for 1.0 atm at $\Phi = 1.00$ are between 5.0 mm and 15.1 mm and for 2.0 atm at $\Phi = 1.00$ are between 5.0 mm and 6.0 mm. The 2.0 atm case only has three historic values from the same research creating a tighter range. The uncertainty bounds for the historic cell size measurements for 1.0 atm at $\Phi = 1.00$ are between 0.0 mm and 30.2 mm and for 2.0 atm at $\Phi = 1.00$ are between 0.0 mm and 12.0 mm. The measured cell size for 1.0 atm at $\Phi = 1.00$ was approximately 8.3 mm with a ± 3.1 mm uncertainty and for 2.0 atm at $\Phi = 1.00$ was approximately 5.7 mm with a ± 2.2 mm uncertainty. This is consistent with historic data and suggests that the method of cell size measurement in this research is valid. The subsequent cases are also consistent with expectations. As the pressure was increased it was expected that the cell size should decrease as was the case illustrated in Figure 28. It was also anticipated that the cell size would increase with a decrease in equivalence ratio holding pressure constant. Figure 29 shows that, indeed, cell size increases with a decrease in equivalence ratio.

Though the trends were as anticipated, the rates of change were not what was anticipated. It was anticipated that the increasing mixture pressures would have a more linear effect on cell size, i.e. it was assumed that the cell size would halve with doubled mixture pressure. This was not the case. The mixture pressure deviation had the greatest effect on a change in cell size. Higher mixture pressure causes small changes in cell size. This could be due to properties of detonations or experimental constraints. Images for higher pressures were not as easily visible as the lower pressure images. Also, the higher pressure tests were at lower equivalence ratios, where such lower equivalence ratios resulted in irregularly shaped detonation waves making it more difficult to measure the cells.

The key conclusions from this research are:

1. Increasing mixture pressure, decreased detonation cell size.
2. The range of elevated mixture pressures had less of an effect on cell size than the range of equivalence ratios.
3. Decreasing equivalence ratio from stoichiometric increased cell size.
4. The change in equivalence ratio had a greater effect on cell size than a change in mixture pressure.
5. Detonation cell size measurements continue to have high uncertainty.
6. Detonation cell size measurements are now possible at mixture pressures up to 10.0 atm.

The research exponent 'n' values in the curve fits in Figure 28 are between 0.177 and 0.381 with mixtures between 1.0 and 10.0 atm and equivalence ratios between 0.65 and 1.00. These are lower than the exponent 'n' values from previous research hydrogen

and air detonation cell size curve fits of 0.419 to 2.571 with mixture pressures between 0.24 atm and 2.5 atm and equivalence ratios between 0.374 and 3.64. Previous research exponent values for each equivalence ratio curve fit were not consistent showing that there is not a clear correlation for all cell size data based on mixture pressure. The data is difficult to compare due to the differing ranges of mixture pressures and equivalence ratios between historic data and the current research. Though the current research hyperbola equations have lower exponents than previous data curve fits, they are close to the lower value. In order to gain more fidelity in research curve fit equation, more tests are required at a range of mixture pressures.

More tests are needed at each case in order to decrease the uncertainty and make more accurate predictions of the average cell size of hydrogen and air detonations. If time allowed more tests would be conducted for each case. Each test can be conducted inside of an hour; however, due to test equipment damage from each experiment, days or weeks were required to repair and reset the experimental setup. In this research there are only two images per case, due to the camera speed, to derive the trend lines and make conclusions; ideally there would be at least 30 images for each case.

Significance of Research

This research has successfully measured hydrogen and air detonation cell sizes without any diluents in elevated mixture pressure above 3.0 atm for the first time. The new data can be added to current detonation databases for use by organizations outside of the Air Force for any detonation related purpose.

Recommendations for Future Research

In addition to this research, the same test equipment is being used to find the cell size of propane and air detonations. This information will be directly used to design an RDE for a proof of design air craft. The propane and air research is measuring detonation cell sizes for multiple equivalence ratios, mixture pressures, as well as elevated mixture temperatures via pre-shocking the detonation tube.

Future research should focus on using the techniques within this research to measure detonation cell sizes for other gaseous mixtures to include methane and ultimately JP-8 or JP-10. Detonation cell size for JP fuels would allow RDEs to be designed for air craft that the Air Force could support more easily than propane or hydrogen.

Summary

The techniques in this research have been used to measure hydrogen and air detonations with mixture pressures up to 10.0 atm. The trend lines through the data match historic trends for lower mixture pressures and validate the techniques. The new data points will be the foundation of further elevated mixture pressure detonation cell measurements.

Appendix A - Previous Research Data

Table A - 1 to Table A - 5 show all previous data used in Chapter II Figure 9 to Figure 13. Table A - 1 to Table A - 5 are the cell size measurements of undiluted hydrogen and air detonation from 5 sources (Ciccarelli et al., 1994, Ciccarelli et al., 1997, Guirao et al., 1982, Stamps et al., 1991, and Tieszen et al., 1987).

Table A - 1. Detonation data, Ciccarelli et al., 1994

Test #	Temp (K)	Equivalence Ratio	Pressure (kPa)	Cell Size (mm)
334	300.9	1.959	101.51	78.5
318	297.6	1.961	101.58	76
258	293.2	1.843	101.71	46
206	298.2	1.691	100.06	25
151	300.0	1.690	101.30	31
317	297.6	1.353	101.71	9.4
207	298.2	1.355	101.71	10
164	300.0	1.011	101.30	9
175	300.0	1.013	101.30	9
146	300.0	1.018	101.30	9
156	300.0	0.843	101.30	12
35	300.0	0.669	101.30	34
254	292.6	0.674	101.85	42
256	294.3	0.677	101.58	47
147	300.0	0.591	101.30	59
187	300.0	0.594	101.30	96
177	300.0	0.592	101.30	98
150	300.0	0.568	101.30	140
343	497	1.690	102.1	10.5
204	500	1.693	102	10
273	504	1.691	102	17
208	498	1.013	102	6
274	508	1.014	101.9	9
341	497	0.740	101.8	8.15
271	510	0.591	102	15
272	506	0.589	102	15
203	498	0.589	101.9	20

Test #	Temp (K)	Equivalence Ratio	Pressure (kPa)	Cell Size (mm)
350	500	0.541	102	24
281	505	0.538	101.9	28.6
355	495	0.473	102	78.5
351	500	0.473	102	78.5
342	497	0.474	102	63
279	500	0.471	101.8	98
344	497	0.439	102.2	105
356	497	0.439	102.1	105
205	643	1.691	102.2	9
287	658	1.690	102.2	10
200	646	1.016	102.2	5
199	648	1.014	102.2	5
184	647	1.014	101	4
201	649	0.590	102.2	12
286	657	0.589	102.1	15.5
282	650	0.504	102.1	16
285	655	0.508	102	16
267	643	0.406	102.7	37
333	652	0.406	102.7	31
337	641	0.406	102.7	36
269	646	0.410	102.7	34
338	640	0.371	102.7	41
290	652	0.373	102.1	37
347	644	0.339	102.7	47
376	644	0.338	102.7	78.5
293	647	0.337	102.5	78.5

Table A - 2. Detonation data, Ciccarelli et al., 1997

Test #	Temp (K)	Equivalence Ratio	Pressure (kPa)	Cell Size (mm)
23	300	1.735968	100	18
18	300	1.002846	100	8
21	300	0.814918	100	11
19	300	0.672958	100	27
22	300	0.584402	100	93
297	300	0.504634	100	187
298	300	0.503282	100	248
107	500	0.999804	100	6
108	500	0.493818	100	52
104	500	0.4225	100	98
109	500	0.377208	100	196
329	500	0.367406	100	429
119	650	0.482664	100	17
122	650	0.385996	100	30
249	650	0.323804	100	46
318	650	0.298454	100	74
254	650	0.296426	100	94
255	650	0.264654	100	213
256	650	0.253838	100	230
373	650	0.313326	170	2
358	650	0.31434	240	85

Table A - 3. Detonation data, Guirao et al., 1982

Temp (K)	Equivalence Ratio	Pressure (kPa)	Cell Size (mm)
293	0.540540541	101.3	245
293	0.557432432	101.3	183
293	0.574324324	101.3	162.3
293	0.591216216	101.3	123.8
293	0.608108108	101.3	110.8
293	0.628378378	101.3	88.9
293	0.641891892	101.3	80
293	0.648648649	101.3	76.2
293	0.675675676	101.3	55.4
293	0.709459459	101.3	44
293	0.743243243	101.3	30.7
293	0.777027027	101.3	25.6
293	0.810810811	101.3	21.4
293	0.844594595	101.3	18.1
293	0.878378378	101.3	17
293	0.912162162	101.3	15.7
293	0.945945946	101.3	15.5
293	0.97972973	101.3	15
293	1	101.3	15.1
293	1.013513514	101.3	15.1
293	1.081081081	101.3	16.2
293	1.148648649	101.3	17.2
293	1.216216216	101.3	19
293	1.283783784	101.3	21.8
293	1.351351351	101.3	22.9
293	1.418918919	101.3	26.7
293	1.486486486	101.3	30.5
293	1.554054054	101.3	37
293	1.621621622	101.3	41.8
293	1.689189189	101.3	50
293	1.756756757	101.3	55
293	1.824324324	101.3	79
293	1.858108108	101.3	95
293	1.891891892	101.3	100
293	1.959459459	101.3	141.5
293	2.027027027	101.3	189.2

Table A - 4. Detonation data, Stamps et al., 1991

Test #	Temp (K)	Equivalence Ratio	Pressure (kPa)	Cell Size (mm)
134	375.5	0.3396	101.39	305
102	372.5	0.3601	101.35	444
101	369.6	0.4163	101.35	150
162	375.3	0.518	102.23	38
100	370	0.5966	101.11	24
99	371.3	1.0081	101.35	20
99II	375.4	1.0026	101.39	7
103	374	2.0202	101.42	14
104	374.4	3.0417	101.35	37
97II	302.4	0.9942	101.62	11
97III	311.3	0.9973	101.46	9
172	298	1.0462	101.52	13
98	281.6	0.9803	101.77	15
135	300.4	0.4996	10.22	56
135II	297.9	0.4901	10.18	210
135III	302.9	0.4977	10.02	250
159	296.4	0.489	15.36	215
136	269.1	0.4779	26.4	450
136II	298.9	0.5026	25.78	260
137	297	0.488	50.73	157
138	296.9	0.4958	101.47	76
139	300.9	0.4919	264.07	100
140	298.1	0.9912	10.02	39
141	296	1.0018	25.43	24
142	296.3	0.9812	51.25	15
143	296.9	0.9817	150.58	7.5

Table A - 5. Detonation data, Tieszen et al., 1987

Test #	Temp (K)	Equivalence Ratio	Pressure (kPa)	Cell Size (mm)
15	281.1	0.3743	97.423	1220
14	277.6	0.3812	97.905	1200
67	294.6	0.3868	100.801	640
68	299.6	0.4071	100.801	420
66	301.1	0.4248	101.008	305
12	277.6	0.4334	99.974	310
69	298.6	0.4335	100.87	265
65	298.6	0.4623	100.732	250
11	276.9	0.4792	99.284	190
64	300.1	0.4867	100.939	150
63	294.1	0.5037	100.801	100
70	302.1	3.6647	100.87	185
71	299.6	4.4655	100.939	475
72	303.6	5.7129	100.939	1350
74	371.6	0.3575	147.685	420
73	373.1	0.3747	148.65	330
77	372.1	0.3827	149.685	295
62	372.1	0.4213	150.236	175
76	372.1	0.4981	155.338	65
60	372.1	0.6059	160.923	25
78	370.6	0.6088	160.647	24
42	368.1	0.6501	161.199	19
80	371.1	0.6985	166.577	14
56	372.6	0.8085	171.817	9
82	371.6	0.8964	176.781	6
84	372.3	0.9957	182.573	5
53	371.6	1.0098	182.641	5
86	372.5	1.5	210.014	6
50	373.1	1.9974	236.698	12
88	372.3	3.0077	290.751	22
96	295.3	0.3989	118.452	400
95	294.6	0.5011	122.726	115
94	292.4	0.6036	126.725	38
93	293.4	0.8038	135.344	13
92	292.9	1.0116	143.962	10
91	295.9	1.9776	186.778	15

Test #	Temp (K)	Equivalence Ratio	Pressure (kPa)	Cell Size (mm)
46	287.6	0.4807	100.801	210
47	323.1	0.4788	101.008	135
48	373.1	0.4701	100.87	106
49	372.1	0.4848	100.87	65
11	276.9	0.4792	99.284	190
44	370.1	0.4853	127.69	130
45	323.6	0.4736	111.902	140

Appendix B - Raw Schlieren Images

Figure B - 1 to Figure B - 60 include all of the raw images of the 15 cases of hydrogen and air detonations. There are two images of each wave to show in color mapping and grey scale. In some instances it was easier to see the transverse waves or triple points in color or in grey. Not all images were used in the analysis. Specifically, Figure B - 20, Figure B - 21, Figure B - 59, and Figure B - 60 were not used due to poor image quality.

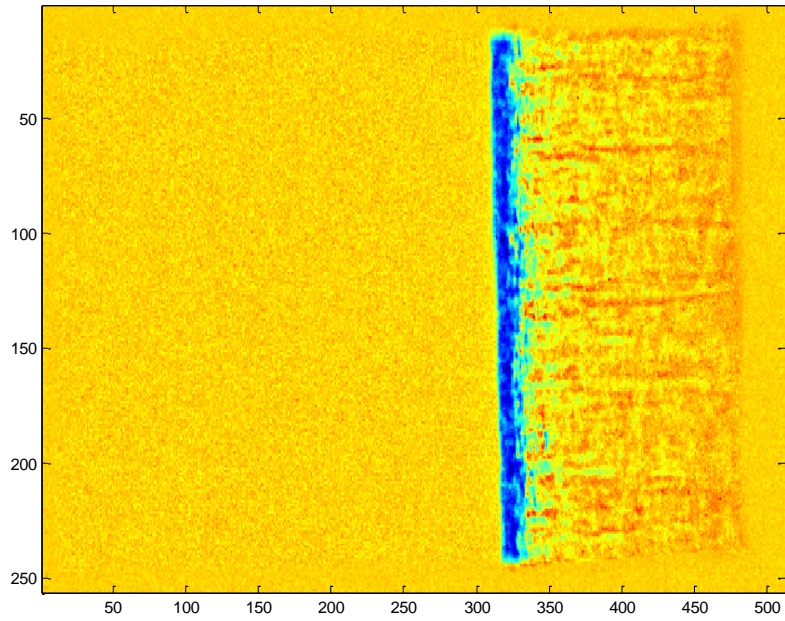


Figure B - 1. Schlieren image of hydrogen and air detonation ($P = 1.0$ atm, $\Phi = 1.0$)

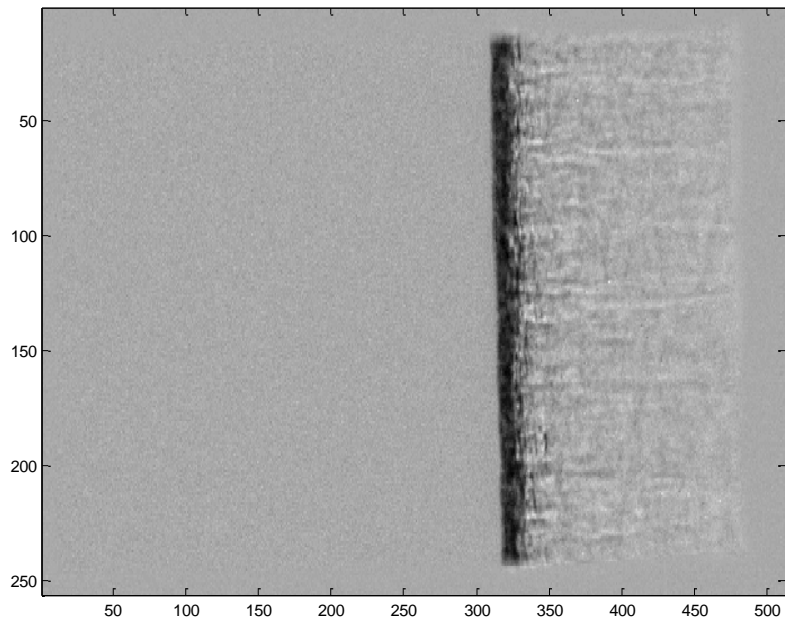


Figure B - 2. Schlieren image of hydrogen and air detonation ($P = 1.0$ atm, $\Phi = 1.0$)

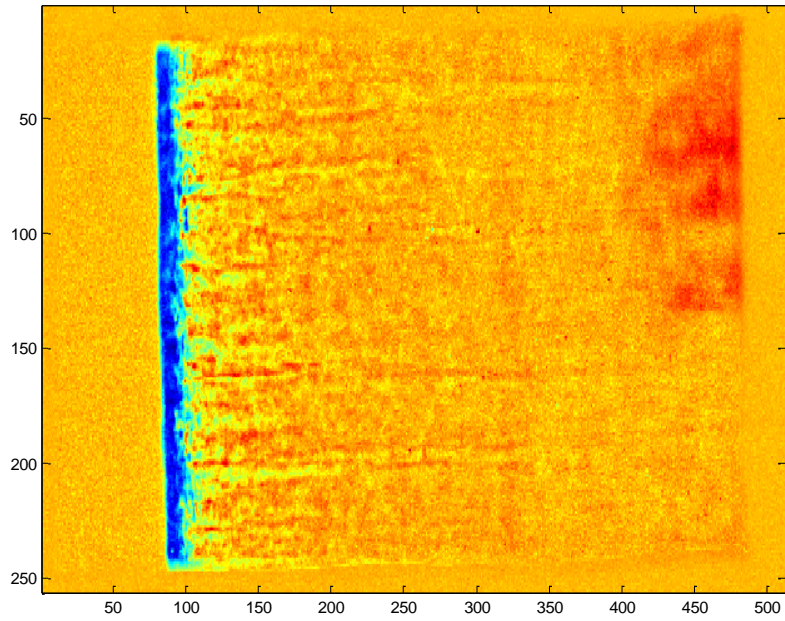


Figure B - 3. Schlieren image of hydrogen and air detonation ($P = 1.0$ atm, $\Phi = 1.0$)

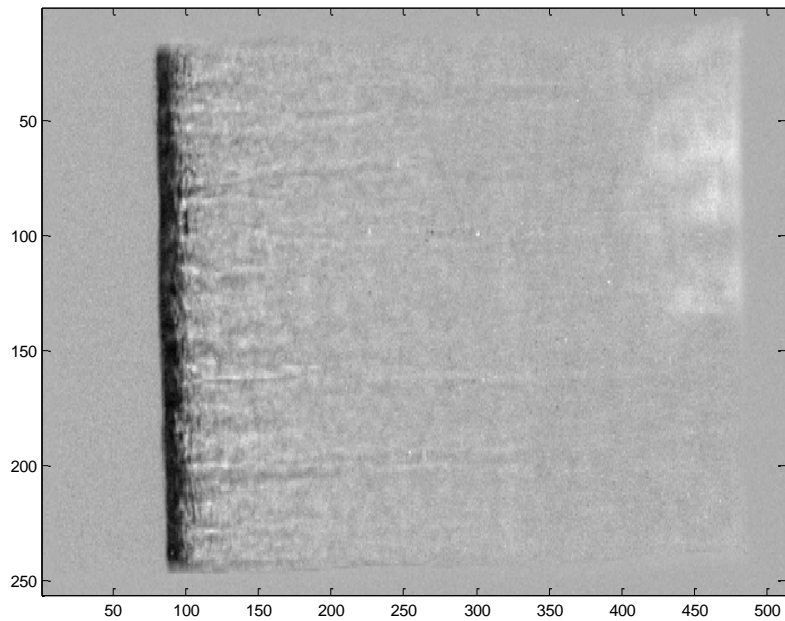


Figure B - 4. Schlieren image of hydrogen and air detonation ($P = 1.0$ atm, $\Phi = 1.0$)

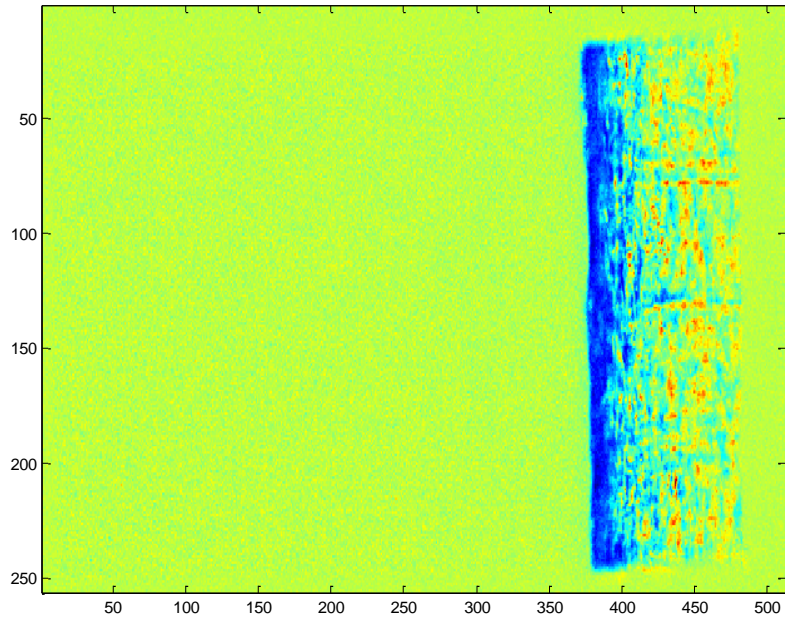


Figure B - 5. Schlieren image of hydrogen and air detonation ($P = 2.0$ atm, $\Phi = 0.8$)

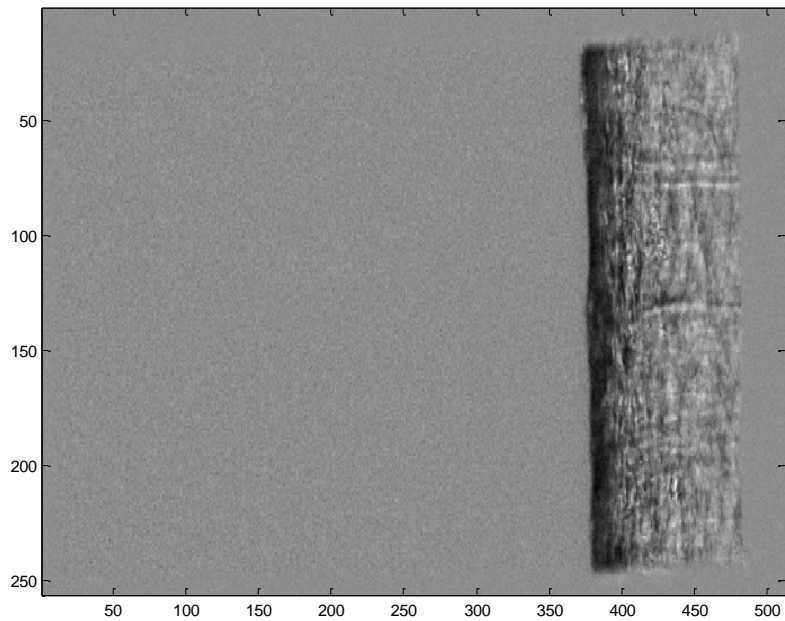


Figure B - 6. Schlieren image of hydrogen and air detonation ($P = 2.0$ atm, $\Phi = 0.8$)

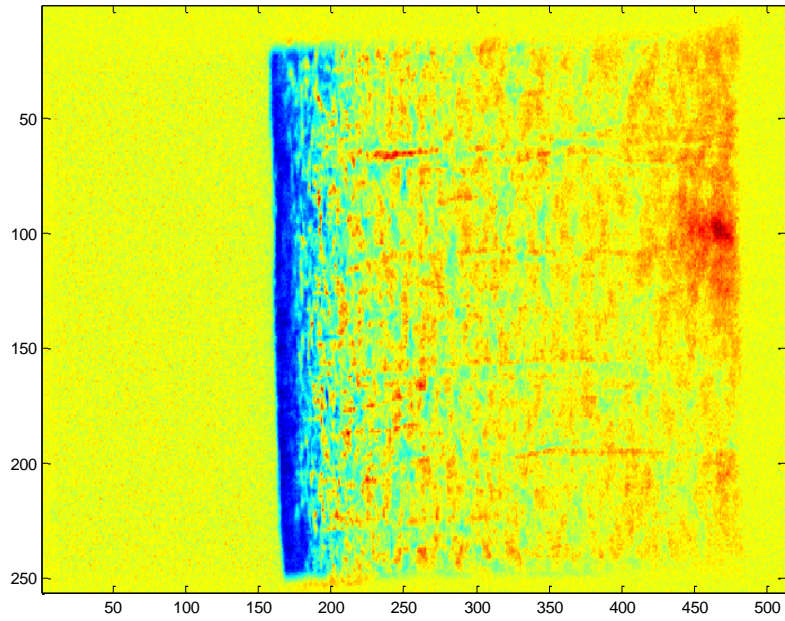


Figure B - 7. Schlieren image of hydrogen and air detonation ($P = 2.0$ atm, $\Phi = 0.8$)

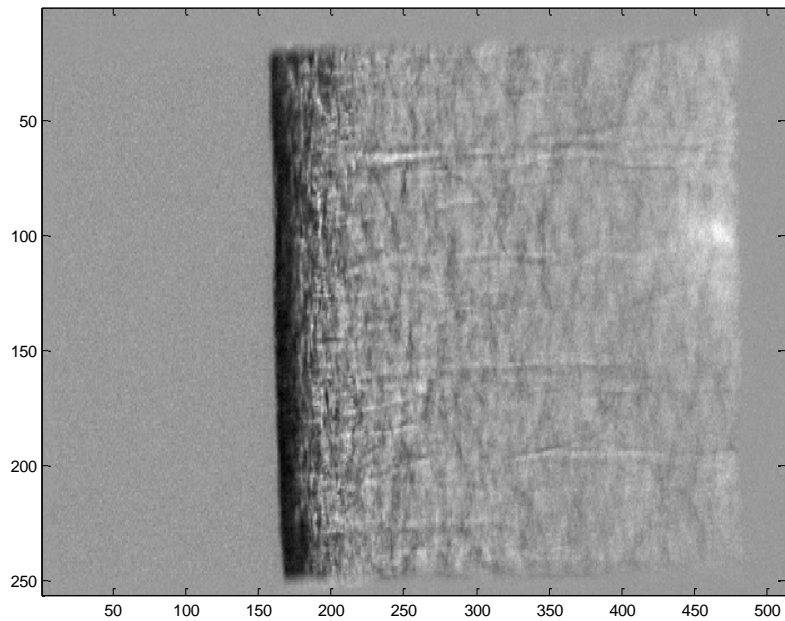


Figure B - 8. Schlieren image of hydrogen and air detonation ($P = 2.0$ atm, $\Phi = 0.8$)

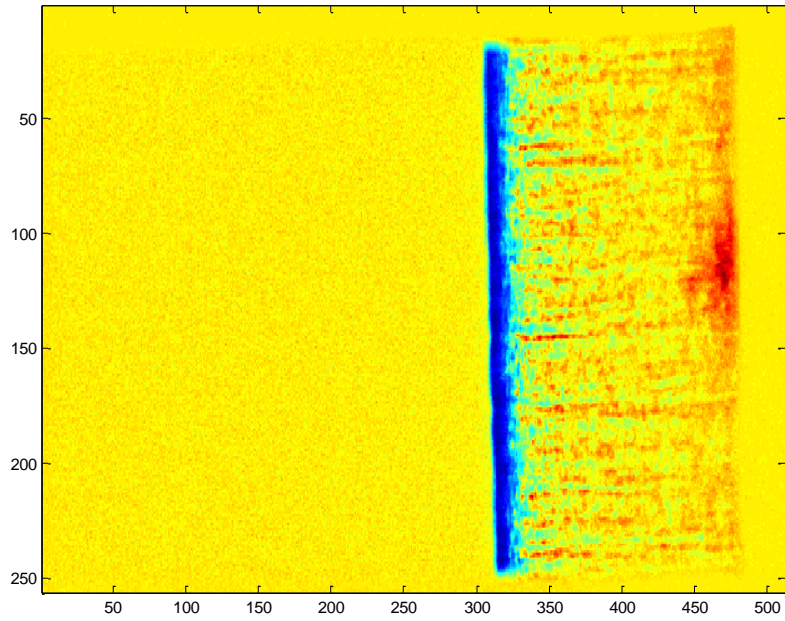


Figure B - 9. Schlieren image of hydrogen and air detonation ($P = 2.0$ atm, $\Phi = 1.0$)

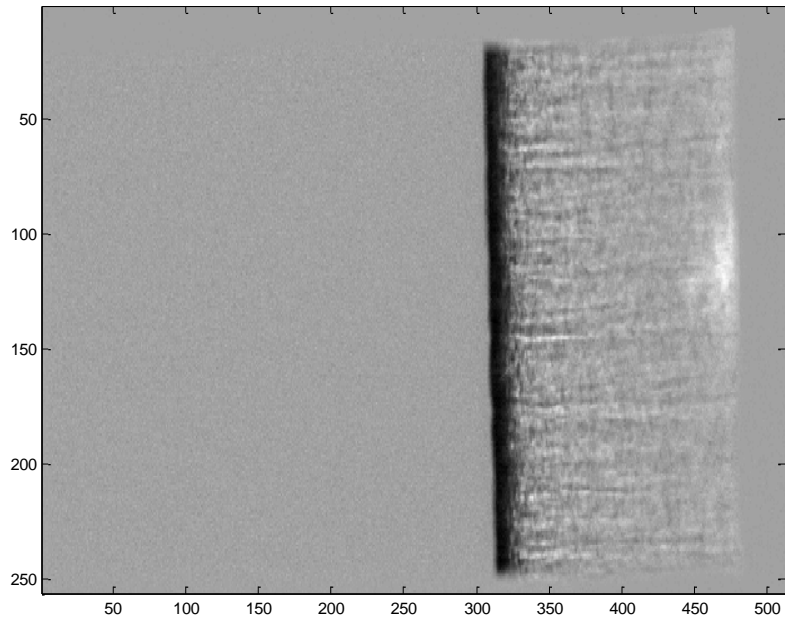


Figure B - 10. Schlieren image of hydrogen and air detonation ($P = 2.0$ atm, $\Phi = 1.0$)

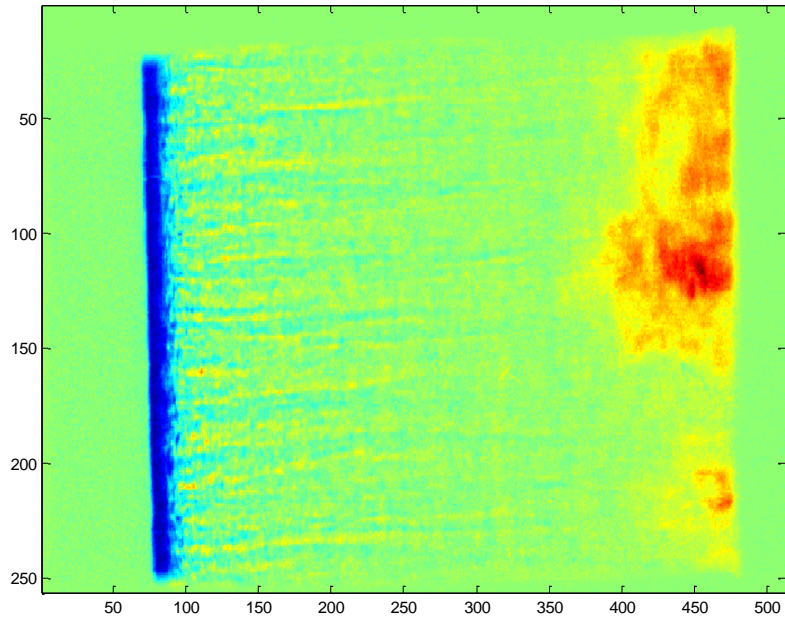


Figure B - 11. Schlieren image of hydrogen and air detonation ($P = 2.0$ atm, $\Phi = 1.0$)

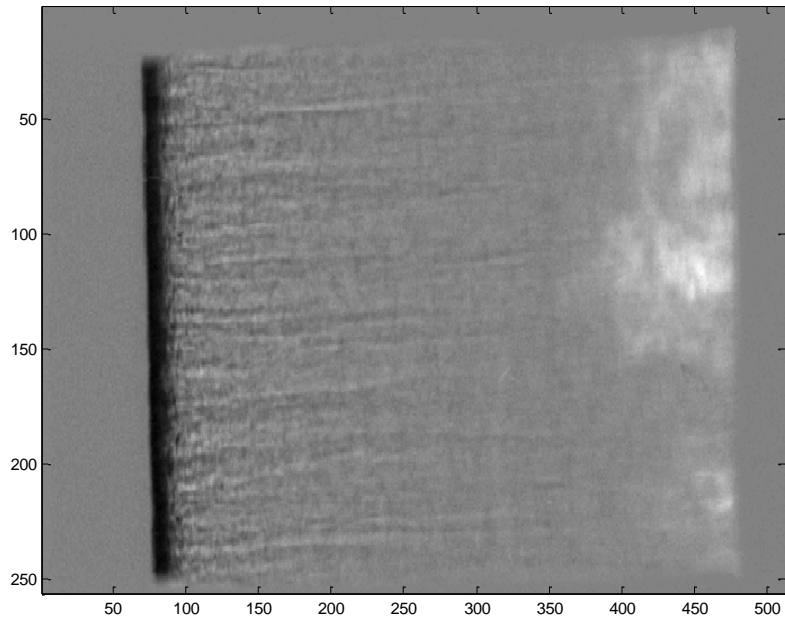


Figure B - 12. Schlieren image of hydrogen and air detonation ($P = 2.0$ atm, $\Phi = 1.0$)

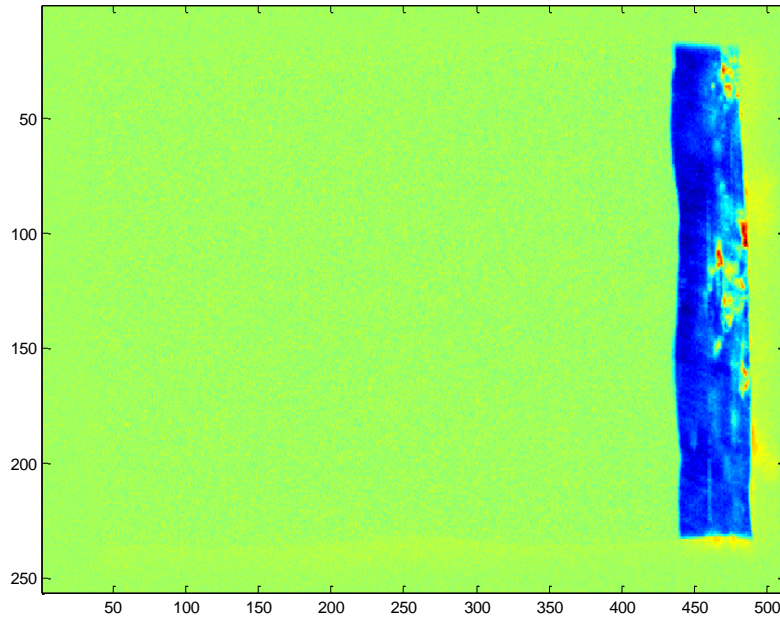


Figure B - 13. Schlieren image of hydrogen and air detonation ($P = 4.0$ atm, $\Phi = 0.7$)

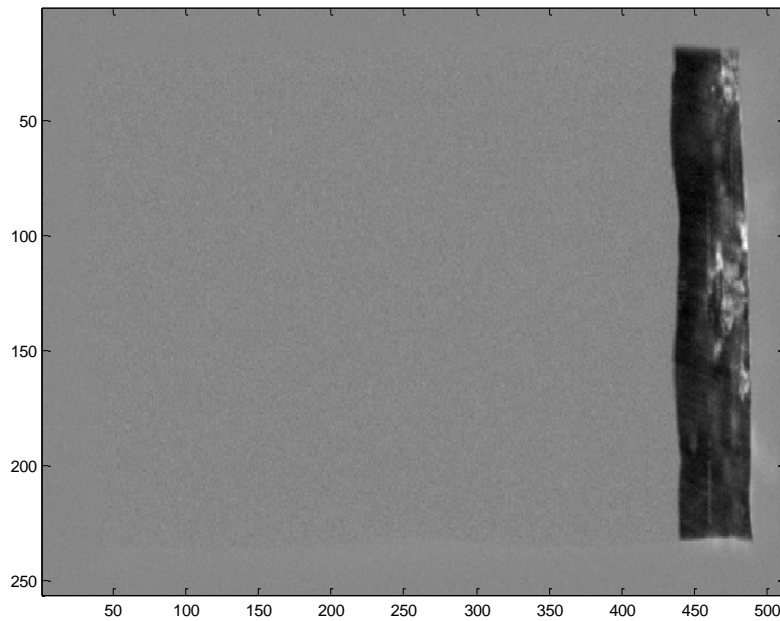


Figure B - 14. Schlieren image of hydrogen and air detonation ($P = 4.0$ atm, $\Phi = 0.7$)

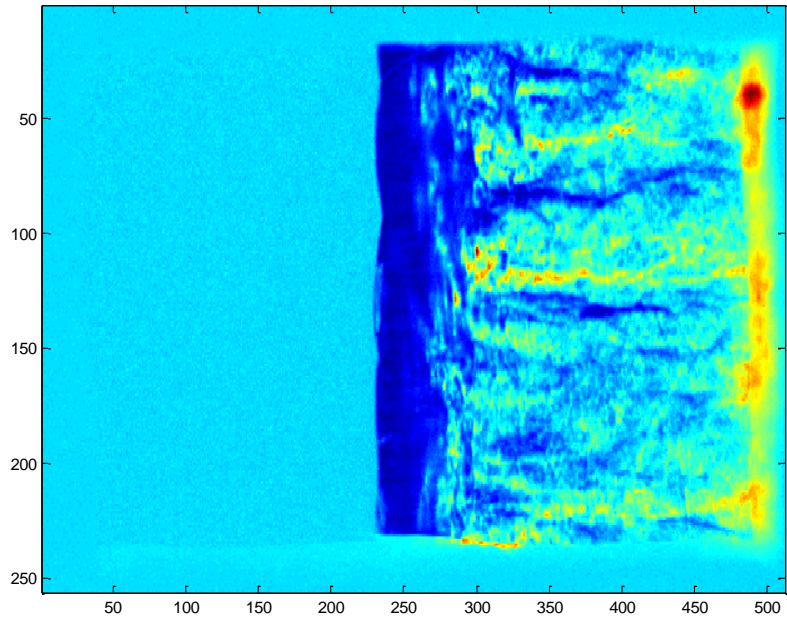


Figure B - 15. Schlieren image of hydrogen and air detonation ($P = 4.0$ atm, $\Phi = 0.7$)

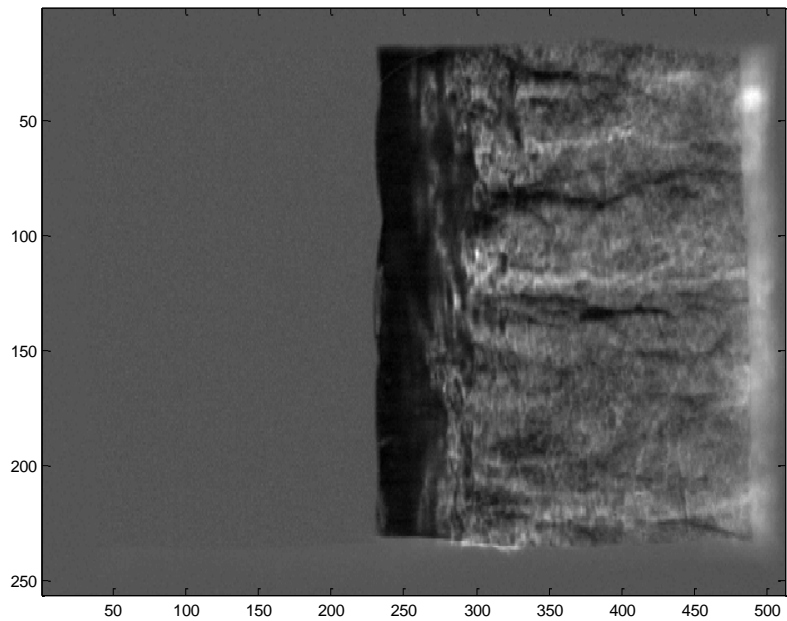


Figure B - 16. Schlieren image of hydrogen and air detonation ($P = 4.0$ atm, $\Phi = 0.7$)

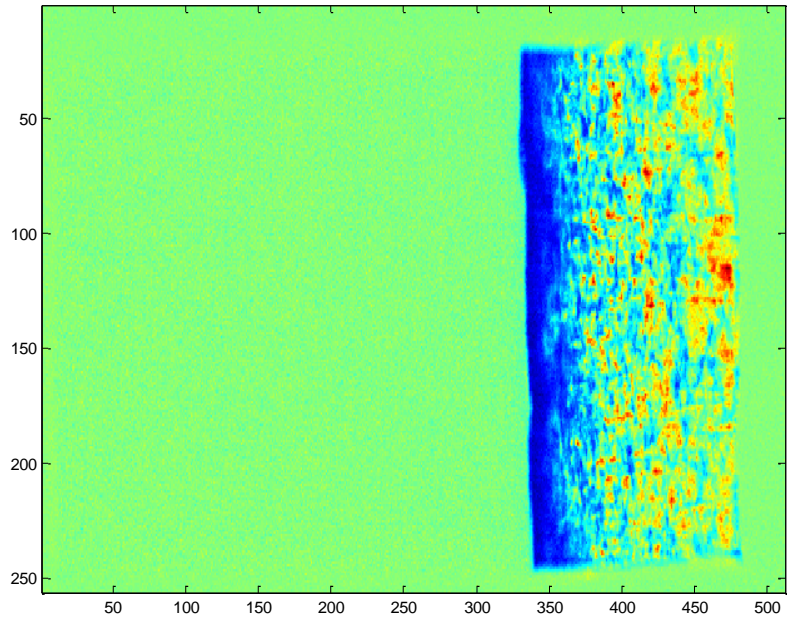


Figure B - 17. Schlieren image of hydrogen and air detonation ($P = 4.0$ atm, $\Phi = 0.8$)

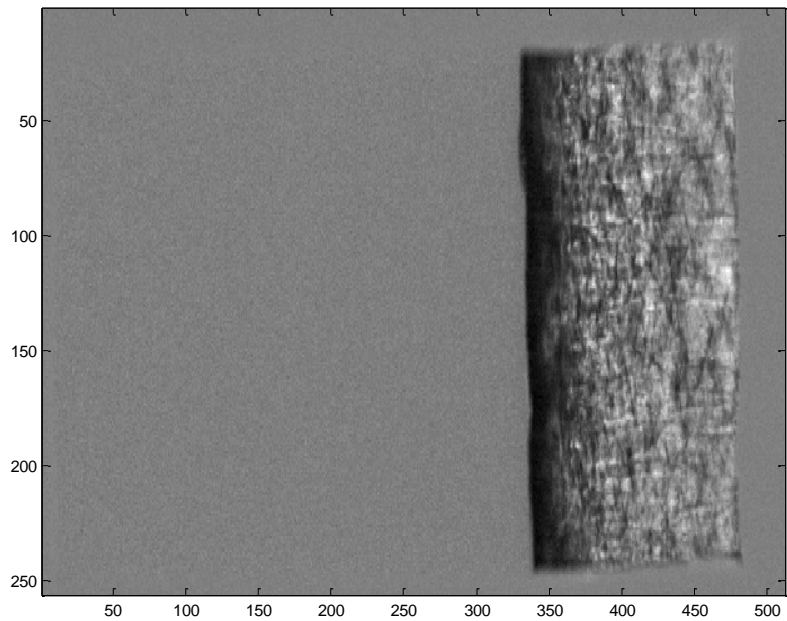


Figure B - 18. Schlieren image of hydrogen and air detonation ($P = 4.0$ atm, $\Phi = 0.8$)

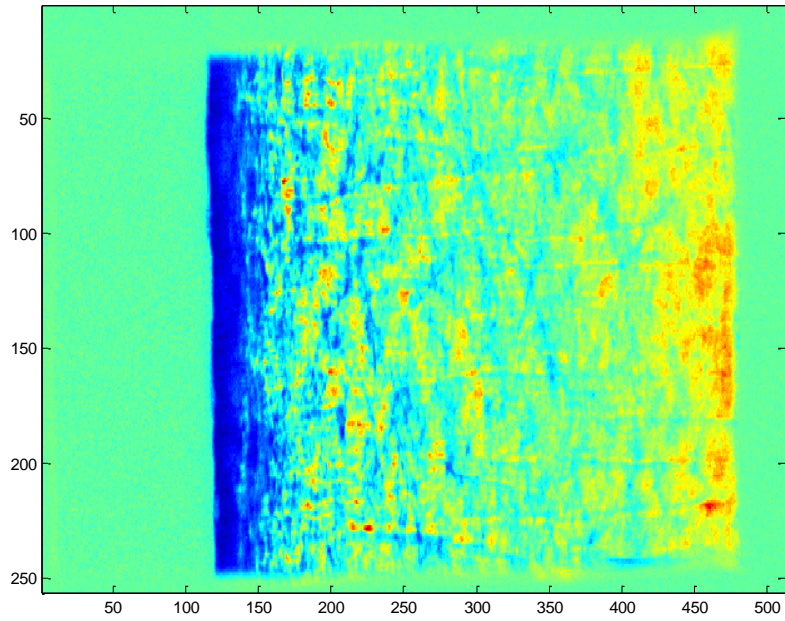


Figure B - 19. Schlieren image of hydrogen and air detonation ($P = 4.0$ atm, $\Phi = 0.8$)

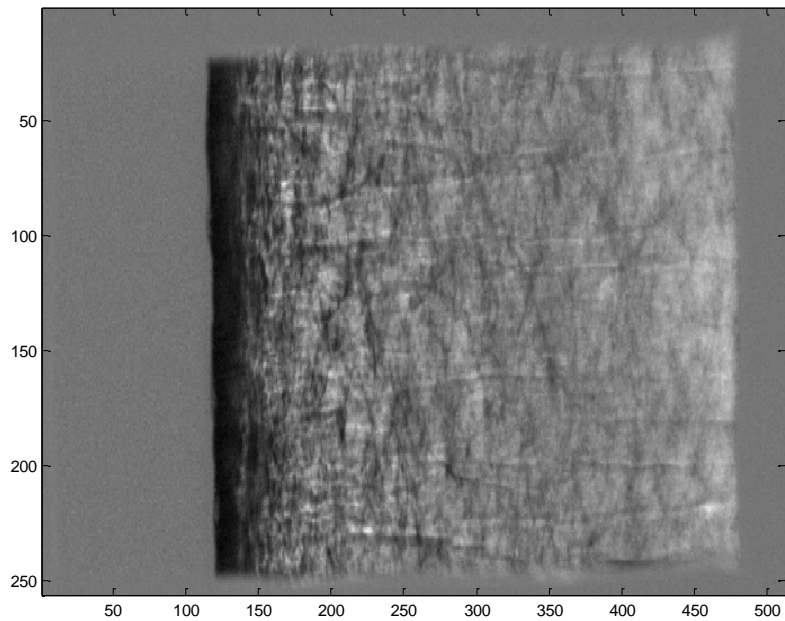


Figure B - 20. Schlieren image of hydrogen and air detonation ($P = 4.0$ atm, $\Phi = 0.8$)

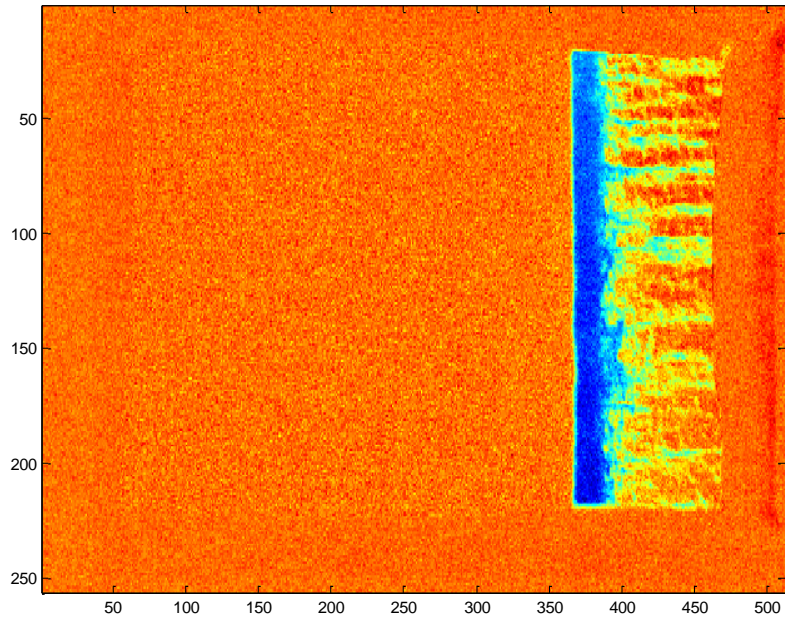


Figure B - 21. Schlieren image of hydrogen and air detonation ($P = 4.0$ atm, $\Phi = 1.0$)

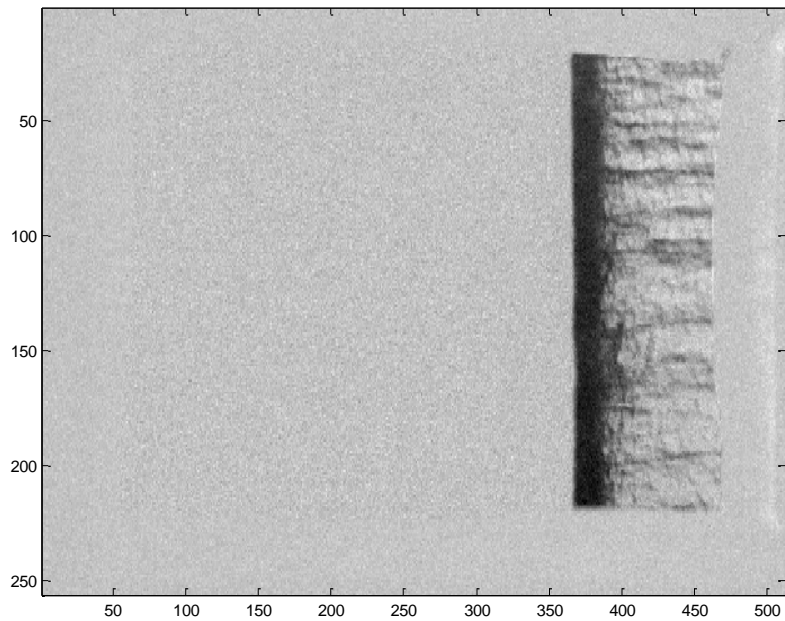


Figure B - 22. Schlieren image of hydrogen and air detonation ($P = 4.0$ atm, $\Phi = 1.0$)

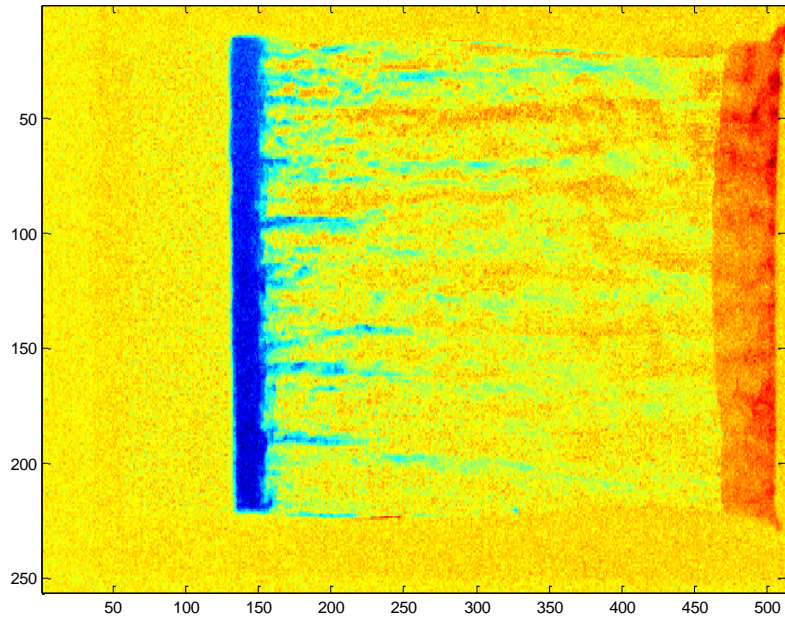


Figure B - 23. Schlieren image of hydrogen and air detonation ($P = 4.0$ atm, $\Phi = 1.0$)

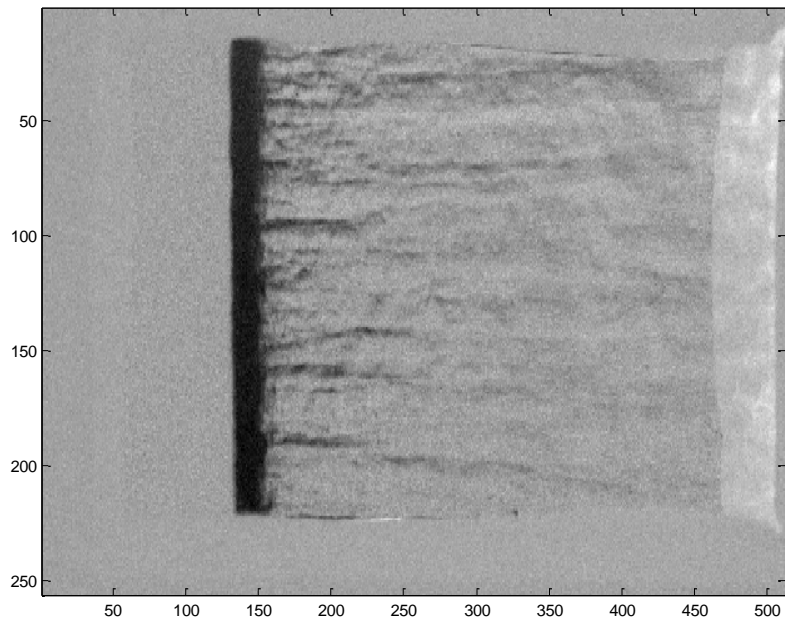


Figure B - 24. Schlieren image of hydrogen and air detonation ($P = 4.0$ atm, $\Phi = 1.0$)

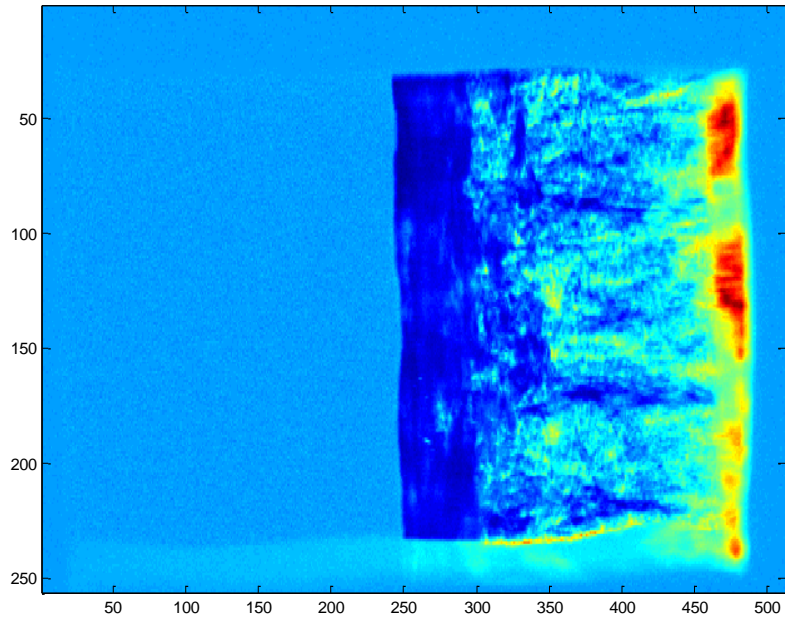


Figure B - 25. Schlieren image of hydrogen-air detonation ($P = 6.0$ atm, $\Phi = 0.65$)

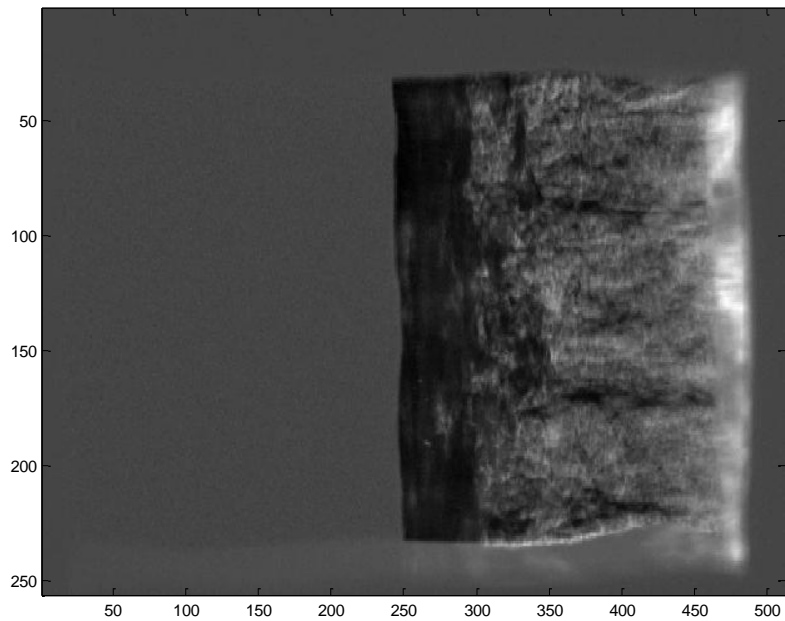


Figure B - 26. Schlieren image of hydrogen-air detonation ($P = 6.0$ atm, $\Phi = 0.65$)

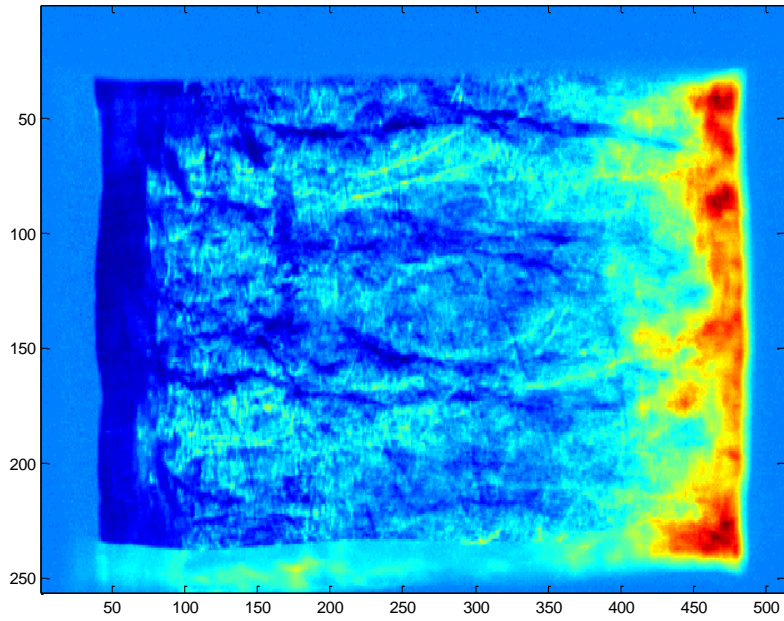


Figure B - 27. Schlieren image of hydrogen-air detonation ($P = 6.0$ atm, $\Phi = 0.65$)

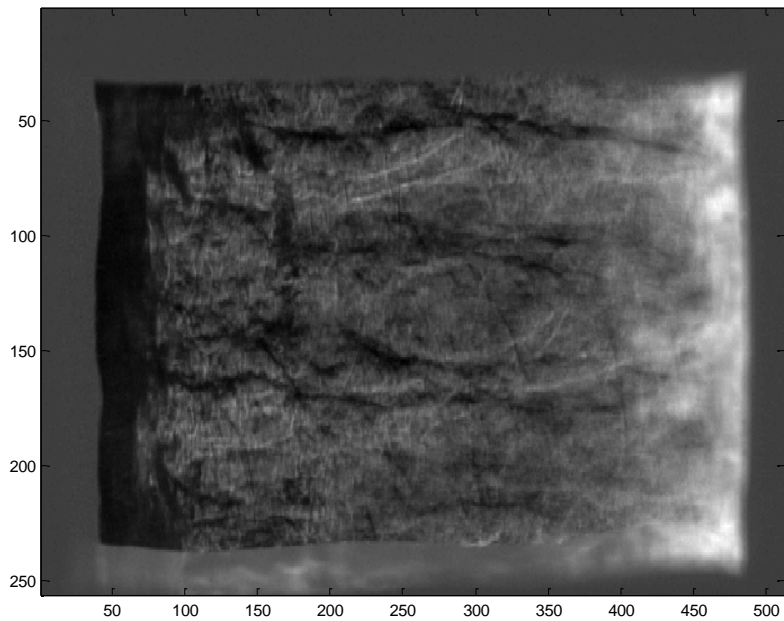


Figure B - 28. Schlieren image of hydrogen-air detonation ($P = 6.0$ atm, $\Phi = 0.65$)

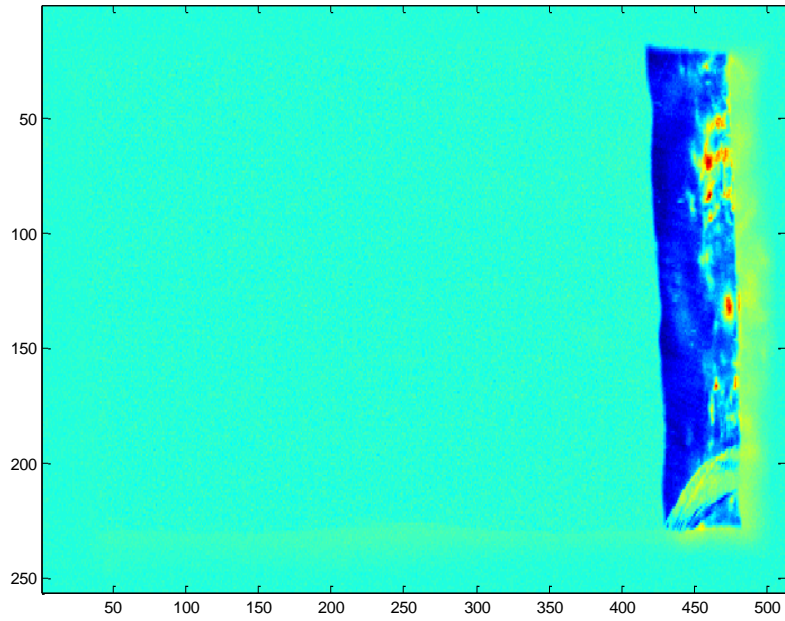


Figure B - 29. Schlieren image of hydrogen-air detonation ($P = 6.0$ atm, $\Phi = 0.70$)

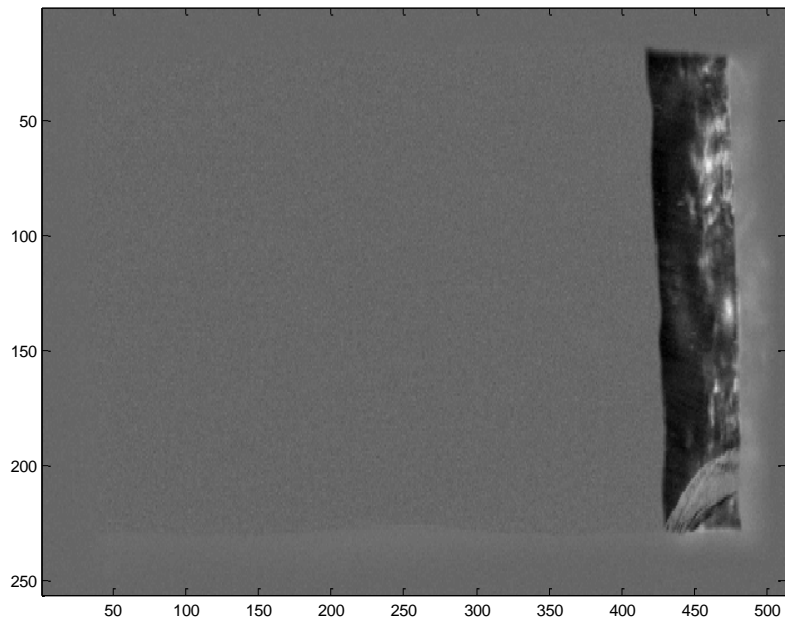


Figure B - 30. Schlieren image of hydrogen-air detonation ($P = 6.0$ atm, $\Phi = 0.70$)

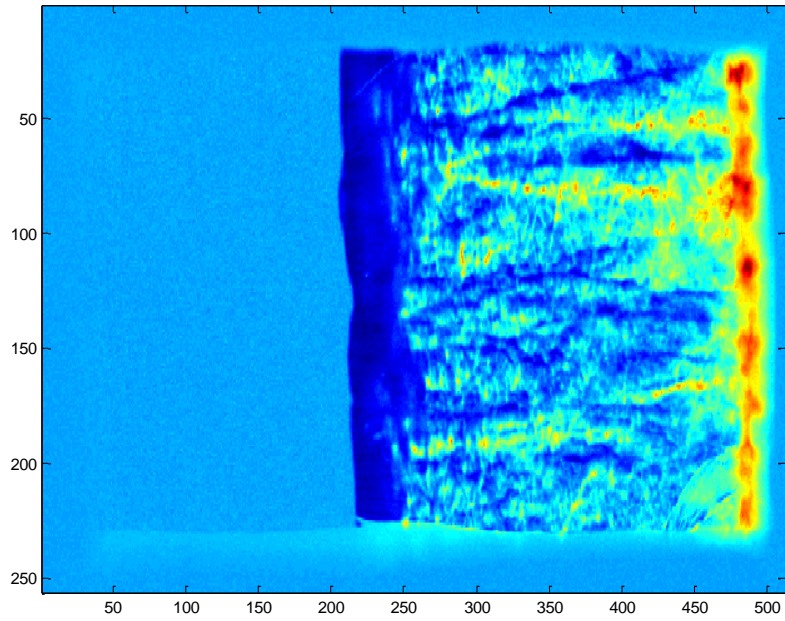


Figure B - 31. Schlieren image of hydrogen-air detonation ($P = 6.0$ atm, $\Phi = 0.70$)

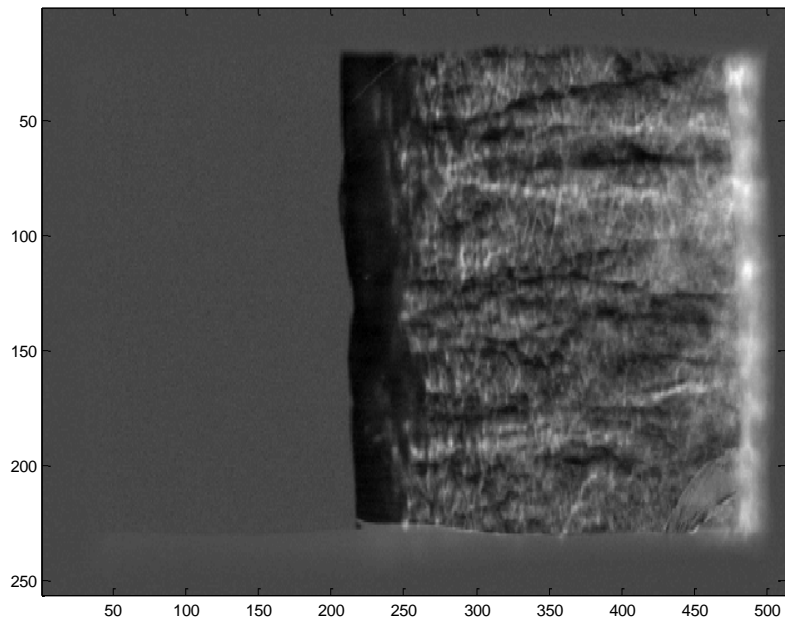


Figure B - 32. Schlieren image of hydrogen-air detonation ($P = 6.0$ atm, $\Phi = 0.70$)

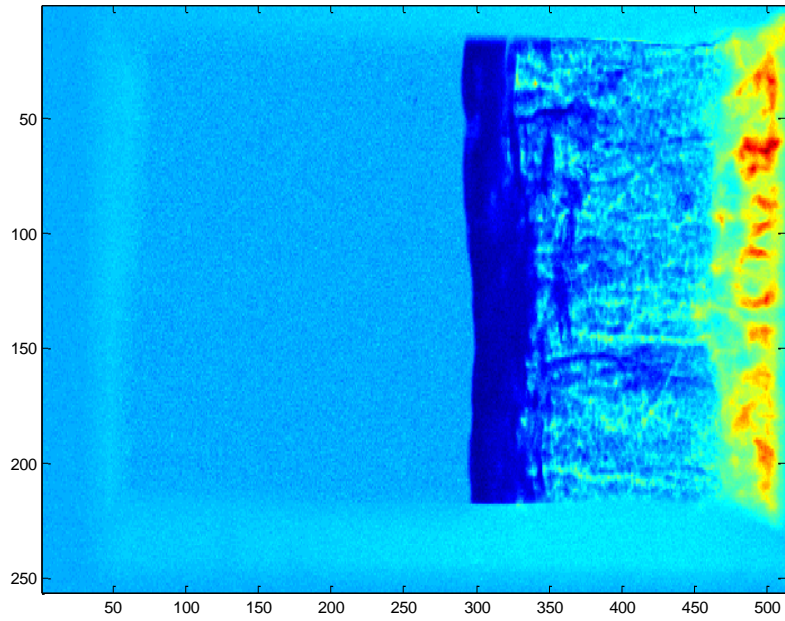


Figure B - 33. Schlieren image of hydrogen-air detonation ($P = 6.0$ atm, $\Phi = 0.80$)

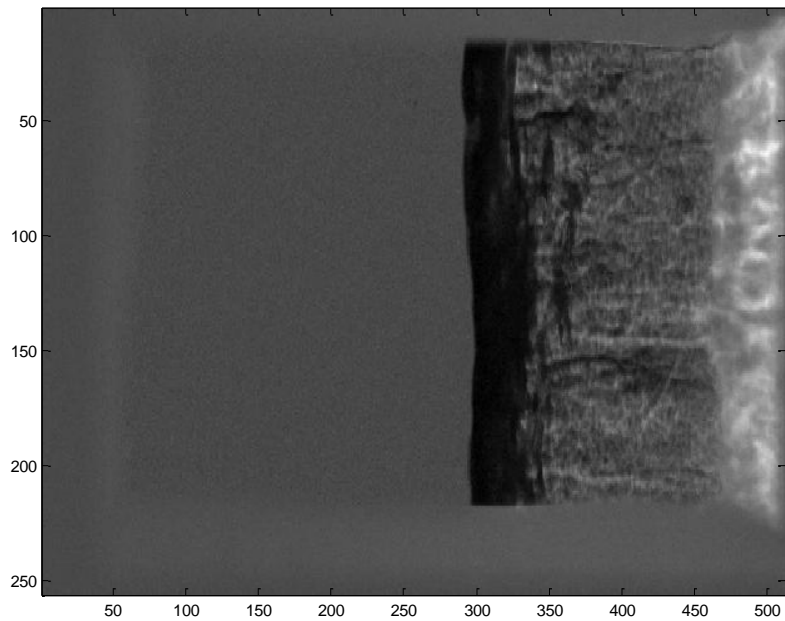


Figure B - 34. Schlieren image of hydrogen-air detonation ($P = 6.0$ atm, $\Phi = 0.80$)

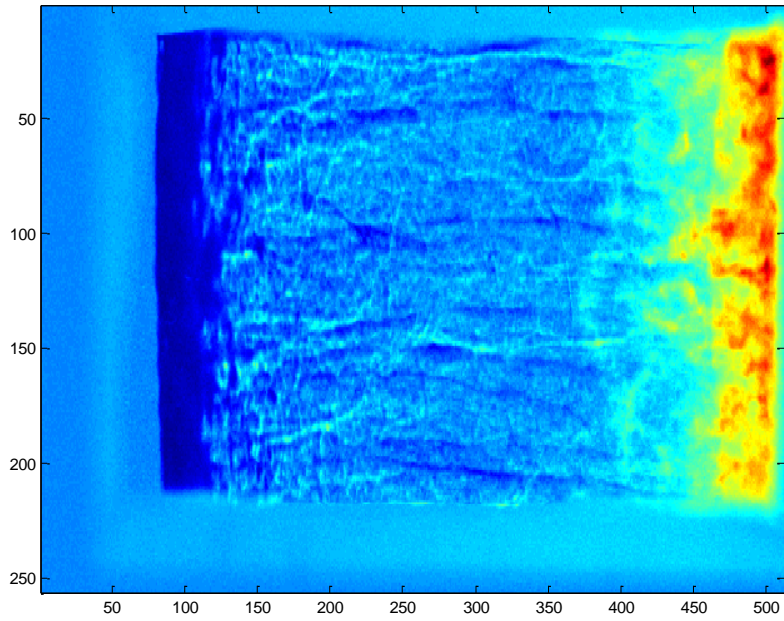


Figure B - 35. Schlieren image of hydrogen-air detonation ($P = 6.0$ atm, $\Phi = 0.80$)

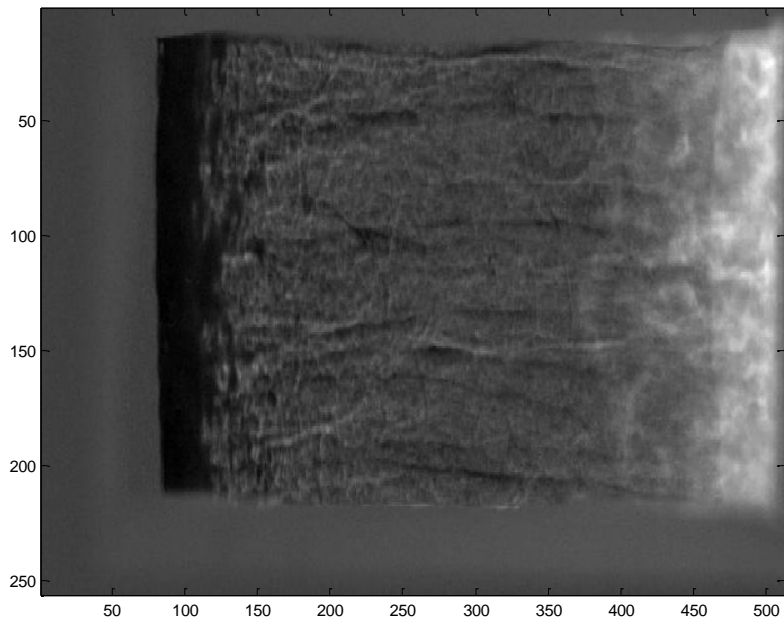


Figure B - 36. Schlieren image of hydrogen-air detonation ($P = 6.0$ atm, $\Phi = 0.80$)

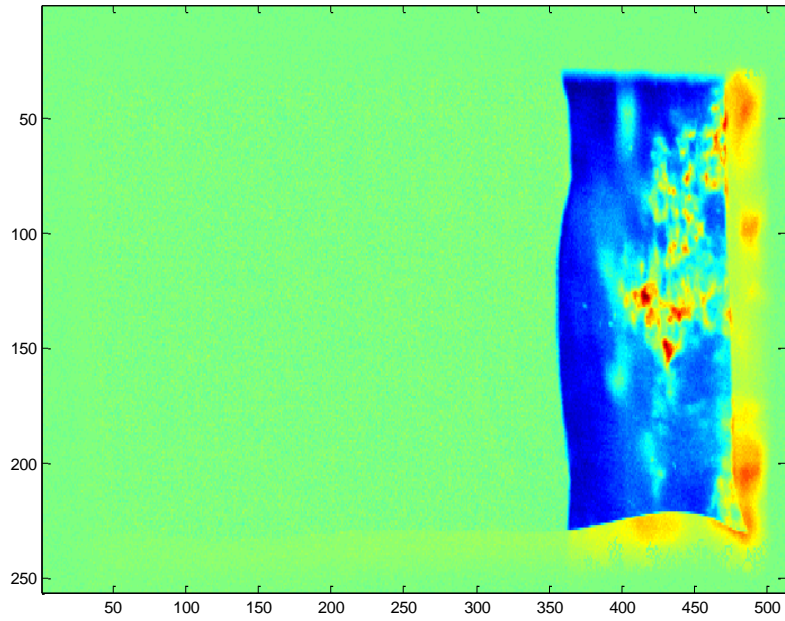


Figure B - 37. Schlieren image of hydrogen-air detonation ($P = 8.0$ atm, $\Phi = 0.65$)

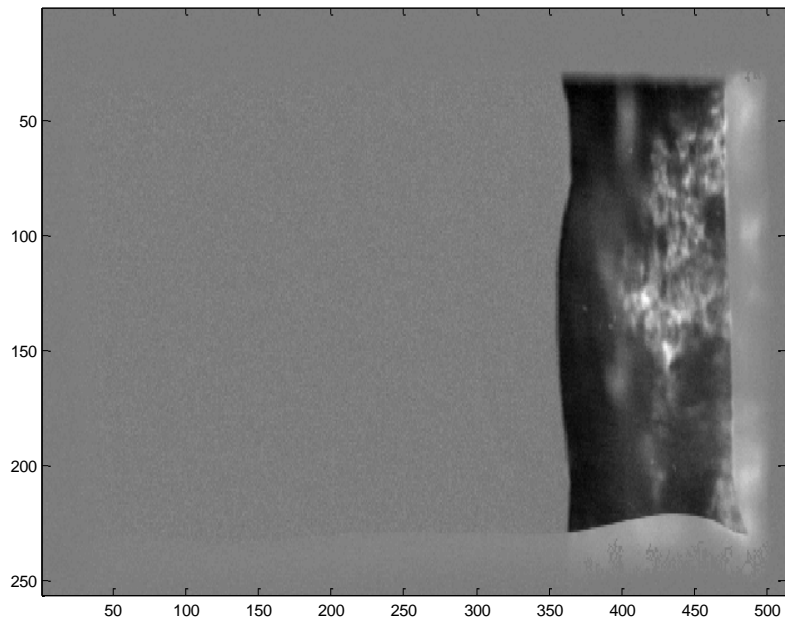


Figure B - 38. Schlieren image of hydrogen-air detonation ($P = 8.0$ atm, $\Phi = 0.65$)

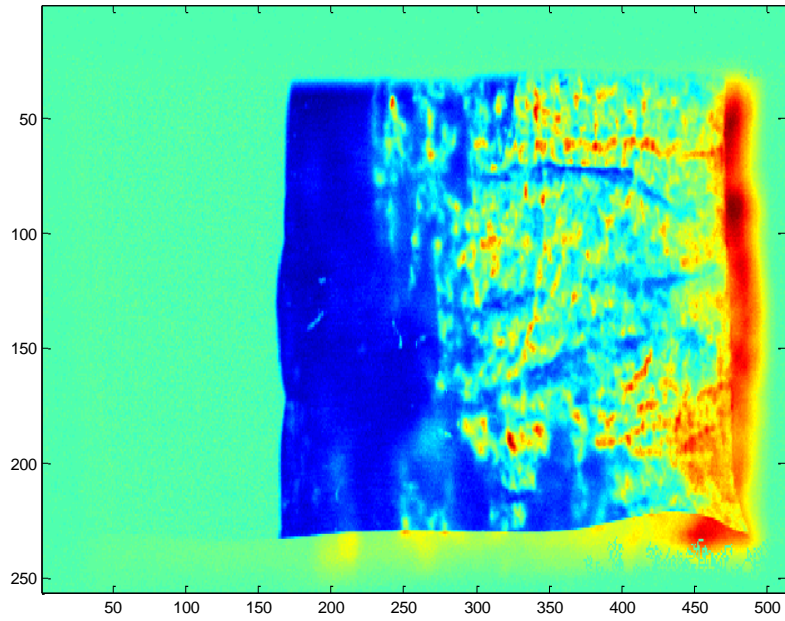


Figure B - 39. Schlieren image of hydrogen-air detonation ($P = 8.0 \text{ atm}$, $\Phi = 0.65$)

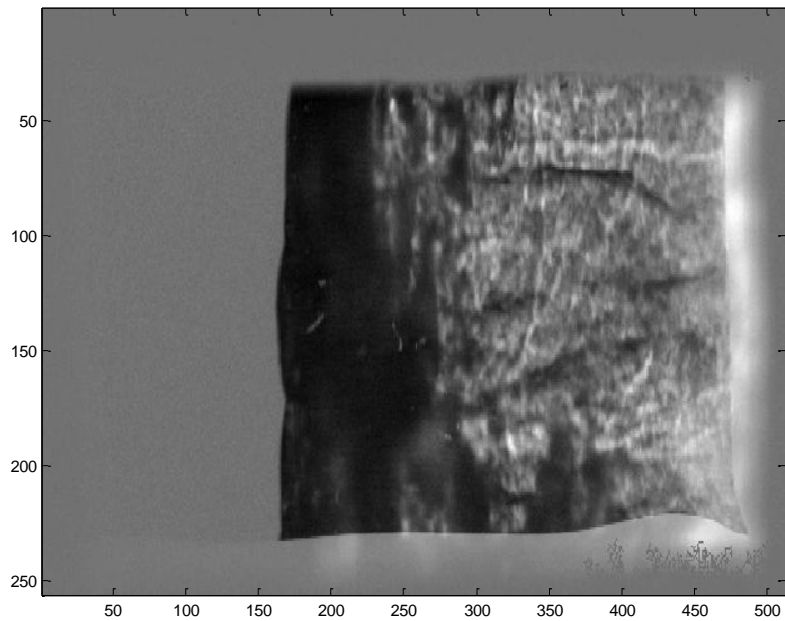


Figure B - 40. Schlieren image of hydrogen-air detonation ($P = 8.0 \text{ atm}$, $\Phi = 0.65$)

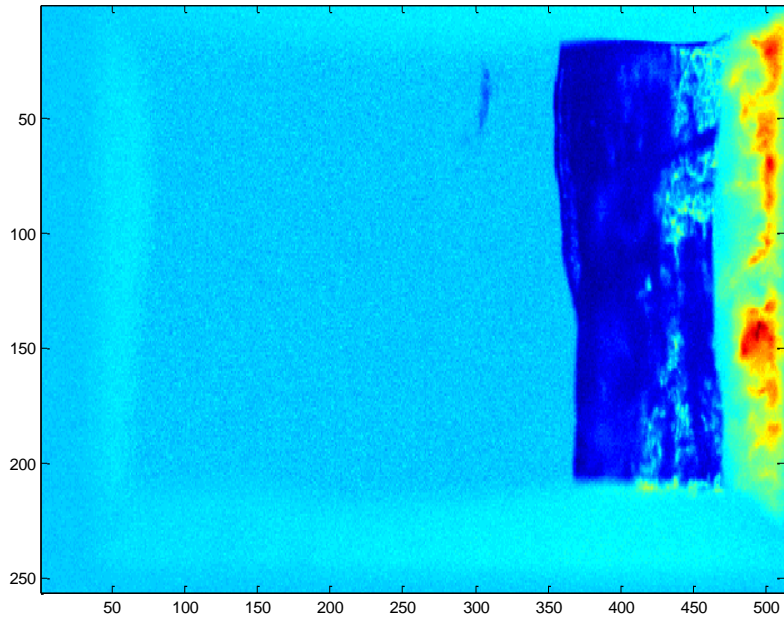


Figure B - 41. Schlieren image of hydrogen-air detonation ($P = 8.0$ atm, $\Phi = 0.70$)

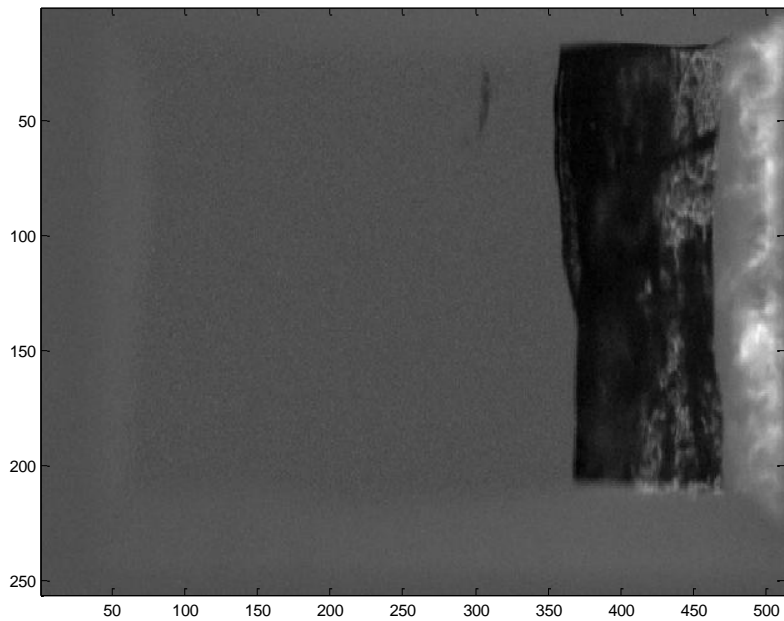


Figure B - 42. Schlieren image of hydrogen-air detonation ($P = 8.0$ atm, $\Phi = 0.70$)

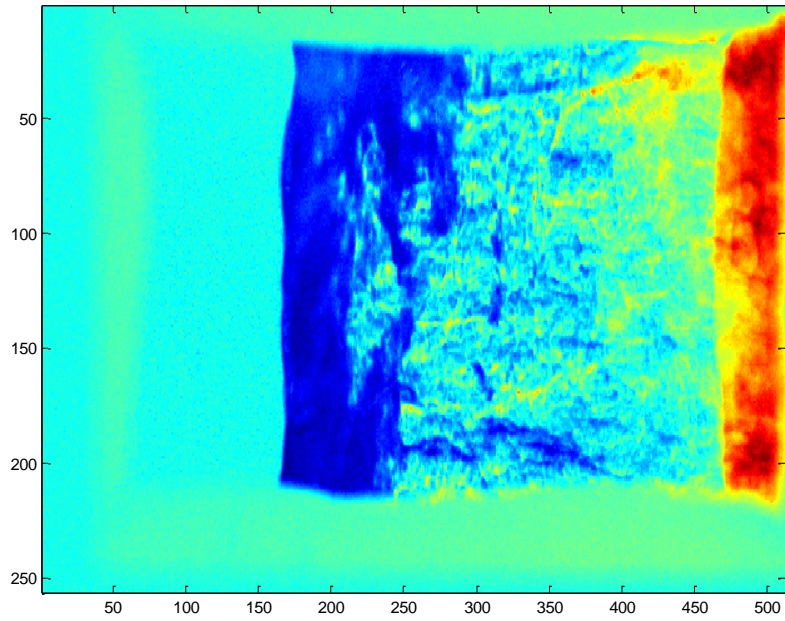


Figure B - 43. Schlieren image of hydrogen-air detonation ($P = 8.0$ atm, $\Phi = 0.70$)

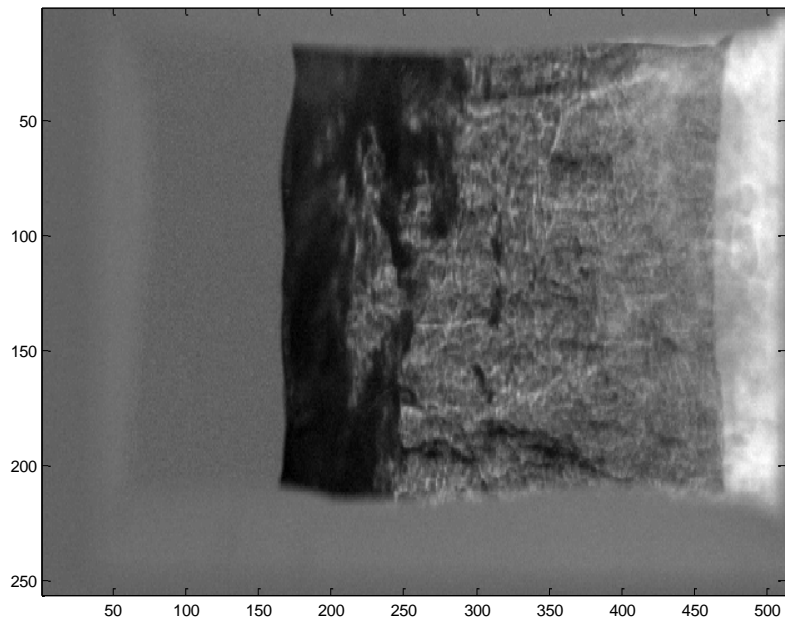


Figure B - 44. Schlieren image of hydrogen-air detonation ($P = 8.0$ atm, $\Phi = 0.70$)

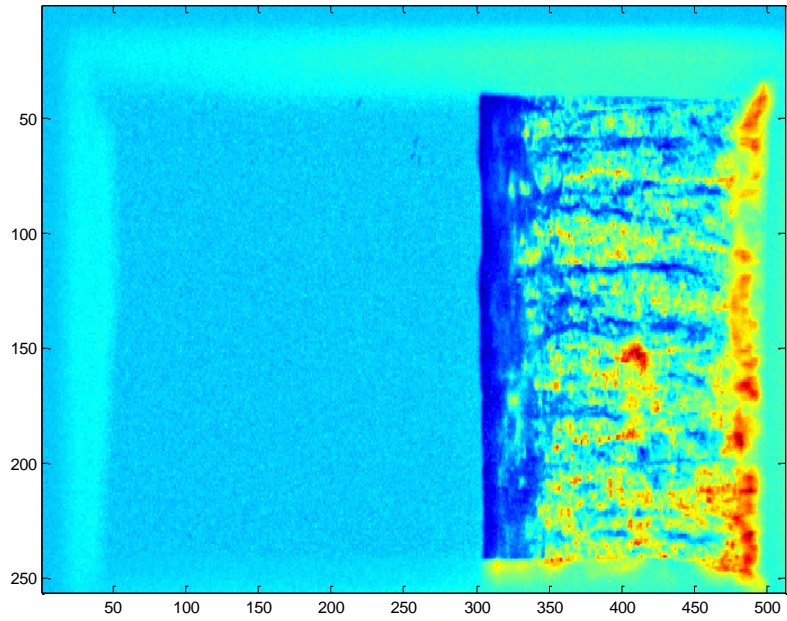


Figure B - 45. Schlieren image of hydrogen-air detonation ($P = 8.0$ atm, $\Phi = 0.80$)

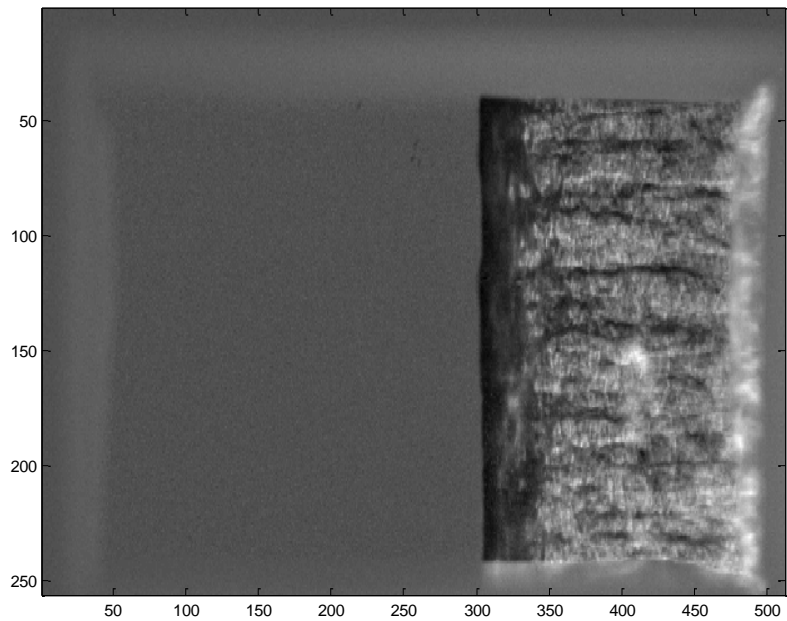


Figure B - 46. Schlieren image of hydrogen-air detonation ($P = 8.0$ atm, $\Phi = 0.80$)

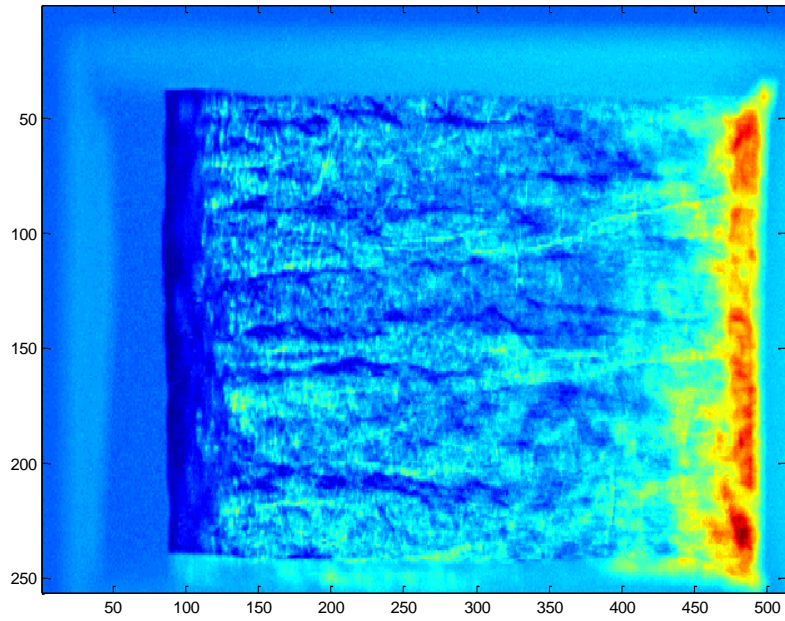


Figure B - 47. Schlieren image of hydrogen-air detonation ($P = 8.0$ atm, $\Phi = 0.80$)

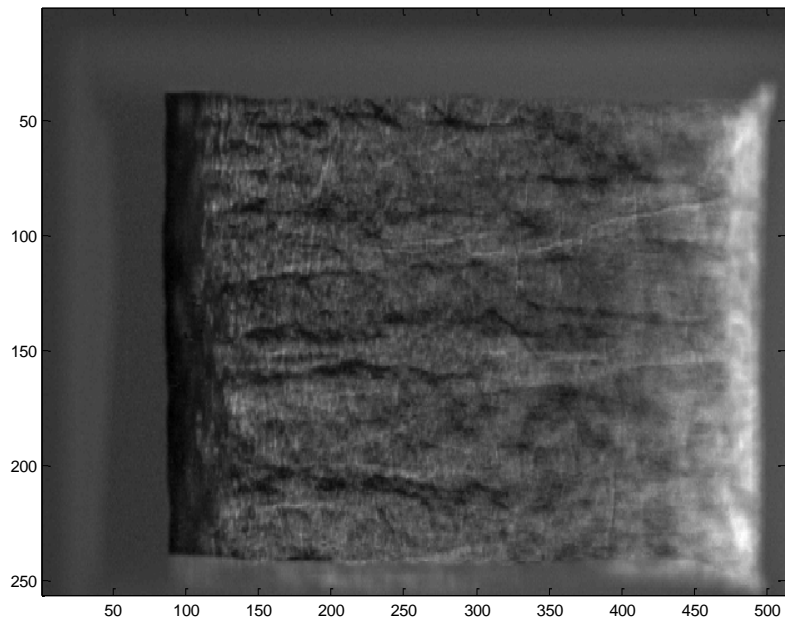


Figure B - 48. Schlieren image of hydrogen-air detonation ($P = 8.0$ atm, $\Phi = 0.80$)

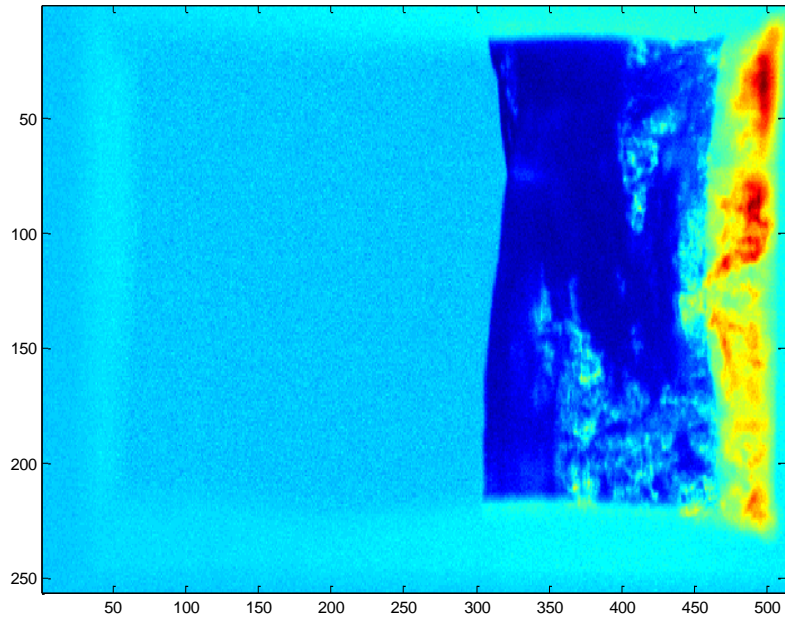


Figure B - 49. Schlieren image of hydrogen-air detonation ($P = 10.0$ atm, $\Phi = 0.65$)

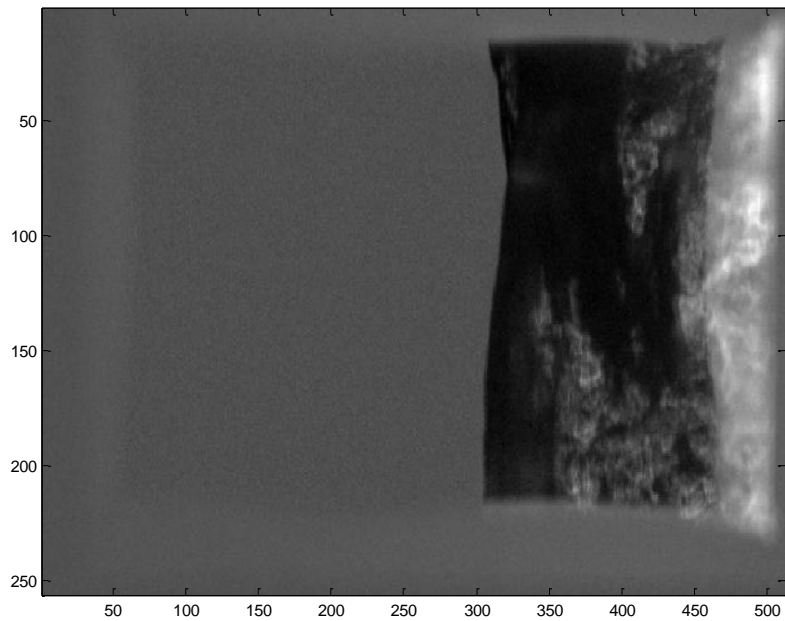


Figure B - 50. Schlieren image of hydrogen-air detonation ($P = 10.0$ atm, $\Phi = 0.65$)

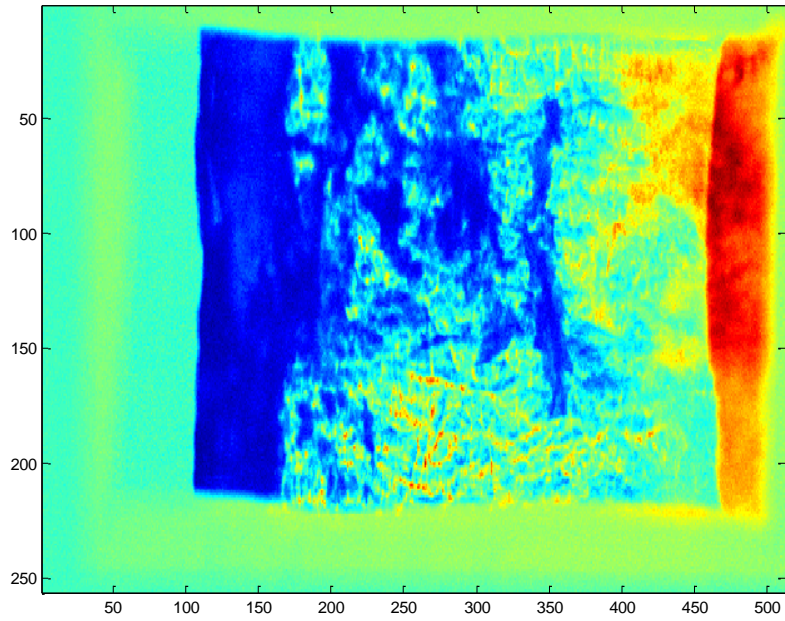


Figure B - 51. Schlieren image of hydrogen-air detonation ($P = 10.0$ atm, $\Phi = 0.65$)

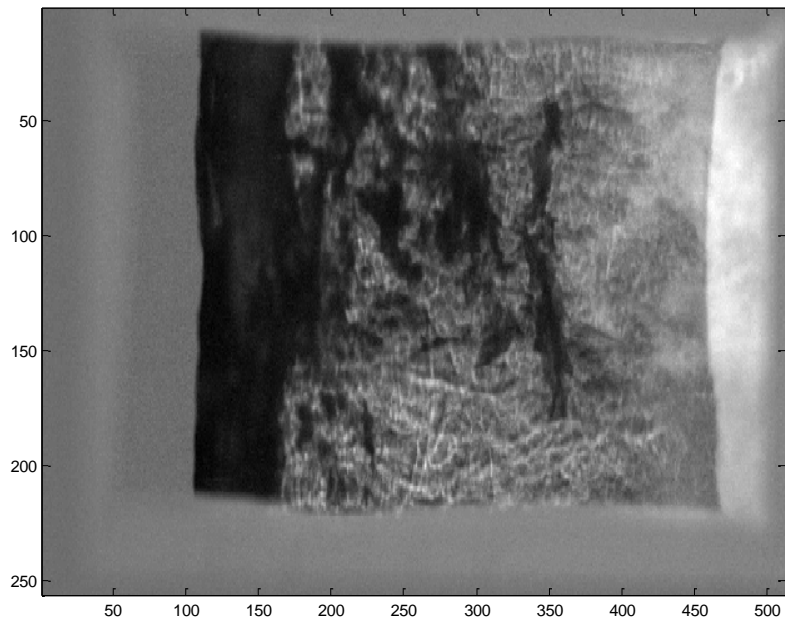


Figure B - 52. Schlieren image of hydrogen-air detonation ($P = 10.0$ atm, $\Phi = 0.65$)

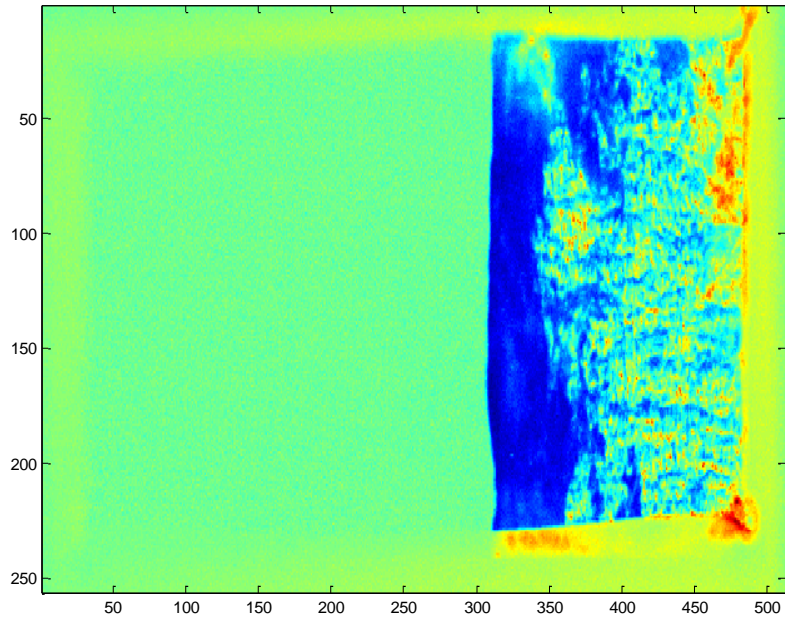


Figure B - 53. Schlieren image of hydrogen-air detonation ($P = 10.0$ atm, $\Phi = 0.70$)

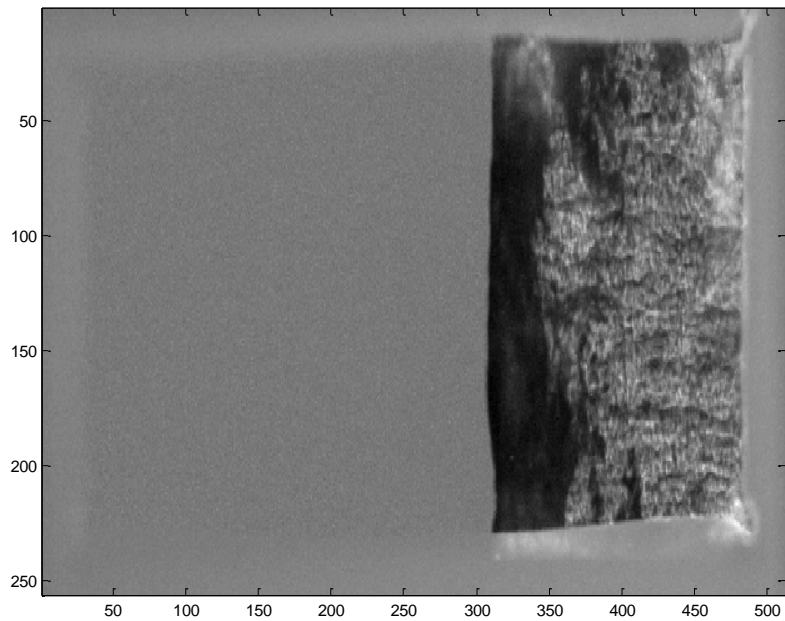


Figure B - 54. Schlieren image of hydrogen-air detonation ($P = 10.0$ atm, $\Phi = 0.70$)

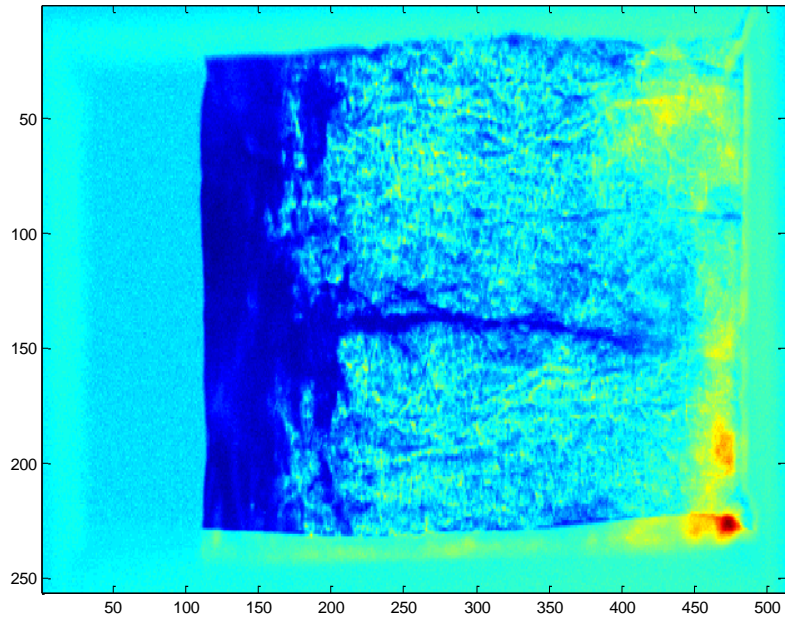


Figure B - 55. Schlieren image of hydrogen-air detonation ($P = 10.0$ atm, $\Phi = 0.70$)

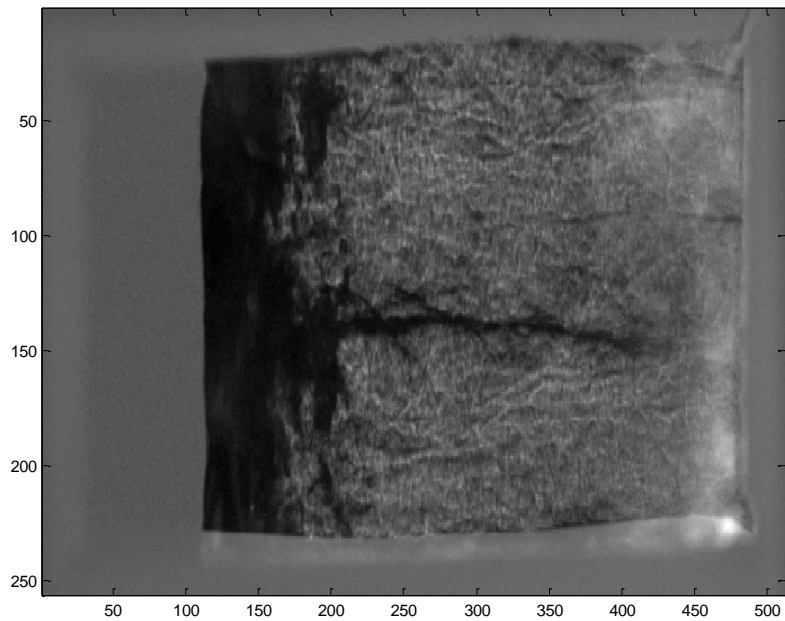


Figure B - 56. Schlieren image of hydrogen-air detonation ($P = 10.0$ atm, $\Phi = 0.70$)

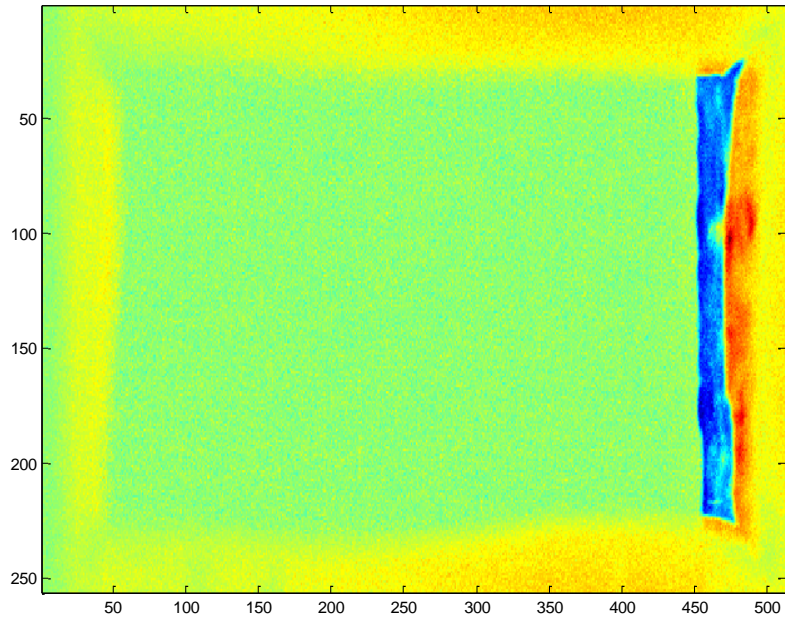


Figure B - 57. Schlieren image of hydrogen-air detonation ($P = 10.0$ atm, $\Phi = 0.80$)

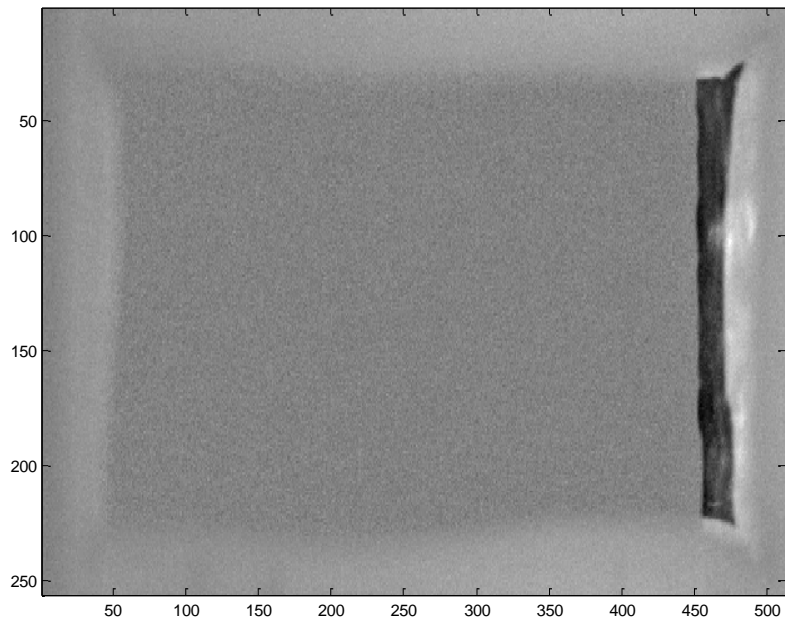


Figure B - 58. Schlieren image of hydrogen-air detonation ($P = 10.0$ atm, $\Phi = 0.80$)

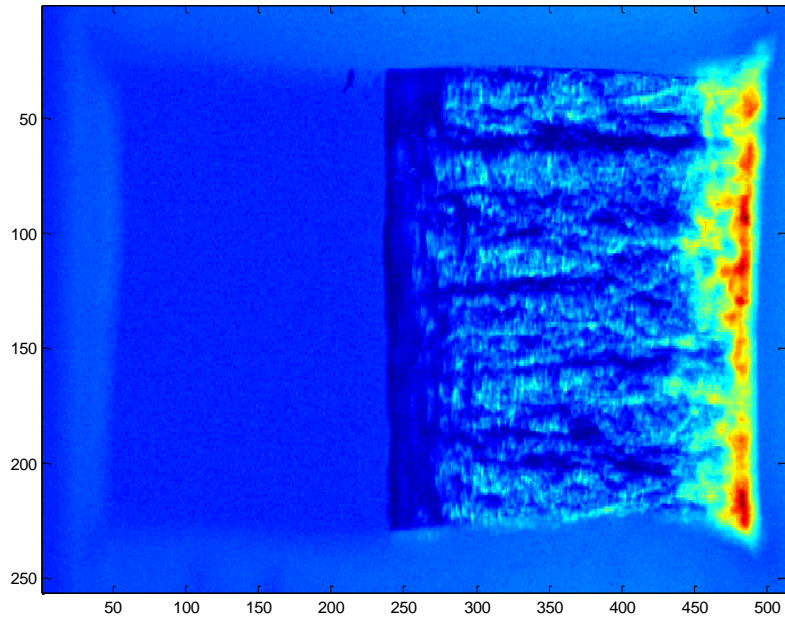


Figure B - 59. Schlieren image of hydrogen-air detonation ($P = 10.0$ atm, $\Phi = 0.80$)

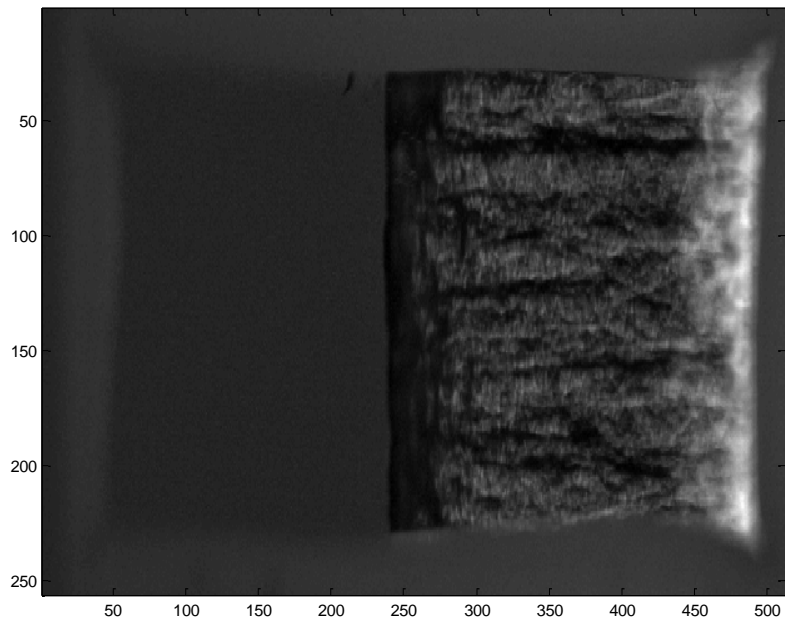


Figure B - 60. Schlieren image of hydrogen-air detonation ($P = 10.0$ atm, $\Phi = 0.80$)

Appendix C - Results by Equivalence Ratio and Pressure

The results by equivalence and pressure display the 15 cases in individual charts to see each trend independently. Each chart contains either a single pressure with changing equivalence ratios or a single equivalence ratio with changing pressures. The charts in Appendix C contain R^2 values and error bars to allow conclusions to be drawn independently of the entire experiment. The R^2 values and error bars were not included into Chapter IV figures because the error bars would overlap. Figure C - 1 to Figure C - 4 show the effect of mixture pressure on cell size by holding equivalence ratio constant with mixture pressure changing. Figure C - 5 to Figure C - 9 show the effect of equivalence ratio on cell size by holding mixture pressure constant with changing equivalence ratios. Figure C - 1 to Figure C - 4 give pressure in torr while Figure C - 5 to Figure C - 9 give trend lines with constant pressure in atm.

Figure C - 1 shows an equivalence ratio of 1.00 with mixture pressures from 1.0 atm to 4.0 atm. This chart contains three data points. The power series trend line yields an exponent of -0.381. The data fits the trend well with an R^2 of 0.958.

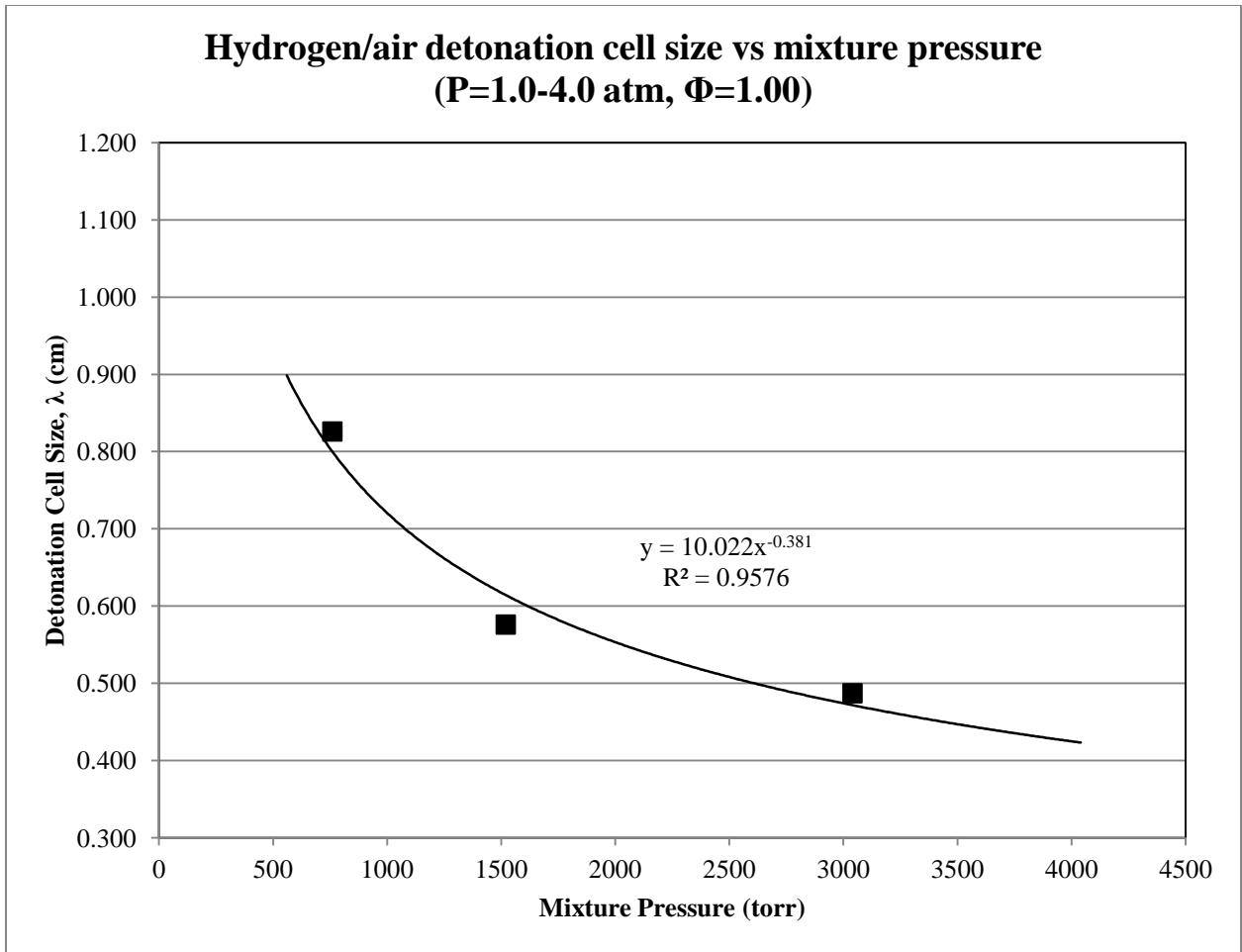


Figure C - 1. Hydrogen/air detonation cell size vs mixture pressure (P=1.0-4.0 atm, $\Phi=1.00$)

Figure C - 2 shows an equivalence ratio of 0.80 with mixture pressures from 2.0 atm to 10.0 atm. This chart contains five data points, the most of any trend in this research. The power series trend line yields an exponent of -0.356. The data fits the trend well with an R^2 of 0.997. Because this trend line contains the most data points and highest R^2 , it has the potential for less error in the results and the best ability to predict true cell size in the range of the tests.

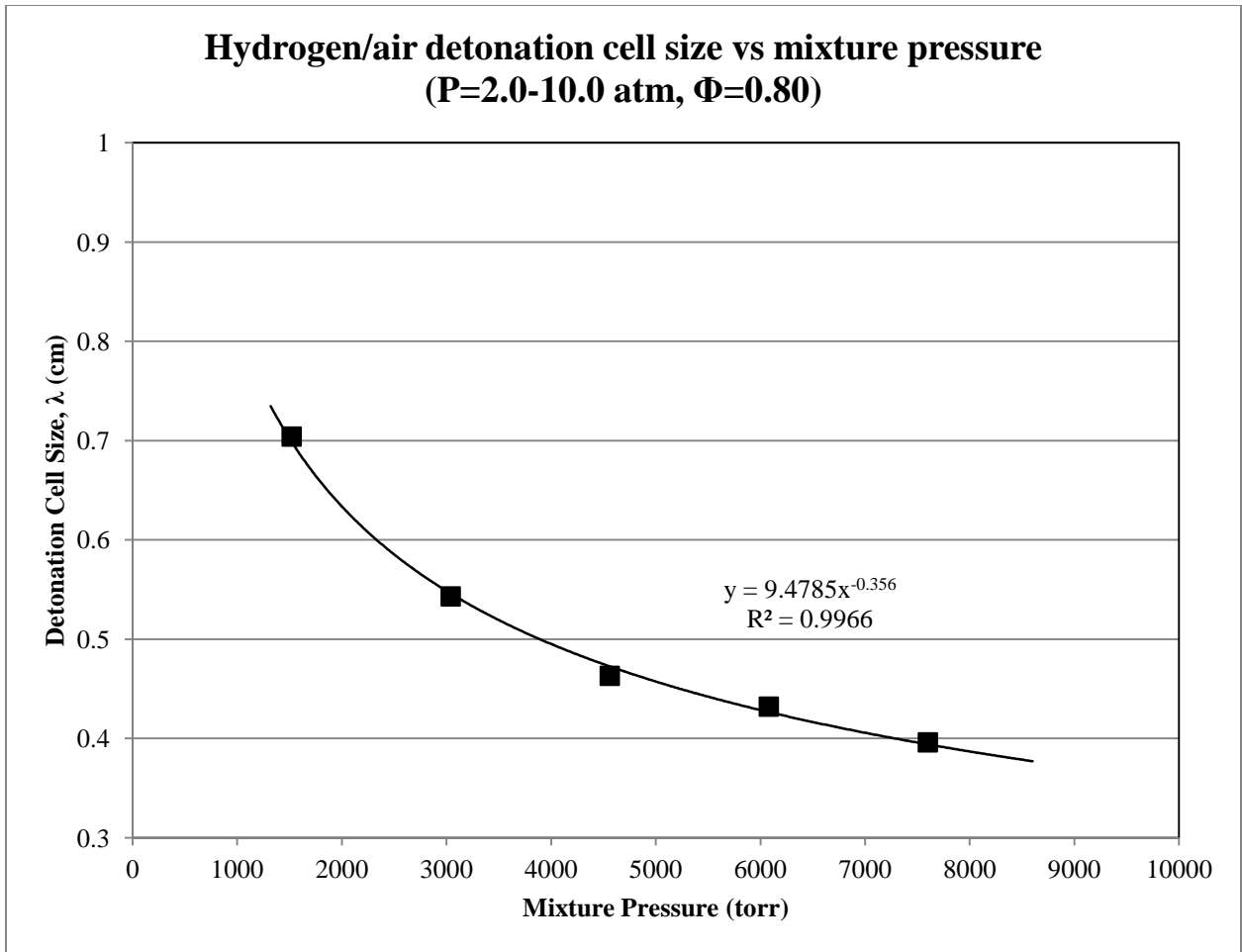


Figure C - 2. Hydrogen/air detonation cell size vs mixture pressure (P=2.0-10.0 atm, Φ=0.80)

Figure C - 3 shows an equivalence ratio of 0.70 with mixture pressures from 4.0 atm to 10.0 atm. This chart contains four data points. The power series trend line yields an exponent of -0.232. The data fits the trend with an R^2 of 0.844. The lower R^2 suggests that the equation has a greater probability to introduce error into predicting the true cell size. It is however, not low enough to disregard the results.

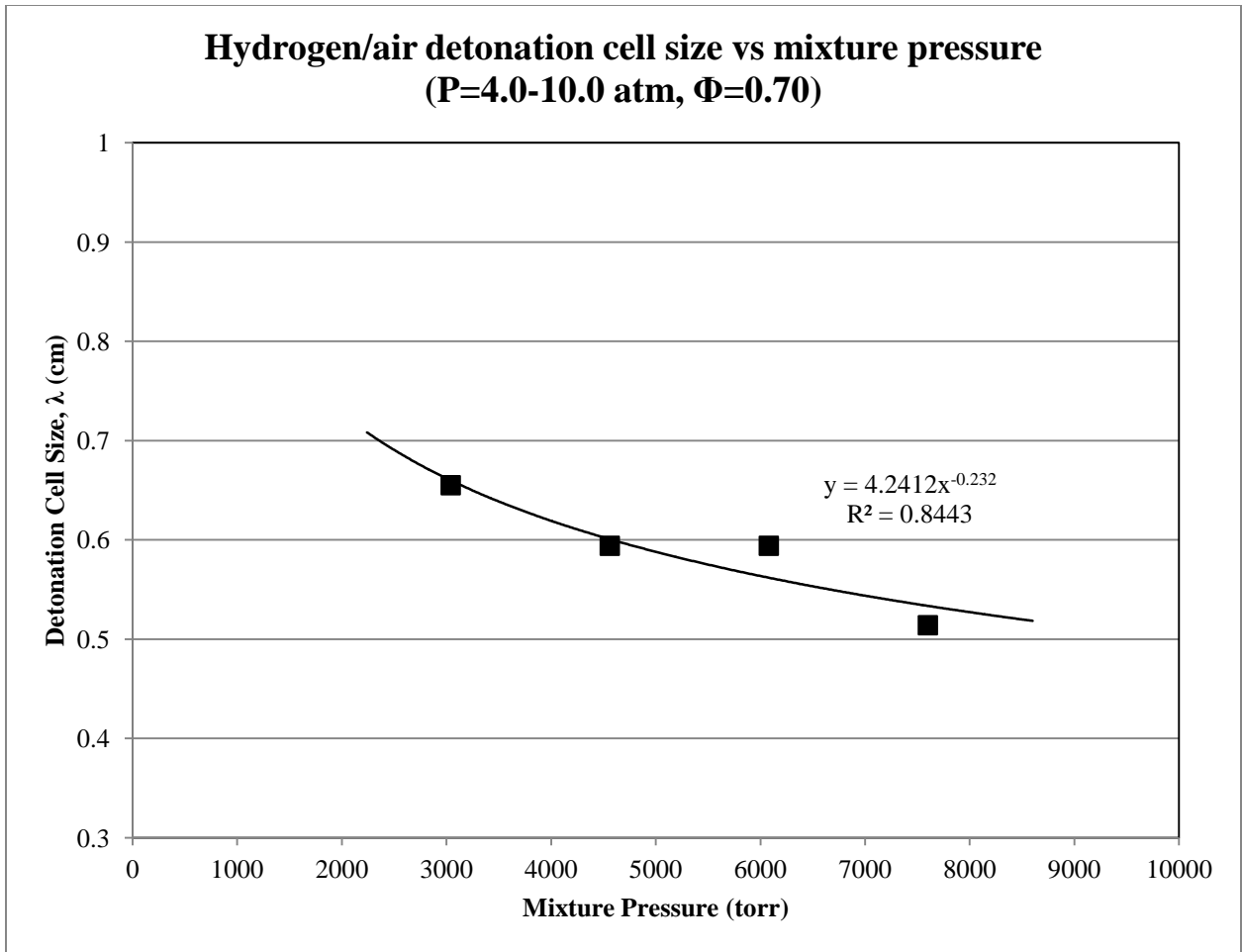


Figure C - 3. Hydrogen/air detonation cell size vs mixture pressure (P=4.0-10.0 atm, $\Phi=0.70$)

Figure C - 4 shows an equivalence ratio of 0.65 with mixture pressures from 6.0 atm to 10.0 atm. This chart contains three data points. The power series trend line yields an exponent of -0.177. The data fits the trend line with an R^2 of 0.810. The low R^2 suggests that the equation has a greater probability to introduce error into predicting the true cell size. It is however, is still not low enough to disregard the results. The lowest R^2 may be due to only having three data points or higher pressures may be more irregular or lower equivalence ratios may be more irregular.

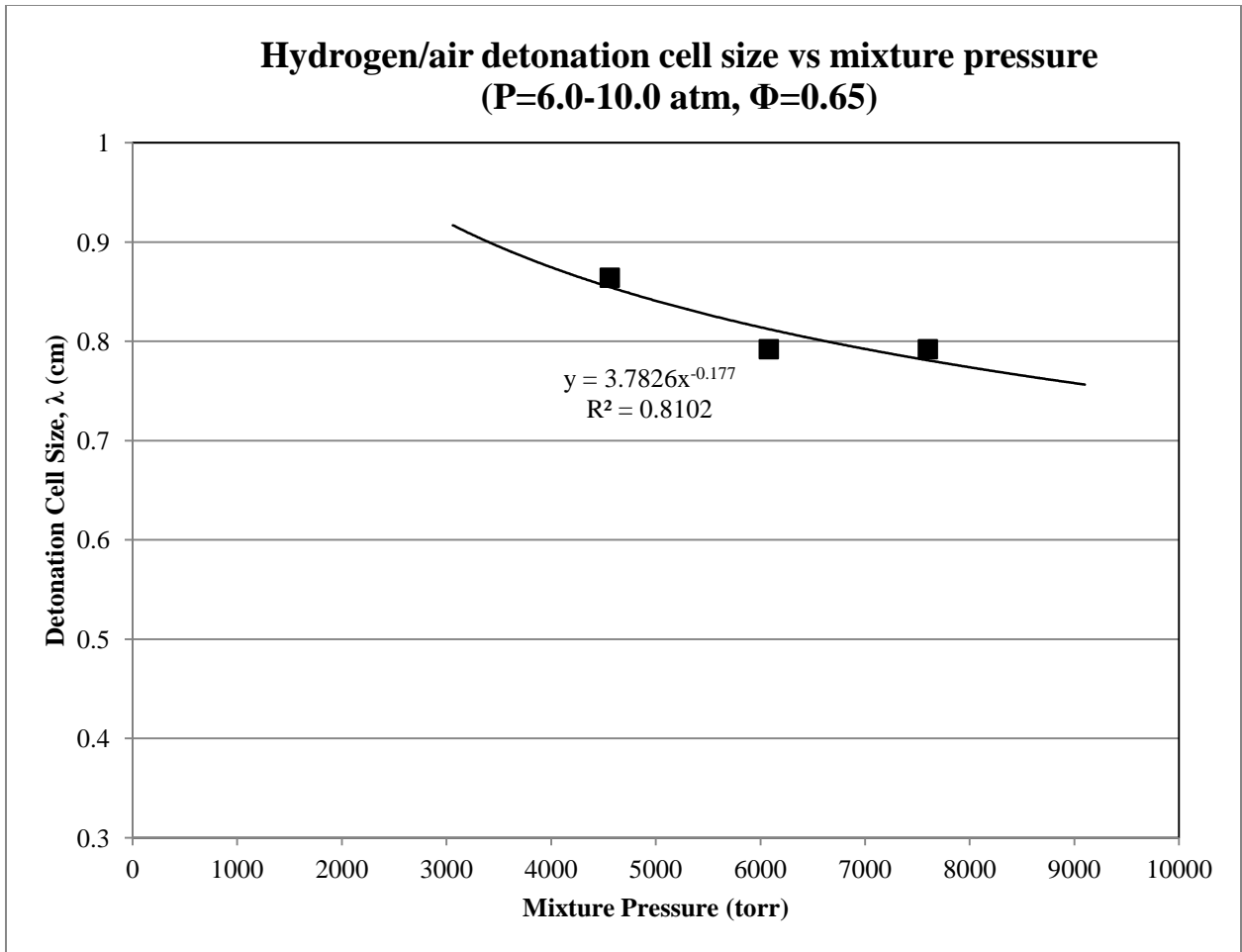
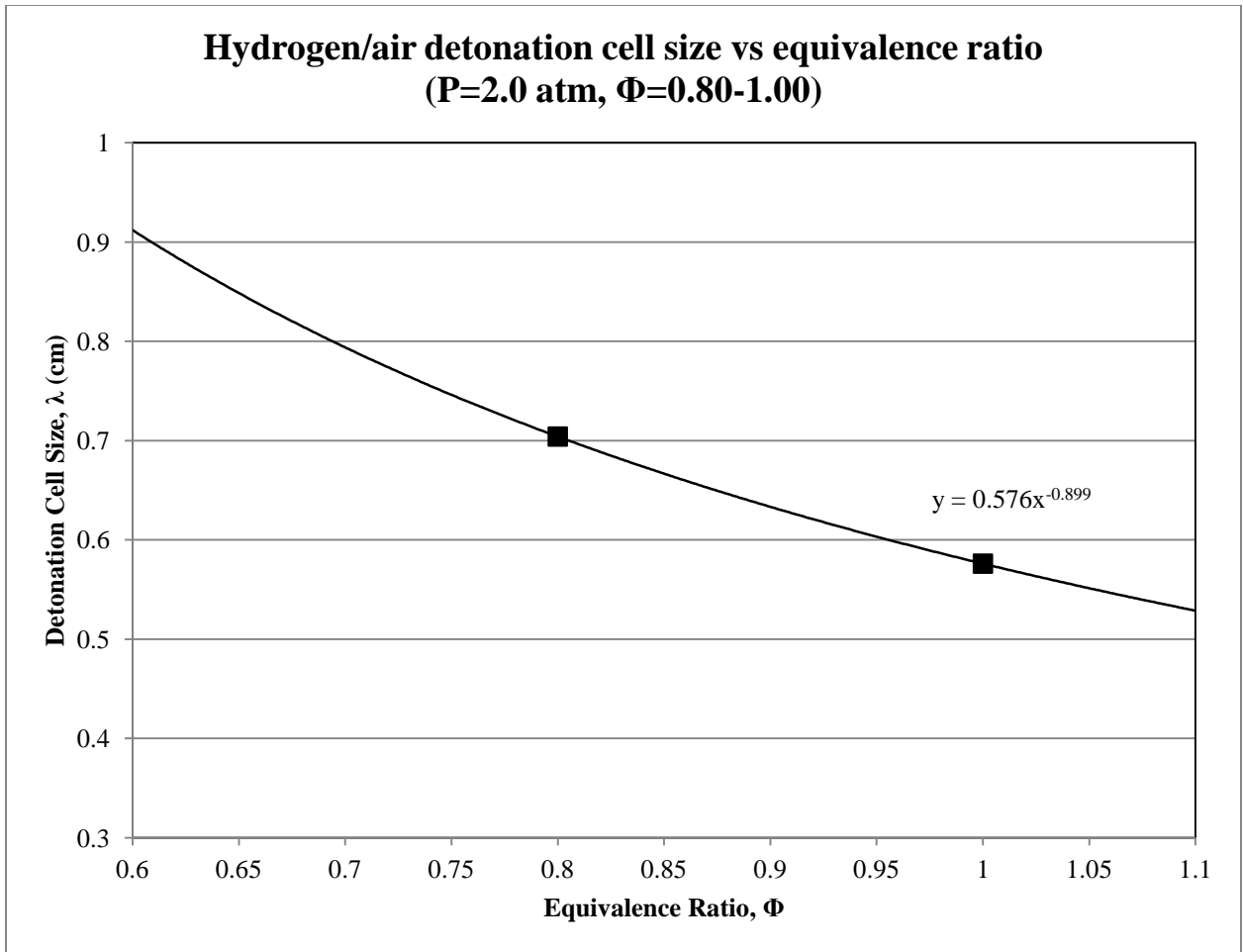


Figure C - 4. Hydrogen/air detonation cell size vs mixture pressure (P=6.0-10.0 atm, $\Phi=0.65$)

Figure C - 5 to Figure C - 9 show trend lines with constant mixture pressure. Figure C - 5 shows an mixture pressure of 2.0 atm with equivalence ratios between 0.80 and 1.00. Because this trend line only contains two data points, the trend line values are not as meaningful. The exponent for the power series is -0.899. The R^2 is not given because it would be 1.00 for two data points.



**Figure C - 5. Hydrogen/air detonation cell size vs equivalence ratio (P=2.0 atm,
 $\Phi=0.80-1.00$)**

Figure C - 6 shows an mixture pressure of 4.0 atm with equivalence ratios between 0.70 and 1.00. This trend line contains three data points. The exponent for the power series is -0.795. The trend line fits the data with an R^2 of 0.91. The R^2 suggests that the trend line should be a good predictor of cell size for the given mixture conditions.

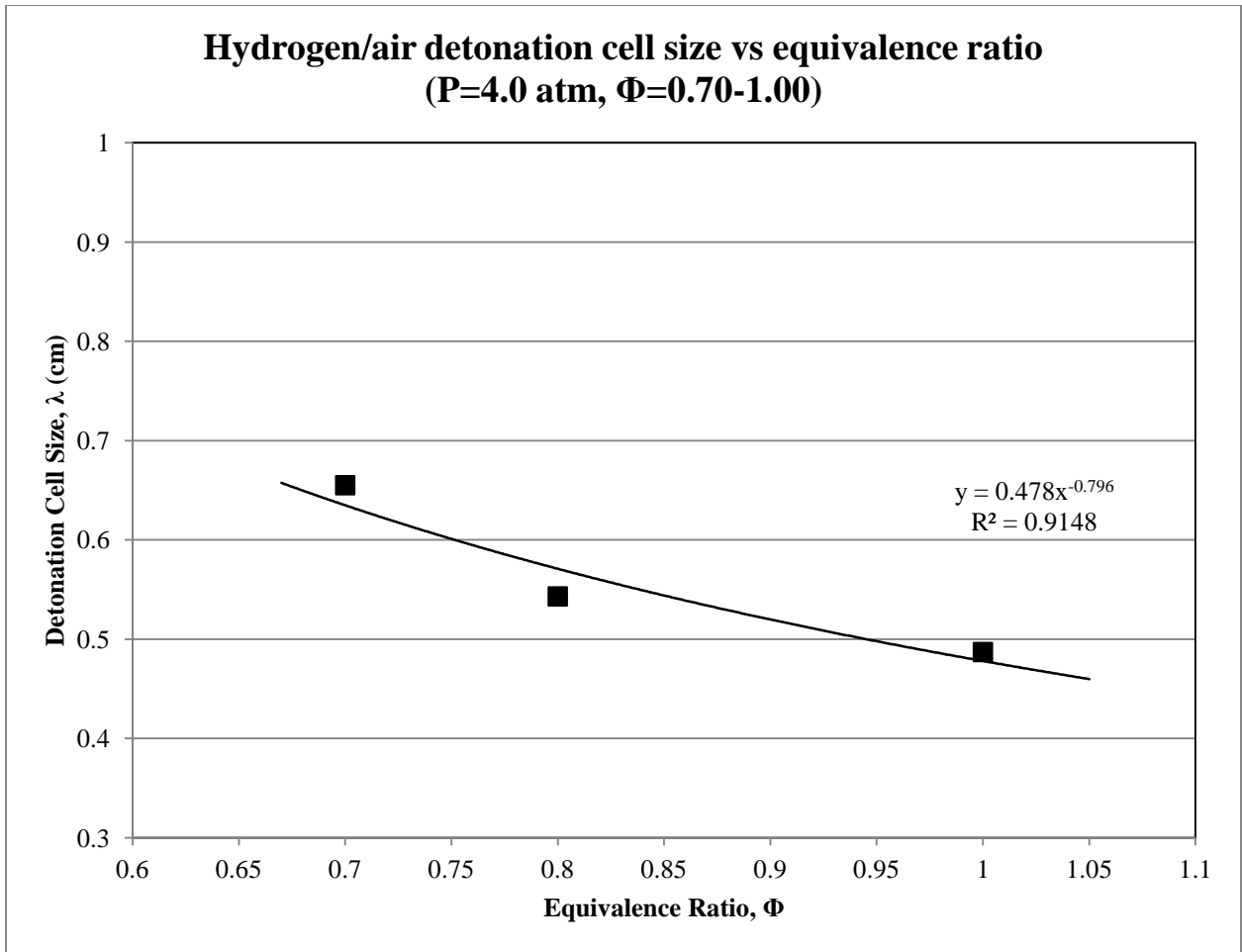


Figure C - 6. Hydrogen/air detonation cell size vs equivalence ratio (P=4.0 atm, $\Phi=0.70-1.00$)

Figure C - 7 shows an mixture pressure of 6.0 atm with equivalence ratios between 0.65 and 0.80. This trend line contains three data points. The exponent for the power series is -2.868. The slope is greater for the 6.0 atm trend line than the 4.0 atm and 2.0 atm trend lines. The larger slope could be attributed to the lower equivalence ratios where the cell size changes the quickest. The trend line fits the data with an R^2 of 0.91. The R^2 suggests that the trend line should be a good predictor of cell size for the given mixture conditions.

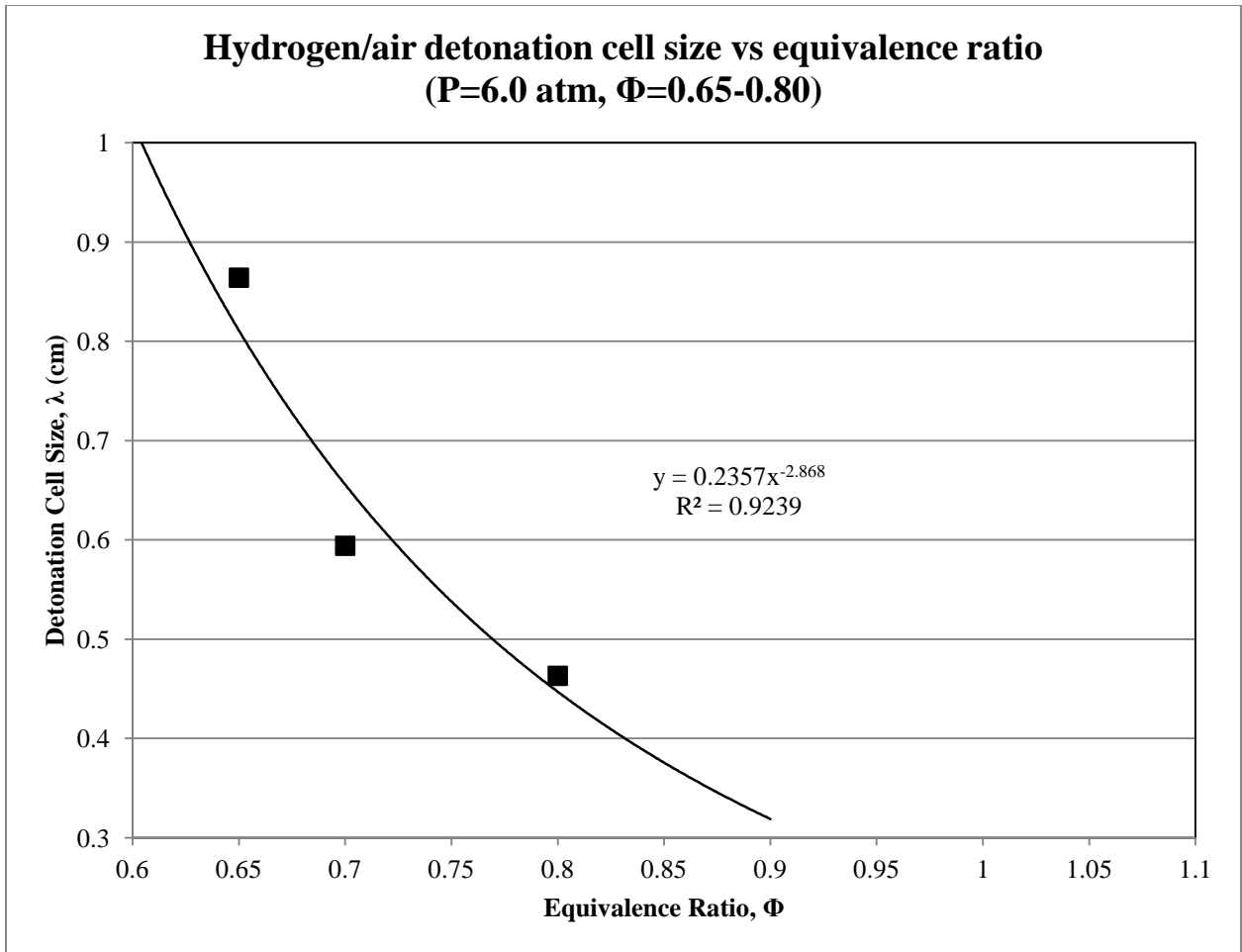


Figure C - 7. Hydrogen/air detonation cell size vs equivalence ratio (P=6.0 atm, $\Phi=0.65-0.80$)

Figure C - 8 shows an mixture pressure of 8.0 atm with equivalence ratios between 0.65 and 0.80. This trend line contains three data points. The exponent for the power series is -2.855. The slope for the 8.0 atm trend line is nearly the same as the 6.0 atm trend line with exponents less than 1.0% different. The trend line fits the data well with an R^2 of 0.98. The R^2 suggests that the trend line should be a better predictor of cell size compared to the other trend lines with constant mixture pressure in this research.

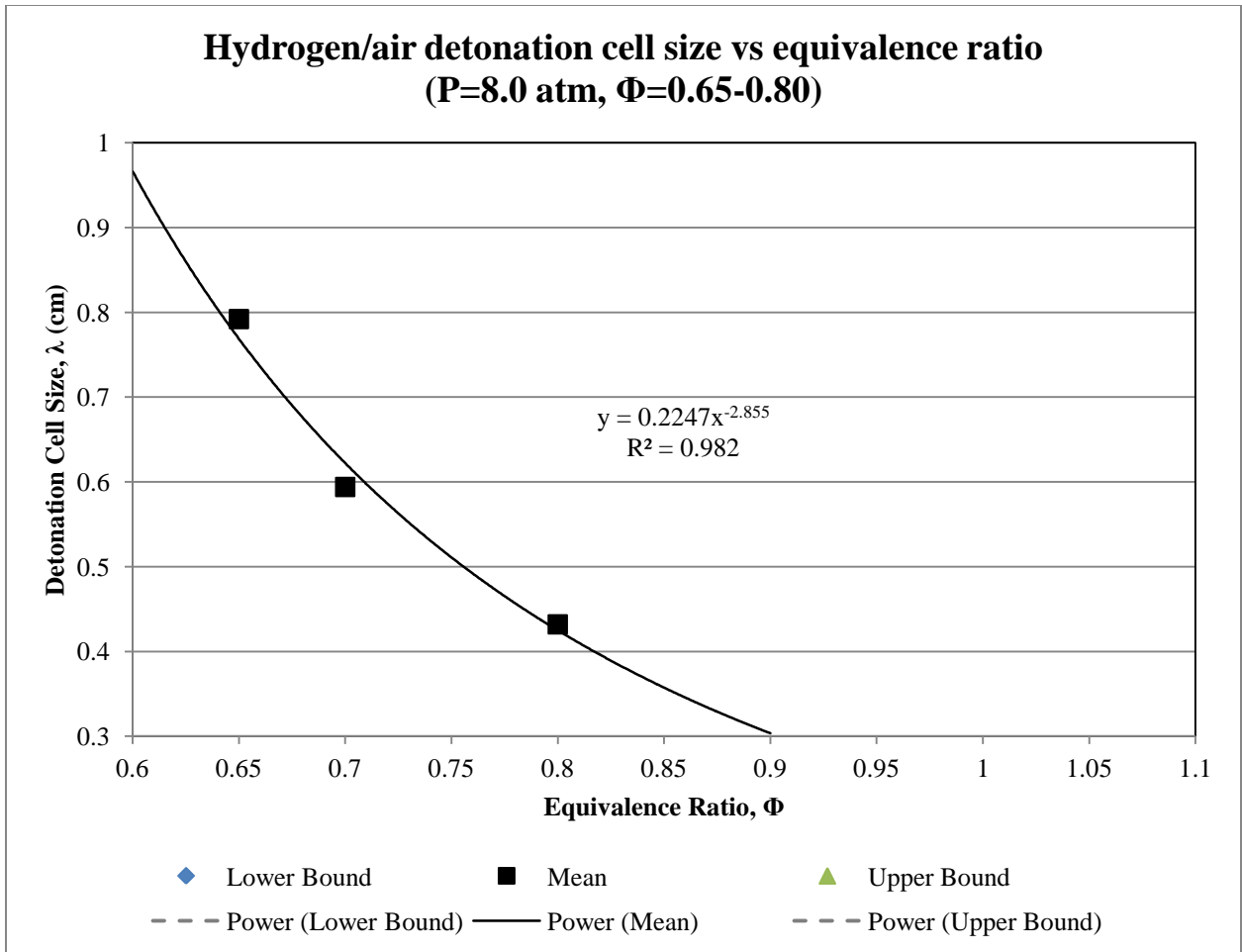
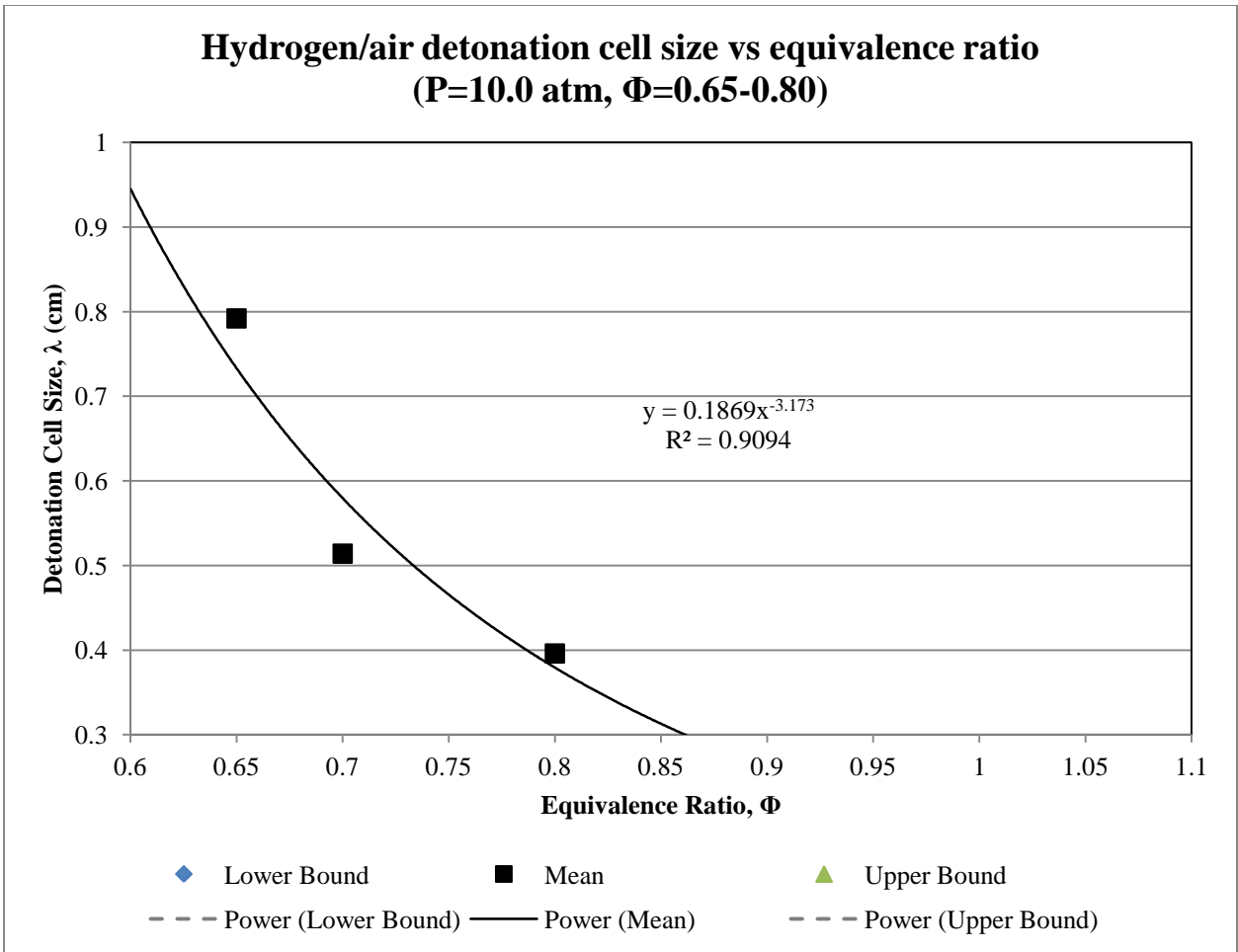


Figure C - 8. Hydrogen/air detonation cell size vs equivalence ratio (P=8.0 atm, $\Phi=0.65-0.80$)

Figure C - 9 shows an mixture pressure of 10.0 atm with equivalence ratios between 0.65 and 0.80. This trend line contains three data points. The exponent for the power series is -3.173. The slope for the 10.0 atm trend line is close to the 8.0 atm and 6.0 atm trend lines with exponents less than 10% different. The trend line fits the data with an R^2 of 0.91. The R^2 suggests that the trend line should be a good predictor of cell size for the given mixture conditions.



**Figure C - 9. Hydrogen/air detonation cell size vs equivalence ratio (P=10.0 atm,
 $\Phi=0.65-0.80$)**

Bibliography

- Bull, D.C., Ellsworth, J.E., and Schuff, P.J. (1982) Detonation cell structure in fuel/air mixtures. *Comb. Flame* 45, 7-22.
- Ciccarelli, G., T. Ginsburg, J. Boccio, C. Economos, C. Finfrock, L. Gerlach, K. Sato, and M. Kinoshita. High-Temperature Hydrogen-Air-Steam Detonation Experiments in the BNL Small-Scale Development Apparatus. Technical Report NUREG/CR-6213, BNL-NUREG-52414, Brookhaven National Laboratory, 1994.
- Ciccarelli, G. T., Ginsberg, J. Boccio, C. Economos, K. Sato, and M. Kinoshita. Detonation cell size measurements and predictions in hydrogen-air-steam mixtures at elevated temperatures. *Combust. Flame*, 99(2):212-220, 1994.
- Ciccarelli, G. T., Ginsberg, J. Boccio, C. Finfrock, L. Gerlach, H. Tagawa, and A. Malliakos. Detonation cell size measurements in high-temperature hydrogen-air-steam mixtures at the bnl high-temperature combustion facility. Technical Report NUREG/CR-6391, BNL-NUREG-52482, Brookhaven National Laboratory, 1997.
- DeBarmore, Nick D., Paul King, Fred Schauer, and John Hoke, "Nozzle Guide Vane Integration into Rotating Detonation Engine," 51st AIAA Aerospace Sciences Meeting including the New Horizons Forum and Aerospace Exposition, AIAA 2013-1030, Grapevine, TX, January 2013.
- Denisov, Yu. N. "Concerning the Analogy Between Combustion in a Detonation Wave and in a Rocket Engine", *ARS Journal*, Vol. 30, No. 9 (1960), pp. 834-840.
- Denisov, Yu.N. and Ya.K. Troshin. Pulsating and spinning detonation of gaseous mixtures in tubes. *Dokl. Akad. Nauk SSSR*, 125(1):110-113, 1959.
- Dupre, G., R. Knystautas, J. Lee, *Prog. In Astro. and Aero.*, Vol. 106, p. 244, 1985.
- Guirao, C.M., R. Knystautas, J. Lee, W. Benedick, and M. Berman. Hydrogen-air detonations. In 19th Symp. Int. Combust. Proc., pages 583-590, 1982.
- Kaneshige, M. and Shepherd, J.E., "Detonation Database," Graduate Aeronautical Laboratories California Institute of Technology, Pasadena, CA, Technical Report FM97-8, July 1997.
- Lee, J.H.S, *The Detonation Phenomenon*, Cambridge University Press, 2008.
- Lee, J. H. S., "Dynamic Parameters of Gaseous Detonations," *Ann. Rev. Fluid Mech.*, 3 1 1-336, 1984.

- Lee, J. H.S., "Initiation of Gaseous Detonations," *Annual Review Phys. Chem.*, Vol. 28, pp. 75-104, 1977.
- Lefebvre, M. H., "Simulation of Cellular Structure in a Detonation Wave," *Dynamic Aspects of Detonations*, Vol. 153, 1993, pp. 64-77.
- Matsui, H., and J.H.S. Lee. On the measure of the relative detonation hazards of gaseous fuel-oxygen and air mixtures. In: *Proceedings of the Seventeenth Symposium (International) on Combustion*. The Combustion Institute, Pittsburgh, pp 1269–1280. 1979.
- Millhouse, Paul T., Stuart C. Kramer, Paul I. King, and Edward F. Mykytka, "Identifying Optimal Fan Compressor Pressure Ratios for the Mixed-Stream Turbofan Engine," *Journal of Propulsion and Power*, Vol. 16, No. 1, January-February 2000.
- Mitrofanov, V. V. and R. I. Solouhkin, *Soviet Phys. Dokl.*, Vol. 9, p. 1055, 1965.
- Moen, I. O., Donato, M., Knystautas, R. and Lee, J. H.: *Eighteenth Symposium (International) on Combustion*, p. 1615, The Combustion Institute, Pittsburgh (1980).
- Moen, I.O., Funk, J.W., Ward, S.A., Rude, G.M. and Thibault, P.A. (1984b) Detonation length scales for fuel-air explosives. *AIAA Progress in Astronautics and Aeronautics*, Vol. 94, 55-79. AIAA, New York.
- Moen, I. O., S. E. Murray, D. Bjerketvedt, A. Rinnan, R. Knystautas, J. Lee, "Diffraction of Detonation From tubes into a Large Fuel-Air Explosive Cloud," *19th International Symposium on Combustion*, p. 635, 1982.
- Settles, G., *Schlieren and Shadowgraph Techniques: Visualizing Phenomena in Transparent Media*, Springer, Berlin, 2001.
- Shchelkin, K. I. and Y. K. Troshin, *Gas Dynamics of Detonations*, Mono :Book Corp., Baltimore, Maryland, 1965.
- Shepherd, J.E., "Chemical Kinetics of Hydrogen-Air-Diluent Detonations," *10th ICDERS*, Berkley, CA, August 1985, pp. 263-293.
- Shepherd, J.E.. Chemical kinetics and cellular structure of detonations in hydrogen sulfide and air. In *Prog. Astronaut. Aeronaut.*, volume 106, pages 294-320, 1986.
- Stamps, D.W., W.B. Benedick, and S.R. Tieszen. Hydrogen-air-diluent detonation study for nuclear reactor safety analyses. Technical Report NUREG/CR-5525, SAND89-2398, Sandia National Laboratories, 1991.

- Stevens, Christopher A., John L. Hoke, and Frederick R. Schauer, "Optical Measurement of Detonation with a Focusing Schlieren Technique," AIAA 53rd Aerospace Sciences Meeting, AIAA-2015-1350, Kissimmee, FL, 2015
- Stevens, Christopher A., John L. Hoke, and Frederick R. Schauer, "Cell Width of Methane/Air Mixtures at Elevated Initial Pressure and Temperature," AIAA-2014-1320, AIAA SciTech, 2014.
- Tellefsen, Johnathan R., Paul King, Fred Schauer, and John Hoke, "Analysis of an RDE with Convergent Nozzle in Preparation for Turbine Integration," 50th AIAA Aerospace Sciences Meeting Including the New Horizons Forum and Aerospace Exposition, AIAA 2012-0773, Nashville, TN, January 2012.
- Tieszen, S.R., M.P. Sherman, W.B. Benedick, and M. Berman. Detonability of H₂-air-diluent mixtures. Technical Report NUREG/CR-4905, SAND85-1263, Sandia National Laboratories, 1987.
- Tieszen, S.R., M.P. Sherman, W.B. Benedick, J.E. Shepherd, R. Knystautas, and J.H.S. Lee. Detonation cell size measurements in hydrogen-air-steam mixtures. In Prog. Astronaut. Aeronaut., volume 106, pages 205-219, 1986.
- Wheeler, Anthony J., and Ahmad R. Ganji, *Introduction to Engineering Experimentation*, Pearson, Upper Saddle River, NJ, 2004, pp. 190-202.

REPORT DOCUMENTATION PAGE

Form Approved
OMB No. 0704-0188

The public reporting burden for this collection of information is estimated to average 1 hour per response, including the time for reviewing instructions, searching existing data sources, gathering and maintaining the data needed, and completing and reviewing the collection of information. Send comments regarding this burden estimate or any other aspect of this collection of information, including suggestions for reducing the burden, to Department of Defense, Washington Headquarters Services, Directorate for Information Operations and Reports (0704-0188), 1215 Jefferson Davis Highway, Suite 1204, Arlington, VA 22202-4302. Respondents should be aware that notwithstanding any other provision of law, no person shall be subject to any penalty for failing to comply with a collection of information if it does not display a currently valid OMB control number.

PLEASE DO NOT RETURN YOUR FORM TO THE ABOVE ADDRESS.

1. REPORT DATE (DD-MM-YYYY) 17-9-2015	2. REPORT TYPE Master's Thesis	3. DATES COVERED (From - To) Sept 2013 - Jun 2015
--	-----------------------------------	--

4. TITLE AND SUBTITLE Effect of Mixture Pressure and Equivalence Ratio on Detonation Cell Size for Hydrogen-Air Mixtures	5a. CONTRACT NUMBER
	5b. GRANT NUMBER
	5c. PROGRAM ELEMENT NUMBER

6. AUTHOR(S) Babbie, Curtis A., Capt, USAF	5d. PROJECT NUMBER
	5e. TASK NUMBER
	5f. WORK UNIT NUMBER

7. PERFORMING ORGANIZATION NAME(S) AND ADDRESS(ES) Air Force Institute of Technology Graduate School of Engineering and Management (AFIT/EN) 2950 Hobson Way Wright-Patterson AFB OH 45433-7765	8. PERFORMING ORGANIZATION REPORT NUMBER AFIT-ENY-MS-15-J-045
---	--

9. SPONSORING/MONITORING AGENCY NAME(S) AND ADDRESS(ES) Department of Aeronautical Engineering 2950 Hobson Way WPAFB OH 45433-7765 DSN 271-0690, COMM 937-255-3636 Email: paul.king@afit.edu	10. SPONSOR/MONITOR'S ACRONYM(S)
	11. SPONSOR/MONITOR'S REPORT NUMBER(S)

12. DISTRIBUTION/AVAILABILITY STATEMENT
DISTRIBUTION STATEMENT A:
APPROVED FOR PUBLIC RELEASE; DISTRIBUTION UNLIMITED.

13. SUPPLEMENTARY NOTES

14. ABSTRACT
Cell sizes of fuel and oxidizer combinations are the fundamental length scale of detonations. The detonation cell size is correlated to dynamic detonation properties. One of the properties, detonability is the motivation for this research. In order to design combustion chambers for detonating engines, specifically PDEs and RDEs, the cell size is needed. Higher than atmospheric mixture pressure detonation cell sizes are important for scaling the combustion chambers, and before this research no data existed for hydrogen and air detonation cell sizes at mixture pressures up to 10.0 atm. This research successfully validated a new detonation cell size measurement technique and measured 15 cases for varying mixture pressures up to 10 atm and equivalence ratios. The results were concurrent with previous trends, as increase in mixture pressure decreased detonation cell size and a decrease in equivalence ratio from stoichiometric increased detonation cell size. The experimental results were used to establish a correlation that estimates hydrogen and air detonation cell size given initial mixture pressure and equivalence ratio.

15. SUBJECT TERMS
^Hydrogen and air, detonation cell size, detonation, cell size, Rotating Detonation Engine, RDE

16. SECURITY CLASSIFICATION OF:			17. LIMITATION OF ABSTRACT UU	18. NUMBER OF PAGES 129	19a. NAME OF RESPONSIBLE PERSON Dr. Paul I. King, AFIT/ENY
a. REPORT U	b. ABSTRACT U	c. THIS PAGE U			19b. TELEPHONE NUMBER (Include area code) (937) 255-3636 x4628 paul.king@afit.edu

Reset